

**Three Unconventional Kinesins Exhibit Novel Microtubule Interactions:
The Characterization of Kar3Cik1, Kar3Vik1, and Nod**

by

Lisa Raenae Sproul, PhD

B.S., Biology, Carlow University, 2001

Submitted to the Graduate Faculty of
The Department of Biological Sciences in partial fulfillment
of the requirements for the degree of
Doctor of Philosophy

University of Pittsburgh

2006

UNIVERSITY OF PITTSBURGH

Biological Sciences

This dissertation was presented

By

Lisa Raenae Sproul

It was defended on

August 31st, 2006

and approved by

Paula Grabowski, PhD, Biological Sciences, University of Pittsburgh

John M. Rosenberg, PhD, Biological Sciences, University of Pittsburgh

William Saunders, PhD, Biological Sciences, University of Pittsburgh

Claire E. Walczak, PhD, Medical Sciences, Indiana University

Dissertation Advisor: Susan P. Gilbert, PhD, Biological Sciences, University of Pittsburgh

Copyright © by Lisa Raenae Sproul

2006

The Characterization of Kar3Cik1, Kar3Vik1 and Nod:

Three Unconventional Kinesins Exhibit Novel Microtubule Interactions

Lisa Raenae Sproul

University of Pittsburgh, 2006

My dissertation work was focused to characterize three members of the Kinesin superfamily *in vitro*. Kinesins are required in the cell for the correct localization and directed transport of proteins, DNA, RNA and cellular organelles. The three molecular motors of the kinesin superfamily studied here are Kar3Cik1, Kar3Vik1 and Nod. These three kinesins are unconventional in that they do not motor to the microtubule plus end transporting cargo over long distances, like Kinesin-1.

Kar3Cik1 and Kar3Vik1 are *Saccharomyces cerevisiae* Kinesin-14s, exhibiting minus end directionality characteristic of Kinesin-14s. Kar3Cik1 is essential for meiosis and for karyogamy, or mating in yeast. Kar3Cik1 also has non-essential roles in mitosis. Kar3Vik1 plays an important role at the spindle pole body during yeast mitosis. My work has shown that the two heterodimers interact with the microtubule in very different ways. Cik1 targets Kar3 to microtubule plus ends and enhances the Kar3-intrinsic depolymerizing ability. In contrast Vik1 binds the microtubule in addition to the Kar3 motor domain and depresses the Kar3 depolymerizing ability. Both of these functions correlate with the *in vivo* phenotypes and suggest different mechanisms of action for the two heterodimers.

Nod is a *Drosophila melanogaster* orphan kinesin proposed to provide a “polar ejection force” to stabilize chromosomes at the metaphase plate in meiosis. Our work characterized Nod as a kinesin that regulates microtubule dynamics by binding to the microtubule plus end and promoting microtubule polymerization. These results provide a mechanistic explanation for the polar ejection force observed *in vivo*.

My dissertation work has provided knowledge about the many ways in which different kinesins can interface with and regulate microtubule dynamics.

TABLE OF CONTENTS

DEDICATED TO.....	XIII
PREFACE	XIV
1.0 INTRODUCTION	1
1.1 THE COMPLEX EUKARYOTIC CELL	1
1.2 MICROTUBULES, DYNAMIC SUPERHIGHWAYS	2
1.3 KINESINS	5
1.4 KINESIN-13, CANONICAL MICROTUBULE DESTABILIZERS.....	10
1.5 KAR3, A KINESIN-14	11
1.6 NOD, AN ORPHAN KINESIN.....	14
1.6.1 Figure 1 Legend.....	17
1.6.2 Figure 2 Legend.....	18
1.6.3 Figure 3 Legend.....	19
1.6.4 Figure 4 Legend.....	21
1.6.5 Figure 5 Legend.....	22
1.6.6 Figure 6 Legend.....	23
1.6.7 Figure 7 Legend.....	24
2.0 MATERIALS AND METHODS	25
2.1 BUFFERS AND EXPERIMENTAL CONDITIONS	25
2.2 MOLECULAR MOTORS	26
OLIGOMERIC STATE.....	26
2.3 CONSTRUCT DESIGN.....	27
2.3.1 Kar3Cik1_L.....	27
2.3.2 Kar3Vik1 and Kar3Cik1.....	27
2.4 PROTEIN EXPRESSION AND PURIFICATION	29

2.4.1	Kar3Cik1 _L , Kar3Cik1, Kar3Vik1.....	29
2.4.2	Kar3MD	30
2.4.3	Vik1MHD and SeMetVik1MHD.....	31
2.4.4	Nod _{FL} -GFP, Nod ₃₁₈ , and Nod ₃₁₈ -GFP	31
2.4.5	Ncd, K401, KHC _R , Kinesin-1	31
2.4.6	Tubulin	32
2.5	ANTIBODIES.....	32
2.6	GEL FILTRATION AND STOKES RADII CALCULATIONS	32
2.7	STEADY STATE ANALYSIS OF MOTOR PROTEINS	33
2.8	MICROTUBULE COSEDIMENTATION ASSAYS	34
2.8.1	Microtubule Depolymerization Solution Assay	34
2.8.2	Microtubule Polymerization Solution Assay	34
2.8.3	Microtubule•Motor Equilibrium Binding Assays	35
2.9	MICROSCOPY ASSAYS OF KINESIN MOTORS.....	36
2.9.1	Preparation of Polarity-Marked Fluorescent Microtubules.....	36
2.9.2	Motility of Kinesin Motor Proteins.....	36
2.9.3	Microtubule Shortening Promoted by Kinesin Motor Proteins ...	37
2.9.4	Microtubule•Motor Immunolocalization.....	38
2.9.5	Analysis of Microtubule Polymerization by Fluorescence Microscopy	39
2.9.6	Error Calculations.....	40
3.0	KAR3CIK1, A NOVEL KINESIN DEPOLYMERASE.....	41
3.1	ABSTRACT	41
3.2	INTRODUCTION.....	42
3.3	RESULTS.....	43
3.3.1	Expression and Purification.....	43
3.3.2	Kar3Cik1 Promotes Robust Microtubule Gliding	44
3.3.3	Kar3Cik1-Promoted Microtubule Depolymerization Requires ATP Turnover	44
3.3.4	Kar3Cik1 Steady-State ATPase Is Only Stimulated by Microtubules.....	45

3.3.5	Kar3Cik1 Promotes Plus-to-Minus End Microtubule Shortening	46
3.3.6	Kar3Cik1 Has a Higher Affinity for the Microtubule End than Kar3MD47	
3.4	DISCUSSION	48
	FIGURES AND FIGURE LEGENDS	50
3.5.1	Figure 8 Legend	50
3.5.2	Figure 9 Legend	52
3.5.3	Figure 10 Legend	54
3.5.4	Figure 11 Legend	56
3.5.5	Figure 12 Legend	58
4.0	CHAPTER THREE <i>ADDENDUM</i>:	59
4.1	KAR3CIK1 AND BIK1, RESPONSIBLE FOR COORDINATING MICROTUBULE DEPOLYMERIZATION FROM THE PLUS ENDS DURING KARYOGAMY	59
4.2	KAR3 AT THE KINETOCHORE, BIK1 TOO	63
5.0	KAR3VIK1, A KINESIN-14 THAT USES A “DEAD” HEAD TO BIND THE MICROTUBULE AND GENERATE FORCE	65
5.1	ABSTRACT	65
5.2	INTRODUCTION	66
5.3	RESULTS	68
5.3.1	Kar3Vik1 is a Minus End Directed Motor	68
5.3.2	Kar3Vik1 Steady State ATPase	69
5.3.3	Kar3Cik1 is a More Robust Microtubule Depolymerase than Kar3Vik1	70
5.3.4	Kar3Vik1 Cooperative Binding Inhibits Microtubule Depolymerization	71
5.3.5	Kar3Vik1 Microtubule Binding Properties – Cosedimentation Experiments	71
5.3.6	Immunolocalization of Kar3Vik1 on the Microtubule	72
5.4	DISCUSSION	73
5.4.1	Kar3Vik1 and Kar3Cik1: Two Distinct Kinesin-14 Motors	73

5.4.2	The Vik1MHD Binds Microtubules in the Absence of Kar3	74
5.4.3	Kar3Vik1 Exhibits Strain Dependent Cooperativity.....	74
5.4.4	Functional Role of Kar3Vik1 in Mitosis.....	76
5.4.5	Figure 13 Legend	78
5.4.6	Figure 14 Legend	80
5.4.7	Figure 15 Legend	81
5.4.8	Figure 16 Legend	83
5.4.9	Figure 17 Legend	85
6.0	DROSOPHILA NOD PROTEIN BINDS PREFERENTIALLY TO THE PLUS ENDS OF MICROTUBULES AND PROMOTES MICROTUBULE POLYMERIZATION <i>IN VITRO</i>	86
6.1	ABSTRACT	86
6.2	INTRODUCTION.....	87
6.3	RESULTS.....	89
6.3.1	Functional Nod _{FL} -GFP Localizes to the Posterior Pole of Stage Nine Embryos in a Fashion That Requires a Properly Organized Microtubule Network	89
6.3.2	Nod _{FL} and Nod ₃₁₈ Show Preferential Binding to Microtubule Plus Ends <i>in vitro</i>	90
6.3.3	Nod Binds Preferentially to the Plus Ends of Microtubules.....	94
6.3.4	Nod _{FL} -GFP and Nod ₃₁₈ Promote Microtubule Polymerization <i>in vitro</i>	95
6.4	DISCUSSION	96
6.5	FIGURES AND FIGURE LEGENDS	98
6.5.1	Figure 18 Legend	98
6.5.2	Figure 19 Legend	99
6.5.3	Figure 20 Legend	100
6.5.4	Figure 21 Legend	101
6.5.5	Figure 22 Legend	102
6.5.6	Figure 23 Legend	104
6.5.7	Figure 24 Legend	105

6.5.8	Figure 25 Legend	107
6.5.9	Figure 26 Legend	109
6.5.10	Figure 27 Legend.....	110
6.5.11	Figure 28 Legend.....	112
7.0	DISCUSSION AND CONCLUSIONS	113
7.1	KAR3, A GENETIC HISTORY.....	114
7.2	CIK1 TARGETS THE MINUS END KINESIN DEPOLYMERASE KAR3 TO THE MICROTUBULE PLUS END	116
7.3	VIK1 BINDS MICROTUBULES TO REGULATE KAR3 BINDING AND DEPOLYMERIZATION.....	118
7.4	CIK1 AND VIK1 CONFER DIFFERENT ROLES TO KINESIN KAR3..	120
7.4.1	The Differences.....	120
7.4.2	The Unanswered Questions.....	121
7.5	NOD, AN ORPHAN KINESIN THAT PROMOTES MICROTUBULE POLYMERIZATION	122
7.6	CONCLUSIONS.....	125
	BIBLIOGRAPHY	126

LIST OF TABLES

Table 1. The Motors Analyzed for the Studies Presented in Chapters 2-6.	26
Table 2. Summary of Motor·Microtubule Depolymerization	56
Table 3. Summary of Motor·Microtubule Binding	58
Table 4. Summary of Nod·Microtubule Binding.....	103

LIST OF FIGURES

Figure 1. The Classification of the Kinesin Superfamily	17
Figure 2. The Stages of Tubulin Polymerization	18
Figure 3. The Hand-Over-Hand Walking Model of Kinesin-1, adapted from ref. [120]..	19
Figure 4. Five Kinesin Structures Show Differences in Loop 11	20
Figure 5. Kar3 Requires Cik1 and Vik1 <i>in vivo</i> , adapted from ref. [229]	22
Figure 6. Microtubule•MCAK Interaction	23
Figure 7. Model: Nod Exerts a Polar Ejection Force To Align Chromosomes in Metaphase.....	24
Figure 8. Model for Kar3Cik1 Function during Karyogamy	50
Figure 9. Kar3Cik1 Characterization	51
Figure 10. Solution Assays of Microtubule Depolymerization.....	53
Figure 11. Microtubule Shortening Promoted by Kar3Cik1, Ncd, and MCAK	55
Figure 12. Immunolocalization of Kar3MD, Kar3Cik1, and Ncd	57
Figure 13. Purification of the Heterodimeric Kar3Vik1, Kar3Cik1 and Monomeric Kar3MD	78
Figure 14. Kar3Vik1 is a Kinesin-14 Heterodimeric Motor	79
Figure 15. Microtubule binding by Vik1MHD, SeMetVik1MHD, Kar3MD, and Kar3Vik1.	81
Figure 16. Immunolocalization of Kar3Vik1, Kar3Cik1, Kar3MD, and Vik1MHD	82
Figure 17. A Proposed Mechanism for Kar3Vik1 Transport of a Microtubule Cargo.....	84
Figure 18. The Structure of the <i>Drosophila</i> Nod Kinesin-Like Protein.....	98
Figure 19. Nod _{FL} -GFP Localizes to both the Oocyte Chromosomes and to the Posterior Pole in Stage 9 Oocytes (Photo by Wei Cui).....	99

Figure 20. Localization of Nod _{FL} -GFP in Stage 9 Oocytes in Which the Microtubule Organization is Disrupted by Mutations in <i>grk</i> (Photo by Wei Cui)	100
Figure 21. Purification of Nod _{FL} -GFP, Nod ₃₁₈ , and Nod ₃₁₈ -GFP From <i>E. coli</i>	101
Figure 22. Nod _{FL} -GFP and Nod ₃₁₈ -GFP Bind to Microtubules <i>in vitro</i>	102
Figure 23. Distribution of Nod Binding Sites Along Microtubules	104
Figure 24. Trapping of the Nod ₃₁₈ -GFP Collision Complex by Glutaraldehyde Fixation	105
Figure 25. Nod Promotes Microtubule Polymerization <i>in vitro</i>	106
Figure 26. Sedimentation Analysis of the Effect of Nod on Microtubule Polymerization	108
Figure 27. Nod Promotes Microtubule Polymerization in a Time-Dependent Manner..	110
Figure 28. <i>E.coli</i> Lysate is Insufficient to Polymerize Microtubules	111
Figure 29. Kar3Cik1 (green) & Bik1 (black) at Depolymerizing Plus Ends Facilitate Nuclear Fusion.....	121

DEDICATED TO

Linda Marie Henry Sproul

and

Blaney Robert Sproul



In Loving Memory of

Margaret Madeline Henry

and

Megan Lillie Dietz

PREFACE

" In every outthrust headland, in every curving beach, in every grain of sand, there is the story of the earth." -*Rachel Carson*

It has been my amazing privilege to study science at an in-depth level for the past five years. The mysteries and the unknowns of this world fascinate me, and I know that if we are patient enough, curious enough, and courageous enough, we will be able to comprehend this amazing universe that has been set in motion. My studies have encompassed much, and produced interesting results and these are but small drops in a bucket too large and too wonderful for me to completely comprehend, but I do believe that if we press on, we will one day come to the beautiful understanding of our remarkable surroundings.

"All I have seen teaches me to trust the Creator for all I have not seen. "

-Ralph Waldo Emerson

This work would not have been possible without the foundation, the inspiration, the encouragement and support of the people I have been blessed with in my life. This work is dedicated to my late Grandmother, Margaret Madeline Henry, the most extraordinary person I've ever encountered. She provided a pathway and a foundation to the Truth that has now spanned three generations and defined my life. Her example of love, kindness and more love with a deep faith in God and Jesus Christ is one that has always inspired and challenged me. Growing up she was one of my best friends, her home was my haven, and her death inspired me to pursue a career that would work to understand, treat, and hopefully prevent deaths from disease. I live my life with the

hope of seeing her again. I am very thankful for my parents, Linda Marie Henry Sproul and Blaney Robert Sproul who did their best as often as they could to build on the foundation my Grandmother helped lay for them, for me, and for my sisters. My parents support over the past five years both through prayer and in other ways has been great and I could not have completed this task in such a manner with out them. Mom and Dad, Thank You. Mom, you are a friend unlike any other, and I hope you know that I value you greatly, not only are you my mom, you are often the best friend I've got. I have three beautiful sisters whose personalities remind me of the awesome genetics that mix and match and are expressed in each of us differently. Leah, you are both a good friend and a great source of inspiration and organization to me! Heidi, it is wonderful to see you grow up into a lovely charming lady with a sense of humor that can always make me smile. Jody, I am so proud of you for attending and completing ABC. You are a wonderful heart and I look forward to the gifts you will develop and share. You three have also been a huge source of support and love. To my immediate family I must say I am forever grateful for and defined by your examples, your faith, and your deep love for me. I will take a moment here to speak briefly to my three adopted sisters, Rebecca, Rachel, and Cami. You three are always in my prayers and where ever I may be, there too you have a place. I love you!

My interest in science has been lifelong stemming from a curiosity of nature and life. This was fostered by my years spent on my Uncle Paul's farm feeding the 'milk cows', 'snipe hunting', 'chasing cats' and 'stacking hay' with Brianne Maryanne Martin and Keith Sproul. These two cousins taught me the value of friendships within family, unconditional love through many hard things, and days. Brianne is an inspiration of a powerful, purposeful woman driven by the past as her guidepost, but never her hitching post. She is a part of everyplace I go and everything I've become. She's my redheaded side, for sure! I have on this earth no biological brothers, but the three humans that come closest to that are my cousins Craig, Shaun, and Neil. These three have always been my best resource for understanding and interacting with men. These three can make me laugh in a heart beat, have always had my back, and are three people I'd love to grab a beer with every night of the week! I am so proud of my 3 cousins and their lives and their beautiful babies and babies to come! Thank you for making my life better

and growing up Sproul a little easier and fun! My cousins mentioned here would not be who they are without the wonderful framework that is the Aimee and Wentzel Sproul clan. My greatest memories growing up span from holiday family dinners at my Grandma Sproul's. For years my preferred friends were MY cousins. This is credit to the amazing job my Grandmother, my Aunts and Uncles did, and to the value of family they managed to instill in all THIRTY of us. Grandma, you have led a great clan, and I am so thankful you are in my life, and here to guide us on. I love you!! To my Uncle Paul and Aunt Linda, my Aunt Beverly (Bee), my Uncle Darwin (Dunk) and Aunt Shirley, my Aunt Sharon (lovingly, Aunt Gook), my Uncle Ron (Dink) and Aunt Donna, my Aunt Louella (Nooch), my Aunt Resia and Uncle Dave, my Uncle Marve and my Aunt Sam, my Aunt Pat, and my Aunt Twila and my Uncle Anthony, thank you for being a great family to grow up and make memories in. Part of those wonderful memories was my recently departed Uncle Marion, I will always remember his staunch love, and loyalty to our family and I respect him for his opinions and willingness to share them always. My only maternal Aunt is my Aunt Judy whose love, support and generosity throughout my life is unsurpassed. Judy, thank you for treating us as your surrogate children, for opening your home and heart to us continually for being a great roommate for the first 3 years of my graduate career. I love you very much! My Grandfather Henry and his wife Lucille have been a pillar of prayer support in my life over the past sixteen years. Thank You both for your love, and your commitment to faith, family and each other. My family members are the friends and fabric of my childhood, they helped define me, continue to root me, and where ever they are, is a place I feel at home. I love you all!

"Aerodynamically the bumblebee shouldn't be able to fly, but the bumblebee doesn't know that so it goes on flying anyway." - Mary Kay Ash

My thesis work was completed in the laboratory of Susan Gilbert. Susan's support and direction has enabled the discoveries described herein and her lab was the place where I grew so much scientifically, spiritually, and humanly. For the scientific lessons, the examples of mentoring and human interactions, I am forever grateful and indebted to Susan. The past five years have been incredible on so many unexpected levels, Thank You. I have learned more about how to properly mentor students by your

example than I have from anyone else, and these are lessons that I will carry with me forever. The Gilbert Lab has always attracted and contained hardworking, dedicated, happy graduate students, undergraduates, and technicians who have become close friends and adopted family to me. Thank you Susan for bringing us all together! To my oldest lab sibling, Andy Mackey, Thank you for helping to recruit, train and mentor me. I think of you every time I cap a column! It was you who taught me to cap and fly so that one could be sure to make happy hour on a Friday at five! I love you and I am so so thankful that you came in for my defense. It meant the world to have you there! Lisa K... my lab sister, and my only lab sister, my kindred spirit, my mentor, my friend. Thank you for two wonderful years in the Gilbert Lab and here at Pitt. Thank you for teaching me so much about science and life and for sharing your life, your family, your friends, your experiences with me continuously. I love you and appreciate your friendship immensely. Thank you for memories which no one can take from me, of mounting Grateful Dead Cows in San Antonio, of dancing with Pauly Shore, of rotors flying dangerously around our lab, and of running the streets of Center City soaked! I love you and SO look forward to our forever friendship, bound together by commonalities that span science, faith, time, and a kindred spirit, and include an amazing state, Texas! Jared and Troy, my successive lab brothers. The bulk of my time growing up as a scientist was with you two, and for that I am forever thankful and grateful and happy for the time we have had together and of course, our trips to Uncle Sam's, a tradition handed down, but one worn well by we three. Jared, we've been together since core course. Thanks for sitting next to me not just through that, but through so so so much over our tenure as Gilbert Lab graduate students. I can remember talking to you on 9.11.01, and from that experience forward, I hoped we'd be labmates. God blessed me with you as that, and thankfully so, for without your friendship, support, and shared experiences through this, my time here would have been less. Thank you for your example as a scientist, a brother, a friend, and as a husband to your own beautiful wife Lisa. Lisa C, you were always our 3rd Gilbert-Lisa. Thanks for sharing Jared and moments with your precious boys with us. They truly enhanced the past 5 years of my life. I love you all! Troykins, you seem to be my twin separated at birth, though our thermal regulating genes did not split like the others! The

past four years of science, travel, food, wine, births of two Cochrans, lab move, bay sharing, and Steeler mania have kept me sane, and have made me look forward to every day. Thank You for becoming not only a great lab mate, a scientist who challenges and inspires me, but also a friend and a brother whom I will forever stay in touch with, come home to see, and whose children I hope to hold. The past 6 months (wow!) of the Troy and Amy show have been amusing and have kept me laughing throughout the thesis writing. I wish you and Amy the very best. You will always have a place at any table I set, and I will forever be honored to share a glass of wine, PBR, or a bag of fruit snacks with you! I love you! Dave Close, what a marvelous addition you have been to my life, and our lab! Thank you for all your help on the Kar3Vik1 paper, for organizing the lab, and taking over ordering (for this i am forever grateful!!). I will always cherish your gentle spirit especially when I was first getting to know you after the hard days of losing Megan. Your sincere care and concern for humans in touching and encouraging. Thanks for playing the role of 'older sibling' with me as we *tried* to help Troy with the Troy and Amy "show"... as I move on, I leave you the responsibility and the stick with which to beat Troy regularly and often so that he doesn't go too far 'astray.' Thank you for wonderful memories! I must mention before I close out the Gilbert Lab section two final fireballs... the future Dr. Thanh Ha. is the first. Thanh, may your brilliance, enthusiasm, and zeal for life never be quenched by anything. Continue to do good, to love, and to look beyond small minds with small problems to be the change you wish to see in this world. I love you and the impression you left on my heart is large. The second is the soon-to-be Dr. Joseph Kielec. Joe, you are a great friend, an amazing person and someone who got me through the long days without Lisa K by throwing me in the bushes once a week and taking me drinking at Docs! Without you, graduate school at Pitt would have been duller for many. Thanks for sharing your warm light with me so often and so caringly. You too, are a forever friend!

My friends are here.

A couple years I've spent. I found I have a second home.

As I'm blazing down my trail to education,

There's no bliss in ignorance for me.

I stop and stare, a breath of air might slow me down some.

***But that's just fine with me.
Surprise, surprise. I traveled here.
Four hundred miles from where I'm known.
My friends are here.
A couple years I've spent. I found I have a second home.
-O.A.R.***

This journey would not have been as enjoyable or as memorable without the staunch surrounding of my classmates and fellow graduate students. I was privileged to live, for the shortest of times with Megan Lillie Dietz. Megan was two years behind me, but a sweet, inspiring soul that won my heart over instantly. We were close, like scientific cousins, both working on the cytoskeleton, and i loved to spoil Megan. She in turn shared with me her rich and deep love of music and gossip! We had a grand time as roommates after Megan came to live with me. She had broken her leg playing softball and needed to be close to work, which i was. Her zest for her life and her work was such that she wanted to miss as little as possible. Within a week of surgery, Megan was back at work, leg in a cast. Megan died at the start of my fifth year on my bathroom floor of a pulmonary embolism, a result of her leg injury. Megan's death and my inability to save or resuscitate her forever changed my life. Her life and death inspire, encourage and challenge me daily. This body of work is dedicated to her memory as well, as she never had the chance to finish her own.

Heather Lynn Hendrickson, Stephen Peter Hancock, Laura Jane Marinelli, Mary Margaret Braun, you four are indisputably the four friends from my graduate career I'd call first with great or bad news. You were the ones I wanted behind me and by my side during the days Megan died. Thank you for helping me through that. Your friendships, your long talks, your hugs, your smiles, your support through five incredibly short years has made my time here memorable in a wonderous way. THANK YOU. Heather Lynn, it is no secret that we share a similar heart and love of life, people, and learning. It is a privilege to be your friend, to share your space and to walk arm in arm with you on both the good and the hard days. I love you and I look forward to our careers and our friendship blossoming and intertwining as we grow beyond the hallowed walls of Pitt's

BioSci. Stephen and Laura, I am so THRILLED that one of these days I'll be getting the call about your engagement, or sitting down to dinner with you as you tell me! I love the two of you as a couple, and treasure your individual friendships greatly! Laura, Heather, Stephen, Red Meat Mondays/Wednesdays will always form some of my happiest memories, again, Thank you, Thank you. Maggie, what a long road we've traveled since A.J. McMullen, eh? Thank You for being a friend through so much, for great fun on basketball trips, at Clarks concerts and for being a good friend to Jason and I. I love the four of you "Sixth years!" immeasurably. I can't wait to see y'all defend!

There are other classmates as well as those who make up the department who've made these precious moments of my life full. Ceyda Acilan, Craig Scott, and Christine Smith Wright are three classmates and wonderful human beings who have shared many long hours on the scope, over dinner and ice cream, or random lunches, respectively with me. Each of these experiences always entailed sharing life experiences and growing as friends and scientists. I have these times etched as beautiful pieces of life in my mind and on my heart, and without them my time here would have been less fun, less invigorating, and less full. Ceyda, thank you for listening and sharing about life, love, and advisors. I look forward to visiting my Dr. Acilan in Turkey soon! Craigers, Wow. What a whirlwind five years! I love you, and wish the best for you. I think you are going to make an impassioned professor where ever you find that dream job. Dinners/ice cream have meant so much to me, they've been a great break from the craziness that can be graduate school! Thank You! Christine, you've been a pure delight to share graduate school moments with. Thank you for the precious bits and moments of your life that you have shared over the past five years! I am so proud of you and happy for you and your new husband!

One of life's greatest gifts are surprises. I want to mention that I have found wonderful friends and comrades in fellow students John James Jennings Jr. and Dr. James P. Cronin in the last year. You are two wonderful human beings whose progress I look forward to tracking!

That brings me to Mick Yoder, Mick, you've been a wonderful friend, confidant and adopted lab brother over the past 5 years. I admire your tenacity, loyalty, and giant

heart. It has been an honor to stand next to you at some of the most terrible moments of our lives, and comfort each other. I will forever have a special place in my heart for the future Dr. Mick Yoder and a hug awaiting his arrivals back into my presence. I love you Micholas!

The faculty that comprise the Biological Sciences at Pitt are formed from some of the very best and brightest faculty and scientists one could hope for. My inspiration as a future scientist has come from watching the absolutely gorgeous science and mentoring that has come from the advising of professors Dr. Graham Hatfull, Dr. Jefferey Lawrence, Dr. Paula Grabowski, Dr. Rick Relyea, and Dr. William Saunders. These four scientists ascribe to a high standard of both science and human interaction. Observing the five of these tenured greats has instilled in me hope and aspirations for becoming a scientist of similar standards in the future.

My hopes and dreams lie not only in becoming a great scientist, but a great mother, lady, and woman at that. Two women in the Biological Sciences at Pitt have touched me and encouraged me 100% along the way. These great ladies are Pat Dean always a loving guide, and Mrs. Christine Glaude Relyea, a pearl among otherwise empty oyster shells. These two have that quiet and gentle spirit of true ladies. I hope one day to be so cloaked. Thank you to both of you for your friendship, encouragement, love and support over the years. You two are amazing friends and examples! I shall carry with me your memories and your life examples as my guides. Christine, it was such a privilege to hold and spoil and hug your little girl as she grew. Thank you for the chance to be a part of Isabelle's life. I shall forever appreciate it.

"A friend may well be reckoned the masterpiece of nature."

-Ralph Waldo Emerson

When I began graduate school, I began with a gaggle of friends so dear, so replete, so wonderous, I was convinced I was fulfilled as far as friends went. I was blessed by God with Karen, Laura, Liza, Marci, and Carey Lynn as my college 'roommates'... the six of us had the time and ruled the Carlow College Campus! We were a force unbreakable and a lot to be reckoned with. These girls were part of the courage that I had as I undertook this long and arduous journey, and without them, none of this would be, would be fun, or would have as much meaning. Ladies, I love

you! Karen, you have never lost touch, or gone more than 3 months without hugging me. I love you for that, and appreciate you being there for me so much since Carlow. You define the essence of a true best friend and I hope my life is a lovely mirror of what strong bonds lie between us. My mentor at Carlow was Dr. Rick Hershberger, and I owe tremendous amounts of my current successes to his guidance, belief and support. Thanks Dicky H!!

In addition, I must mention Christopher Lyle Kerby, Gina Marie Kerby, Judy Read, Jennifer Kelley, Ted Wilson, and Kylie Westfall. These 6 were my best friends from 1995 on. They still occupy huge heart space. Without the unconditional support and love of these dear precious ones, life would have been less lived for me. I love, value, and long for the 6 of you often and for us to be sitting on the floor, pleasantly over some Yuengling in a cabin in Killbuck, in a kitchen with a moveable island. How I miss those long gone days!

Chris, you taught and still teach me the lesson of true, pure friendship. Dating you was a life experience I'll always cherish. It is your friendship pre, during, and post our dating that amazes and centers me. You are a true gift to me. I don't know where I'd be without you, and somehow, where ever I go, I know that your light, example, and i pray your friendship, will guide me. I love you so much.

None of the aforementioned folks would have colored my world had it not been for amazing UCG summer camps. For running and organizing these beautifully, I must thank Mr. and Mrs. McNeely, Mr. and Mrs. Dobson, Mr. and Mrs. Mark Winner, Mr. Paul Suckling, Mr. Fred Kellers, and Mr. and Mrs. Doug Johnson. Some of my life's most poignant moments have happened on the parade grounds in Farmington, PA and as the fog lifted in Blount County, AL. Out of these camp experiences grew friendships and extensions of friendships that i cherish and revel in daily and five of those MUST be mentioned here... Heidi, Tarah, Rich, Gregg, and Matthew, so much of us flows through each other, I see us as forever intertwined. I love you each so much. My greatest goes with you and my greatest moments, I hope, reflect each of you.

To Mrs. Patronas, Jerry McClurg and Shawn Moon, I take with me a piece of you as I walk forward every day and I am forever changed by your presence in my life.

"Sometimes our light goes out but is blown into flame by another human being. Each of us owes deepest thanks to those who have rekindled this light."

-Albert Schweitzer

Finally, I come to my Jason Todd. You've definitely been my best friend these past 3 years. Thank You for teaching me to be a better scientist, for standing next to me through really hard days, for crying for me a time or two when I couldn't, and when faced with something really hard, for backing me 100%, and NEVER leaving me. The weekends you allowed me to play scientifically with you at PLE have forever changed my life and made my graduate school career bearable. I have loved every minute of every day with you. Nothing makes me smile like you and nothing in the world can back me better than you. Thank you for touching and changing my life forever. I hope to live my life to do the same for you. I love you! Hovermans, Korey, Bob (Madia, I know!), Teresa, Roan, Dillon, Cody, Barbara and Gary... your support of Jason and I has been soul touching and magnificent! Thank You!

I shall close this section by stating that I have had a very rich and fulfilling career as a human and as a graduate student. I look forward to the next stages of my life with great anticipation based on the amazing life I have lived to this point. So many people have been a part of that. I am grateful to them all for their love, friendships, prayers, concern and light in my life.

1.0 INTRODUCTION

1.1 THE COMPLEX EUKARYOTIC CELL

Eukaryotic cells depend on intracellular transport, temporal delivery of cargoes and spatial organization for survival. Cytoskeletal filaments and their associated protein partners have enabled the cell to achieve these tasks. Cytoskeletal motors bound to filamentous actin (F-actin) or microtubules participate in virtually every cell biological process. They are involved in building and maintaining the mitotic spindle, faithfully segregating chromosomes in mitosis and meiosis, ensuring cytokinesis, transporting organelles, localizing cytoplasmic mRNAs, membrane trafficking, cellular locomotion, and neuronal transport (reviewed in [1-6]). Cytoskeletal motors, also interact with the filaments to establish, maintain, rearrange, modify and regulate the cytoskeleton to accomplish cell functions [7-22]. The cytoskeletal motor superfamilies are the myosins, kinesins, and dyneins [23-25]. The motors share the ability to convert the chemical energy from hydrolysis of the substrate ATP to ADP·Pi to perform work in the cell [1, 26-28].

Myosins bind to F-actin while the kinesins and dyneins are both microtubule-based. The roles of the cytoskeleton and their associated motors in cell division and many other crucial cell events has made them valuable targets for cancer therapeutic drugs [29-31]. This interest, combined with the present ability to perform rapid genetic and molecular biological screens, has sustained discovery of myosins, kinesins and dyneins in eukaryotes for over two decades [23-25]. The focus here is on the kinesin superfamily (Figure 1- www.proweb.org/kinesin). The kinesin motor proteins are essential to all eukaryotic cells and play roles in unidirectional microtubule transport and regulation of microtubule dynamics. Although much information has been gained from

early studies of kinesins and their interactions with microtubules, it is evident that due to the diversity of the kinesin superfamily and their specific functions *in vivo* (Figure 1), kinesin discovery has only just begun.

1.2 MICROTUBULES, DYNAMIC SUPERHIGHWAYS

Microtubules are long polymers that serve as superhighways for structure and function, including intracellular transport [5, 32-34]. Microtubules are not static tracks. When one considers the changing cellular landscape, it is evident that microtubules must be continuously remodeled for cell function. Imaging of living cells shows microtubule plus ends rapidly probing the cytoplasm undergoing rapid growth and shrinkage [35]. Microtubule dynamic instability persists until the microtubules are stabilized or bound to a specific target, like the kinetochore in mitosis [36-40]. Such dynamic behavior [41], which is regulated by microtubule binding proteins *in vivo* can also be seen in solutions of purified microtubules, suggesting the behavior is intrinsic to the tubulin itself [42]. This phenomenon is referred to as dynamic instability [42-45]. Microtubules undergo these cycles of growing (rescue) and shrinking (catastrophe) by the polymerization and depolymerization of $\alpha\beta$ -tubulin [45-48]. These processes are important for microtubule spatial organization and for their ability to generate the forces necessary for cellular function (reviewed in [49, 50]).

Dimers of $\alpha\beta$ -tubulin polymerize in a head-to-tail manner forming linear protofilaments. Approximately 13 protofilaments interact laterally to produce a polarized cylinder, the microtubule, of nearly 25 nm in diameter, and several microns in length (Figure 2) [46-48, 51-53]. Microtubules have a faster growing plus end and a slower growing minus end that is anchored at the microtubule-organizing center (centrosome/spindle pole body) in the cell. Several *in vitro* experiments show that dynamic instability is dependent on the nucleotide, GTP or GDP, that is bound at the nucleotide exchangeable site, or E site, of β -tubulin (reviewed in [32, 48, 49, 51, 52, 54]). Initial kinetic/thermodynamic studies showed that GTP bound β -tubulin exhibits a

high affinity for the growing microtubule, while GDP bound tubulin has a low affinity for the polymerizing microtubule (reviewed in [49]). Further evidence for GTP-tubulin promoting microtubule growth was the fact that GDP added to a soluble tubulin solution failed to polymerize any microtubules, yet once GTP was added, microtubule assembly occurred (reviewed in [49]). This led to the hypothesis that GTP-tubulin promoted microtubule growth, whereas GTP hydrolysis to GDP by all subunits in a polymer could not support microtubule stabilization, and shrinking of the microtubule occurred (reviewed in [49]). An observed kinetic lag between microtubule polymerization and GTP hydrolysis could generate a build up of GTP tubulin subunits at the end of the growing polymer, creating a “GTP cap [55]”. When the GTP cap is lost at the growing end because of GTP hydrolysis, catastrophe ensues. While no definitive evidence for or against such a cap exists, experiments performed *in vitro* using GMPCPP (a slowly-hydrolysable GTP analog) provide support for this hypothesis [56]. Early reports showed that tubulin polymerized with GMPCPP produces extremely stable, straight microtubules that do not display dynamic instability. If severed in the center, these microtubules do not undergo catastrophe, like GTP polymerized microtubules do [55, 57].

Recent cryo-electron microscopy of growing and shrinking microtubules offers a mechanistic view based on structures solved with both GDP and GMPCPP tubulin that complements the GTP cap hypothesis. When microtubules depolymerize, the protofilaments curve outward at the ends (reviewed in [58]) (see Figure 6). In the presence of certain microtubule binding proteins, or divalent cations, these protofilaments bend back on themselves and form stable GDP tubulin rings as they dissociate from the microtubule [14, 58, 59]. It was proposed that GTP hydrolysis destabilized the microtubule by promoting outward curving to facilitate dynamic instability. It was unknown how GTP hydrolysis was coupled to protofilament curvature. The Nogales lab found conditions where they could polymerize short GDP protofilaments that form stable, one turn helices formed by two laterally interacting protofilaments [48, 60]. The experiments provided the first view of the lateral interactions of GDP tubulin not bound by proteins or tubulin binding compounds. They compared the structures of these GDP protofilaments with that of the microtubule

structure formed using Taxol [33]. This comparison showed the GDP protofilaments to be significantly bent at both the inter- and intra-dimer contacts making the protofilaments curve outward, distinct from the contacts observed for the dimers in the microtubule lattice. In the microtubule polymer, tubulin subunits also have GDP bound, thus the tendency would be for the protofilaments to curl outward. However, lateral contacts within the lattice force a straight conformation. GMPcPP-bound tubulin protofilaments also display slight curvature outward, when polymerized at 4 °C, though to a much lesser extent than the GDP-tubulin helices. When the temperature is returned to room temperature or temperatures normal for tubulin polymerization, these helices unwind and associate into straight microtubules, showing that GTP hydrolysis is not required for the zipping of the microtubule together [60]. These results suggest that GTP-protofilaments interact laterally initially and then add onto the growing ends of microtubules. Importantly, the Nogales study showed that unconstrained lateral GDP-tubulin interaction is incompatible with the canonical straight protofilaments observed in the microtubule [48, 58, 60]. The microtubule utilizes the energy stored in GTP-bound tubulin as it polymerizes onto the end of a microtubule, in the form of mechanical strain to keep the microtubule straight and the protofilaments together. Depolymerization of the plus end, either actively (by a microtubule destabilizing protein), or intrinsically (all β -tubulin hydrolyzing GTP to GDP at the microtubule end) releases this strain, the protofilaments dissociate, curl outward, and catastrophe follows (reviewed in [48, 58]). With this study, the Nogales lab has provided more evidence that GTP-bound protofilaments must be at the growing microtubule plus end to maintain the polymer growth. These results add to the data showing the GTP-microtubule lattice (plus end) to be structurally and energetically different from the GDP-microtubule lattice [58, 61, 62], which likely has meaning for microtubule dynamics *in vivo*.

The cell has a battery of stabilizers and destabilizers to regulate microtubule dynamics. Classic regulators, such as microtubule-associated proteins (MAPs) including MAP1, MAP2, and tau have been long characterized, while newly discovered regulators such as microtubule plus end binding proteins, or tip-tracking proteins have been identified [63-69]. Some of the tip-tracking proteins are transported to the plus end by kinesin motors. Others appear to skate along the microtubule via electrostatic

interactions, yet for others the mechanism of targeting the plus end is unknown. One hypothesis to explain the tip-tracking protein localization is that the proteins associate with GTP-protofilament structures and are thus targeted to the growing end. Though the plus ends of microtubules may contain GTP *in vivo*, protofilament destabilization by motor proteins or other MAPs suggests a mechanism for inducing catastrophe. Future characterization of proteins found at microtubule plus ends and their interactions with different tubulin lattices will better define *in vivo* microtubule regulation.

1.3 KINESINS

Kinesin motor proteins were first discovered late in the twentieth century as MAP-like proteins that bore vesicles down the axon to the synapse in neurons [70-73]. These nanomachines were able to efficiently transport vesicles traversing long distances without falling off the microtubule [73, 74]. Biochemical and genetic probing of these first kinesins found them to be enzymes similar to myosins. They have a homologous catalytic core, structurally similar to myosin, but kinesin proved to be functionally distinct [75-78]. Kinesin is the smallest of the molecular motors with ~ 350 amino acids comprising the motor domain [78], (myosin is ~ 850 residues [79-81] and dynein is ~ 1000 residues [25]). However, kinesins form a large and diverse family, which is grouped into fourteen subfamilies plus an undefined orphan kinesin group. The classifications are based on conserved family-specific sequences within the homologous motor domains, directionality, oligomeric state and *in vivo* function [24] (Figure 1). The orphan kinesins have unique characteristics or functions that have limited their classification thus far.

Since the discovery of conventional kinesin more than 450 kinesins have been added to the growing kinesin database [6]. The kinesins can be broadly grouped into three categories, KinN, KinI and KinC kinesins, dependent upon where in the polypeptide sequence the catalytic motor domain can be found [6, 24]. It was observed that kinesins having an N-terminal motor domain, KinN kinesins, glide toward the faster growing microtubule plus end, while the KinC motors differ, they glide or motor to the

less dynamic microtubule minus end [82]. Kinesins possessing an internal motor domain, KinI kinesins, do not motor or glide. Instead they diffuse along the microtubule lattice in either direction and bind to both of the microtubule ends [83]. These different directionalities and modes of microtubule travel allow kinesins to play diverse roles in nearly every cellular event examined. Every role that kinesins fulfill results from the energy transmitted through the molecule upon ATP hydrolysis coupled to interaction with the microtubule lattice. Understanding how this family of motor proteins hydrolyzes the same nucleotide to accomplish such a diversity of functions is of great interest.

Conventional kinesin is N-terminal and is classified as Kinesin-1. Kinesin-1 is a heterotetramer containing two heavy chains that contain microtubule binding catalytic motor domains at the N-terminus which dimerize through a C-terminal coiled-coil stalk [78, 84-90]. In conventional kinesin, the dimeric heavy chains associate with two light chains at the C-terminus where these light chains act as binding sites for kinesin adaptors or cargo, such as axoplasmic vesicles. Subsequent kinesin discovery showed that not all kinesins are cargo carrying, or have light chains that associate as cargo binding domains. In addition, the oligomeric states of the different kinesins vary. Kinesin motors have been found to perform functions as monomeric, dimeric, trimeric and tetrameric motor proteins. Two decades of elegant biochemical, fluorescence and single molecule studies have dissected the mechanism of how conventional Kinesin-1 coordinates ATP turnover on the microtubule with translocation along the polymer for very long run lengths in the cell.

Conventional kinesin walks hand-over-hand along the microtubule (Figure 3) ([91-93] reviewed in [94]). Studies show that in solution kinesin has MgADP bound at the active site, and many kinesins are crystallized in this manner [78, 95-99]. Upon binding to the microtubule at a β -tubulin site with one motor 'head', kinesin releases its ADP, and ATP rapidly binds to the active site [100-104]. This induces conformational changes on the first, attached head [104-113]. One of the changes is neck linker docking, which causes kinesin to propel the second motor head forward onto the microtubule. ATP is hydrolyzed on the first head [75, 76, 100, 105, 114-116]. The second head binds tightly to a β -tubulin site, 16 nm away from the β -tubulin site bound by head number one. The ATP hydrolysis on the first head causes the second head to

bind tightly to the microtubule, releasing its ADP and introducing tension between the two heads [117-120]. This strain prevents ATP binding to the second head [118, 120], allowing the first head to release the hydrolyzed γ -phosphate as Pi which is followed by detachment [120]. Detachment releases the tension between the heads and allows for ATP to rapidly bind to the second forward head to restart the cycle so that kinesin can take another step [118, 120]. These in-depth biochemical studies, combined with single molecule work, has shown that for each ATP hydrolyzed conventional kinesin moves approximately 8 nm, while each individual head steps 16 nm ([91, 93, 94]). This is diagrammed in Figure 3, adapted from [120].

The unique kinesin structure allows ATP turnover and microtubule interaction to be coupled. N-terminal human Kinesin-1, kinesin heavy chain motor domain (KHC), and a characterized C-terminal kinesin, *Drosophila* Ncd motor domain, were the first kinesin structures solved. The two structures began to give insight to the coupling of nucleotide turnover to microtubule interaction. Kinesin was shown to have an arrowhead-like appearance (Figure 4A & a) with two very different sides. One side is negatively charged near the nucleotide binding pocket (4A), and one is positively charged, hypothesized to be the microtubule binding face (4a, microtubule binding residues are colored in green), providing preliminary clues as to the interaction domain of kinesins with the microtubule [78, 121]. A major difference between the N- and C-terminal kinesins was found in the sequence directly C- or N-terminal to the KHC or Ncd motor domain. The sequence was class specific, and was shown through elegant biochemical experiments to be the defining factor for directionality along the microtubule [122-124]. However, this left the mechanism of the kinesin microtubule interaction ambiguous. Subsequent biochemical studies using site-directed mutagenesis and electron microscopy reconstructions confirmed the microtubule-binding interface to involve β 5a-Loop 8- β 5b, Loop 11 (arrowheads Figure 4), α 4-Loop 12- α 5, and α 6 [125-140] (Figure 4, green).

As more kinesin crystal structures were solved, it became clear that these residues differ subtly between the crystal structures (Figure 4a, b-f, residues in green) (reviewed in [140-142]). The diversity of functions (from walking along microtubules, to destabilizing or stabilizing the microtubules) the kinesin superfamily performs is linked to

the nature of the specific microtubule•kinesin interface, and thus differences located at this site are of importance. The structure showing the most variation is Loop 11 [141]. Loop 11 differs in length and composition among the plus end directed, minus end directed, and canonical destabilizing kinesins, contrast KHC (elongated, C), Kar3-R298A (shorter, F) and pKinI (shortest, E) in Figure 4. Loop 11 plays a crucial role in how these kinesins specifically interface with the microtubule [135, 140, 141]. In most kinesin crystal structures Loop 11 is disordered, and assumed to become ordered upon microtubule association [140, 142]. In the crystal structures presented in Figure 4, Loop 11 is modeled in for KHC (C, c) [78], and is ordered in the Kar3 R598A mutant (F, f) [143] and the pKinI kinesin crystal (E, e) [98]. In the Kar3 [96] (D,d) and Ncd (B,b) [95] motor domains, the majority of Loop 11 is missing.

Loop 11 is of importance because it contains the conserved Switch II motif (N3 motif in other ATPases or G-proteins) made up of the canonical DXX**G**XE found in all kinesins, myosins and G-protein superfamily members [28, 140, 142, 144-146]. The **G**lycine, is conserved in all Switch II motifs and interacts with the γ -phosphate of the nucleotide at the active site, the Switch II motif moves in response to the release of the γ -phosphate as inorganic phosphate (Pi) following nucleotide hydrolysis [28, 140, 142, 144-147]. The disordered state of Loop 11 in the crystal structures is indicative of the flexibility it retains to interact with, and move dependent upon, the nucleotide bound at the active site. Loop 11 connects the Switch II kinesin motif to the Switch II cluster [28, 140, 142, 144-147]. The Switch II motif is DLAG**S**E, conserved in KHC, Ncd, Kar3, and pKinI (all shown in Figure 4) [142, 143]. The Switch II cluster that is made up of α 4-Loop 12- α 5 interfaces directly with the microtubule. Movement by the Switch II motif is amplified through Loop 11 to the Switch II cluster, communicating between the active site and the kinesin-microtubule interface (reviewed in [140, 142]).

Loop 11 also mediates kinesin binding to the microtubule in the protofilament groove [96, 98, 135, 141, 147], acting as one of the two 'arms' that help bind kinesin to the microtubule, based on cryo-electron microscopy reconstructions [135, 146, 147]. The C-termini of α 4 and α 5 lie close to the docked neck linker in the crystal structure of rat kinesin-1 (reviewed in [140]), suggesting Loop 11 may also signal to the neck linker, which reorients based upon the nucleotide found at the active site. The length and

positioning of Loop 11 is likely to modulate the amplification of intra-molecular structural transitions and thus dictate how the specific kinesin then interacts with the microtubule [135, 140, 146, 147]. One study argues that the binding of Loop 11 to the microtubule is the tight binding state, important for processivity [146]. The elongated Loop 11 of conventional kinesin is proposed to enable kinesin to glide processively down the microtubule preventing motor binding too deeply into the protofilament groove, while the shorter Loop 11s are thought to allow the kinesin motor domains to bind closer to the protofilament groove [96, 146]. The deeper protofilament groove binding affects the motility and the way in which kinesins interface with the microtubule. Such binding may disturb the lateral contacts of the protofilaments, leading to microtubule destabilization caused by unzipped protofilament curling [96].

Mutations in Loop 11 of Kar3 have been shown to decouple the microtubule-stimulated ATPase and weaken the affinity of the motor for the microtubule [143]. Another mutation in the Switch I region, **SSRHSX** (conserved in kinesins, myosins and G-proteins superfamily members, also involved in nucleotide sensing of the γ -phosphate) of Kar3 designated R598A, which normally forms a salt bridge with Switch II (DLAGS**E**631 in Kar3), causes Loop 11 to become ordered in the absence of the salt bridge in the crystal (Figure 4F,f). The salt bridge forms between the Arginine (**R**) and the Glutamate (**E**) of Switches I & II, respectively. The Kar3 R598A mutation binds very weakly to microtubules and has no microtubule-stimulated ATPase activity [143]. These studies collectively provide the evidence of communication between the active site and microtubule interface coordinated through Loop 11. The many differences in this structure affect function and suggest that the variation found here will specify the communication that each kinesin has with the microtubule, such that each kinesin-microtubule interaction will be uniquely coupled to its ATPase. As more kinesins are found and crystallized, the importance of this structure will be assessed.

While a detailed and thorough analysis of conventional kinesin stepping coordinated to ATP turnover has dominated the last twenty years, less is known about how unconventional kinesins couple their ATPase to very different microtubule interactions [148]. The push to understand the different interactions kinesins have with

the microtubule partner has been intensified by the ability to specifically inhibit kinesins and block events like cell division [149, 150].

1.4 KINESIN-13, CANONICAL MICROTUBULE DESTABILIZERS

It is not unexpected that the large diverse family of kinesin contains microtubule motors that participate in regulating microtubule dynamics. The canonical microtubule destabilizers are the Kinls, or the Kinesin-13s [9, 14, 18, 19, 66, 68, 151-153]. Kinesin-13s or MCAK (*mitotic centromere associated kinesin*, the founding member [151]) was shown to associate with the ends of microtubules *in vitro*, specifically the curled protofilament peels at the plus ends of microtubules [20, 59, 66, 98, 154-157]. MCAK accelerates the rate of microtubule catastrophe, even in the absence of ATP, if the tubulin-to-motor ratio is high enough [14, 154, 156]. MCAK has been shown to target to the microtubule ends by one dimensional diffusion, where it binds to the ends, inducing protofilament curling [14, 19, 59, 66, 152, 154, 156] (Figure 6). The protofilament peeling then induces rapid depolymerization or catastrophe of the microtubule [44, 158, 159]. Depolymerization of the microtubule in the presence of MCAK proceeds with sigmoid kinetics [156] and induces catastrophe.

It has not been shown definitively that MCAK is a processive depolymerase [83]. MCAK has been shown to release with tubulin as it is peeled from the rings of depolymerizing microtubules (Figure 6), and the ATPase is thought to be important for releasing it from the tubulin [14, 19, 59, 66, 68, 83, 156]. MCAK is unique in that its ATPase is stimulated by both the microtubule polymer and soluble tubulin [19, 59, 66, 68, 83, 99, 155, 156, 160, 161]. MCAK also differs in the microtubule binding region, as determined from both mutagenesis studies and from the crystal structures [59, 98, 99, 155, 162, 163] (Figure 4E, e, arrow, and arrowhead). The arrow points out Loop 2, which in MCAK is thought to bind to the intra-dimer face of $\alpha\beta$ -tubulin. Loop 2 contains three class specific residues, KVD, that have been shown to be important for MCAK microtubule depolymerizing activity [98, 99]. The Loop 2 is not colored green, as it does not bind the microtubule in the other four kinesins. Combined with a very different

microtubule binding interface, MCAK exhibits an extremely short and very ordered Loop 11 stabilized by family-conserved residues [98, 99]. As discussed above, the very short “arm” formed by Loop 11 in the Kinesin-13 structure may alter binding to the very straight microtubule lattice, promoting diffusion, such that binding to the split ends of the microtubule is more favorable. Both mutational and structural studies provide evidence for this atypical binding. Evidence for this hypothesis is given from the Ogawa *et al* crystal structure of Kif2C, another Kinesin-13 whose crystal structure is docked onto the curved conformation of tubulin [99]. Here the Loop2, Loop8, Loop 11- α 4-Loop 12- α 5 microtubule interface fits better onto the curved tubulin subunit reconstruction than it does onto the straighter microtubule lattice [99].

Kinesin-13s are responsible for regulating microtubule length during both mitosis and in interphase in most eukaryotes (reviewed in [68, 153]). No Kinesin-13s exist in yeast, where microtubule dynamics are governed by Kip3, a Kinesin-8 during mitosis [164] and Kar3, a Kinesin-14 during karyogamy [164-168]. To understand the role of different kinesins in microtubule depolymerization, comparative studies between these different classes is needed.

1.5 KAR3, A KINESIN-14

Saccharomyces cerevisiae, or budding yeast kinesin Kar3 was discovered in 1990 in a genetic screen for mutations in genes that blocked the mating event in yeast referred to as karyogamy (nuclear fusion - see Figure 8) [169]. The deletion of Kar3 stalls karyogamy at step 5, just after cell fusion, preventing microtubule interaction to promote nuclear fusion (Figure 8) [169]. Kar3 is a C-terminal kinesin, essential for mating and meiosis I [168-172], and important for mitosis and astral microtubule integrity in vegetatively growing yeast [7, 8, 12, 164-168, 170-185].

The *in vivo* localization of Kar3 was shown to be dependent on one of two distinct polypeptides, Cik1 (also essential for karyogamy and meiosis [172, 186-190]) and Vik1 (important for mitosis and vegetative growth [184, 188]) (See Figure 5). If Cik1 were

deleted (*cik1Δ*), and the yeast *cik1Δ* cells were challenged with mating pheromone, karyogamy was again blocked at Step 5, Figure 8. Kar3 became mis-localized throughout the nucleus and was unable to associate with cytoplasmic microtubules (Figure 5B) [187-189]. In vegetatively growing *cik1Δ* cells, mitosis proceeded similar to wild type with increased chromosome segregation defects (Figure 5B) [179, 186-189, 191]. However, if Vik1 were deleted, mitotic chromosomal segregation was normal, but Kar3, normally localized to the spindle pole body (SPB) was absent and Kar3 re-localized onto the spindle microtubules dependent upon Cik1 (Figure 5C) [188]. If both Cik1 and Vik1 were deleted, Kar3 no longer localized to the SPB or the microtubules. Instead, there was diffuse nuclear localization of Kar3 (Figure 5D). These studies showed that Kar3Cik1 and Kar3Vik1 played distinct roles *in vivo*.

These genetic studies suggested that there were specific functional roles for Kar3Cik1 different from those of Kar3Vik1 during the yeast life cycle. Support for this hypothesis came with immunoprecipitation of Kar3 from yeast extract showing that Kar3 immunoprecipitated with either Cik1 or Vik1 [164, 188-190]. Reciprocal immunoprecipitations showed Cik1 or Vik1 co-precipitated with Kar3 [164, 188-190].

In 1994, a Kar3 motor domain with neck linker and N-terminal coil-coil sequence fused to GST was shown to promote minus end directed microtubule gliding, while at the same time shortening microtubules from both ends, with a preference for the minus end, *in vitro* [192, 193]. The combined genetic and biochemical data led to the hypothesis that Kar3 formed heterodimers with either Cik1 or Vik1 *in vivo* for function where it motored to the minus ends of microtubules, and then acted on the minus ends to limit the length of microtubules *in vivo*. Elegant genetic experiments examining Kar3 function during vegetative growth provided further support for this hypothesis [8, 12, 173-175, 177, 179-181, 183, 194].

The crystal structure of Kar3 provided yet more evidence for Kar3 regulating microtubule dynamics. In the Kar3 sequence, Loop 11 is shorter as compared to KHC and Ncd, but longer than the Loop 11 of Kinesin-13, and was hypothesized to allow the motor to bind deep in the protofilament groove, leading to destabilization of the microtubule and promoting shortening [96]. Loop 11 is also disordered in the crystal structure of native Kar3, suggesting that it retains flexibility for interaction with the

microtubule, and may become ordered upon contact with the filament (Figure 4C gray arrow points to missing Loop 11) [96]. Loop 11 is ordered in a Kar3 salt bridge mutant (R598A), showing its intermediate length between that of KHC and Kinesin-13. Interestingly Kar3 is reported to both glide and depolymerize microtubules, which may require an intermediate length Loop 11 to accomplish both. What is unknown is how the complex of Kar3Cik1 and Kar3Vik1 change the Kar3 structure and microtubule binding face, particularly Loop 11.

Recent advances in microscopy and fluorescent probes have allowed better imaging of microtubule dynamics *in vivo* [195]. Maddox et al. have shown that yeast do not exhibit tubulin subunit turnover at microtubule minus ends, with the microtubule dynamics governed predominantly at the microtubule plus-end [196]. Further work from the same laboratory showed that Kar3 is actually found at the shortening microtubule plus ends during karyogamy [165]. Other evidence for Kar3 acting at microtubule plus ends, despite being a minus end directed motor, has been reported [184, 185, 193].

The new reports on microtubule dynamics in yeast reopened dialogue about Kar3 function *in vivo*, especially since the complexes relevant for Kar3 function and localization had never been examined in conjunction with Kar3 *in vitro*. What was unknown was how the heterodimeric complexes of Kar3Cik1 and Kar3Vik1 interacted with the microtubule, and how these two complexes differed, if at all in modulating Kar3 function. This was a crucial missing link in understanding Kar3 function *in vivo*, as genetics had clearly demonstrated that in the absence of either Cik1 or Vik1, Kar3 failed to function [188]. What was needed was a comparison of the *in vitro* microtubule gliding, depolymerizing, and binding properties of the Kar3Cik1 and Kar3Vik1 motors compared to the Kar3 motor domain, a characterized Kinesin-14 family member, such as Ncd [95, 197-202], and the canonical Kinesin-13 destabilizers [9, 14, 18, 19, 66, 68, 151-153].

Our work in examining the Kar3 motor in complex with Cik1 (Chapter Three) [167] and Vik1 (Chapter Five) was designed to understand if the intrinsic biochemical properties of the motors we observed *in vitro* could account for the multiple Kar3 *in vivo* functions reported. This work not only increased understanding about the different roles of Kar3Cik1 and Kar3Vik1 in their specific interactions with the microtubule, it gave

insight into the interactions different kinesin motors can have with their tubulin filament partner through complex formation with non-catalytic polypeptides.

1.6 NOD, AN ORPHAN KINESIN

Drosophila melanogaster Nod, an orphan kinesin [24] was discovered as a gene required for the accurate distributive segregation of non-exchange chromosomes in female meiosis [203]. Distributive segregation in *Drosophila* meiosis refers to the faithful disjunction (separation and segregation) of homologous chromosomes that do not undergo exchange at the metaphase plate (reviewed in [204-215]). Loss-of-function mutants result in non-disjunction, and loss of non-recombining chromosomes from the metaphase plate in meiosis I and in subsequent mitotic divisions [208, 210]. Sequencing the gene revealed it to be similar to conventional kinesin in the N-terminus, but unlike any other kinesin in the C-terminus [208].

Meiotic arrest in *Drosophila* has shown the meiotic spindle to be a long tapered spindle in which the majority of microtubules do not terminate at the poles [213]. Non-exchange homologous chromosomes are seen to orient on the spindle away from the exchanging chromatin mass, both contacted by microtubules in the absence of what seems to be a direct linkage [213]. In the absence of Nod function however, these non-exchange chromosomes are lost and/or exhibit excessive poleward migration [213]. This observation, coupled with microtubule attachment to the chromosomes suggested that in some way Nod may exert an anti-poleward force to maintain the non-exchange chromosomes properly aligned on the metaphase plate, pushing the chromosomes away from the poles, also referred to as a “polar ejection force” [213, 216]. Mutations in both the conserved kinesin-like motor domain and in the unique C-terminus produced the non-disjunction phenotype, suggesting that Nod requires both N- and C-terminal domains to function [217, 218]. It should be noted that mutations affecting the putative nucleotide pocket in Nod produce more severe phenotypes suggesting that the ability to bind and/or hydrolyze ATP is critical for Nod function [217]. It was shown that Nod could in fact bind to chromatin through its C-terminus, and that Nod bound along the

chromosomal arms, providing molecular localization to explain the polar ejection force [219, 220]. The motor domain of Nod was not shown to bind chromatin, but instead localized only to microtubules *in vivo* [220]. These results suggested that in some way the motor domain of Nod through its ATPase and/or microtubule binding abilities provides the anti-poleward force that helps align the non-exchange chromosomes, which do not undergo homologous recombination along the spindle in meiosis. How does Nod do this?

This question remained unanswered at the beginning of our studies described in Chapter Six. As an N-terminal kinesin, Nod was assumed to be plus end directed, as nearly all N-terminal kinesins known to date [6], but it was known that this directionality was not for movement [221]. However, the plus end localization of Nod was called into question based on a report about Nod:KHC fusion proteins that had been visualized *in vivo* on what were presumed to be microtubule minus ends [222]. If Nod were a plus end directed motor how does one account for both the anti-poleward force provided by the motor at the microtubule plus ends near the chromosomes [217, 218], and the minus end microtubule localization (as minus ends are oriented at the poles)? Clues as to how Nod might facilitate an anti-poleward force came from studying a tubulin mutant where chromosome segregation was aberrant [223]. The mutation caused slower microtubule polymerization [223]. It was found that decreasing Nod function concurrent with the tubulin mutation decreased the segregation defect [223]. This observation suggests a role for Nod in regulating microtubule dynamics in some way to produce the anti-poleward force. This microtubule binding was proposed to be transient and not for motor walking, as Nod does not glide microtubules [221]. As has been pointed out above, the microtubule binding region is variable among kinesins, this holds true for Nod as well [221]. The Nod kinesin microtubule binding region differs from all other kinesins, and is the least conserved among the kinesins [221]. While no crystal structure of Nod exists, residues from the Nod microtubule binding domain inserted into conventional kinesin drastically reduced its motility rate [221]. This finding suggests that Nod may interact in a novel way with the microtubule as compared to Kinesin-1s, Kinesin-13s (MCAK) or Kinesin-14s (Kar3). My work in collaboration with Wei Cui from the Scott Hawley lab, examined the specific interactions of both full-length Nod and the

Nod motor domain *in vitro*. We examined the hypothesis that Nod bound to microtubules at the plus end to either stabilize or promote microtubule polymerization. We proposed that Nod would bind to the chromosomes through the C-terminal domain and to the microtubule using its N-terminal domain to provide the polar ejection force by promoting microtubule polymerization at this site, or stabilizing the microtubule plus end from depolymerization to hold the chromosomes on the metaphase plate (diagrammed in Figure 7). I contributed data to all *in vitro* experiments reported examining microtubule•Nod interaction [224]. The genetics presented in Chapter 5 as well as the Nod domain constructs and *in vitro* data were contributed by Wei Cui.

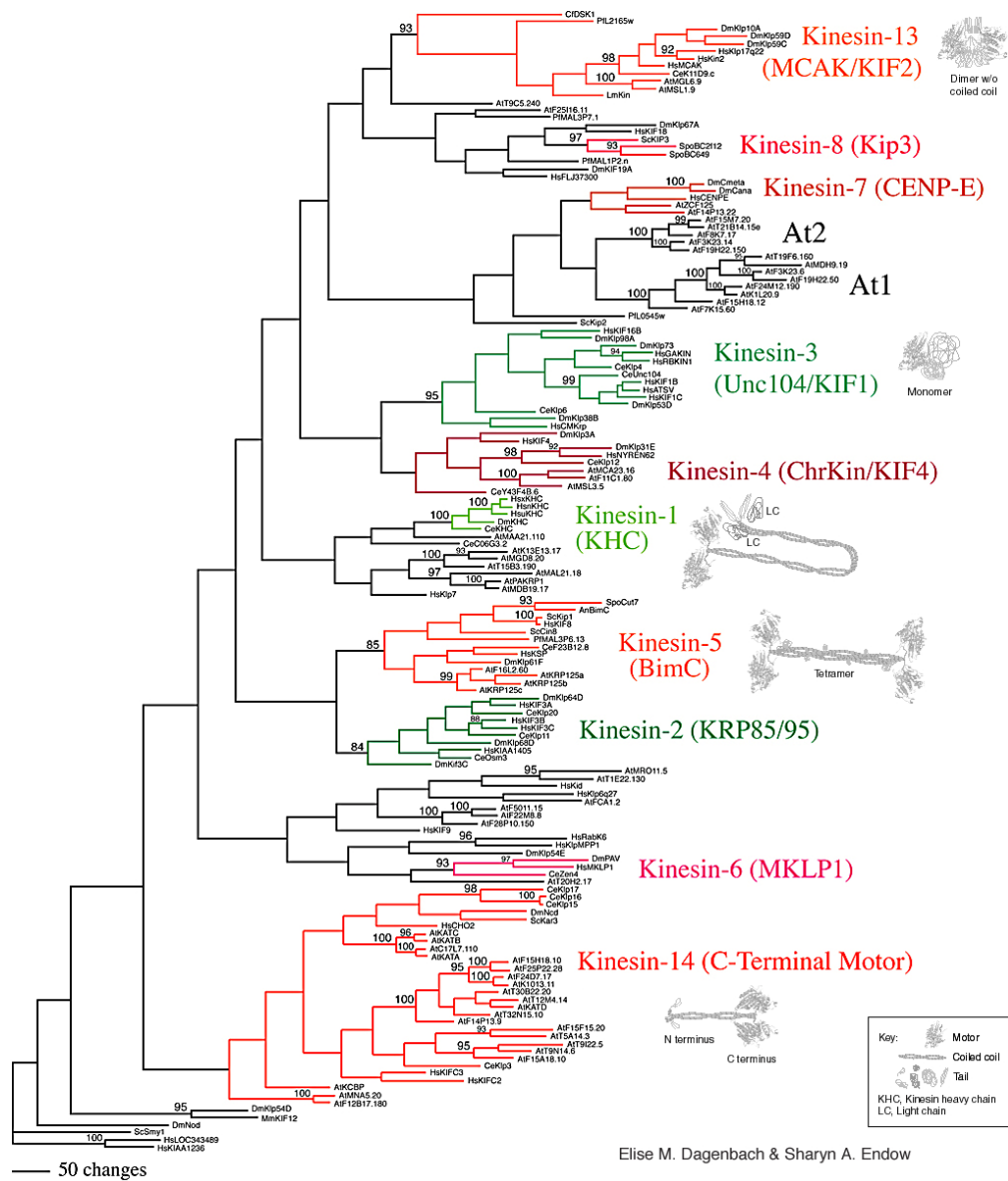


Figure 1. The Classification of the Kinesin Superfamily

1.6.1 Figure 1 Legend

The Diverse Kinesin Superfamily

The Kinesin Superfamily Tree showing the 14 sub-family classifications plus an orphan group yet to be classified (www.proweb.org/kinesin and ref.[24]).

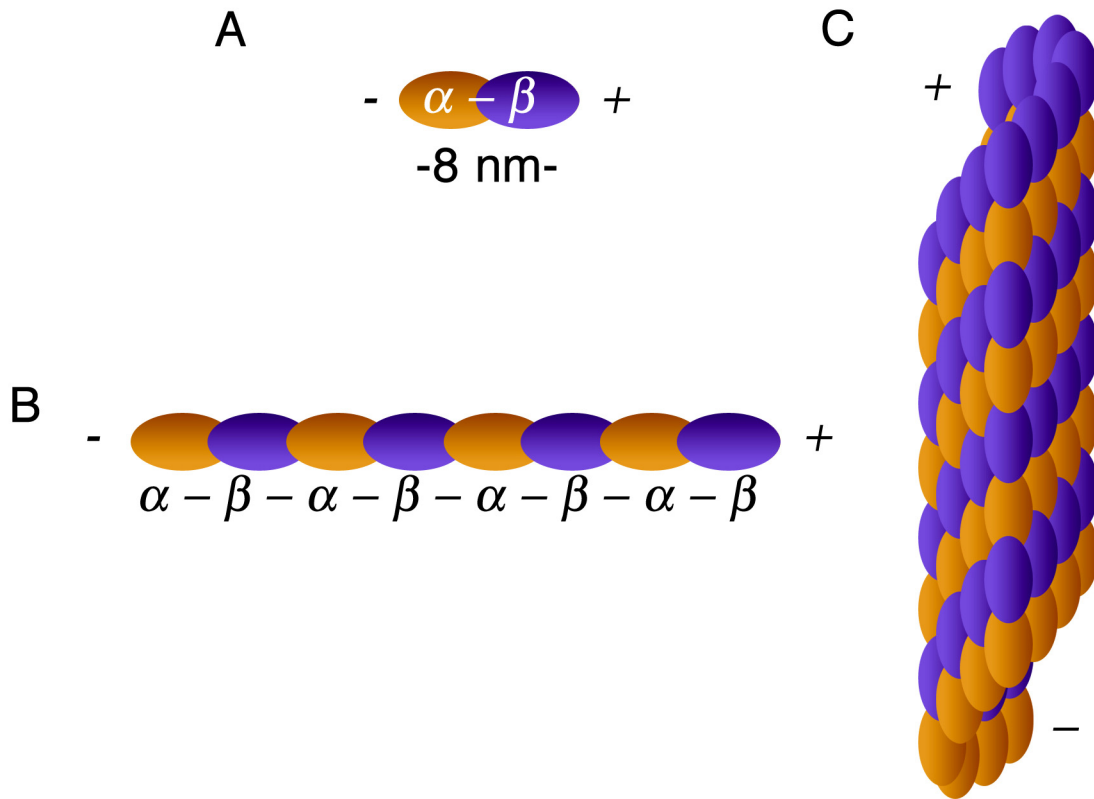


Figure 2. The Stages of Tubulin Polymerization

1.6.2 Figure 2 Legend

Building a Microtubule

The $\alpha\beta$ tubulin heterodimer (A) associates head to tail to form a protofilament (B). Lateral interactions with other protofilaments form the microtubule, a hollow tube comprised of approximately 13 protofilaments, and around 25 nm in diameter [33, 48] (C).

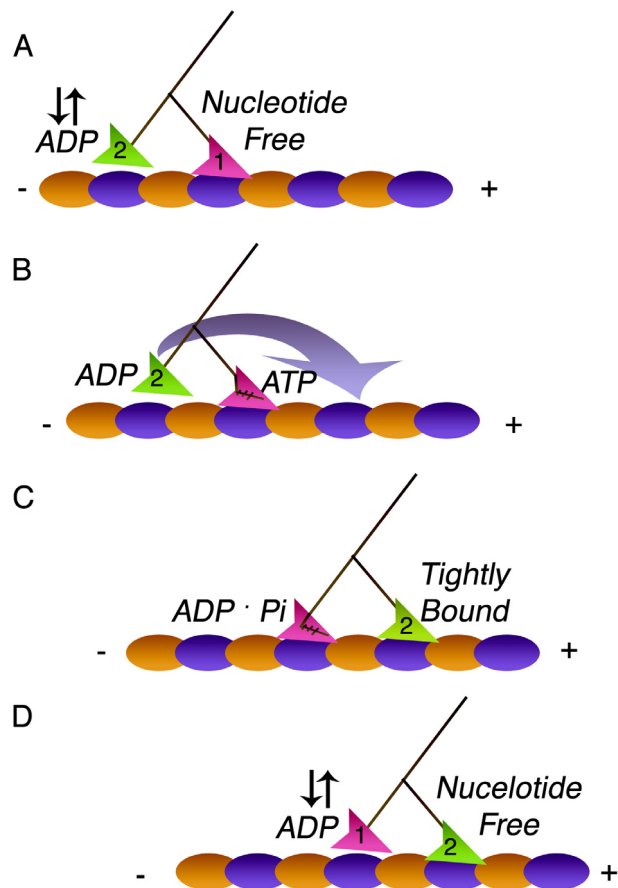


Figure 3. The Hand-Over-Hand Walking Model of Kinesin-1, adapted from ref. [120]

1.6.3 Figure 3 Legend

Kinesin-1 Asymmetric Hand-Over-Hand ATPase Cycle

Conventional kinesin walks hand-over-hand; the heads alternate stepping, coordinated with ATP turnover toward the microtubule plus end [5, 94]. (A) Kinesin binds tightly to the microtubule with rapid ADP release resulting in a nucleotide free Head 1. Head 2 is tethered to the microtubule with ADP at the active site [107, 225, 226]. (B) Head 1 binds ATP inducing a series of structural transitions in the motor [104-113], such that the neck-linker zippers onto the motor domain. Neck-linker docking on Head 1 propels Head 2 to the next microtubule binding site. (C) Hydrolysis on Head 1 causes Head 2 to bind tightly to the microtubule, releasing ADP [117, 119]. Phosphate is released on Head 1, and results in Head 1 detachment from the microtubule as the ADP intermediate [120]. (D) Head 2 awaits ATP binding to repeat the cycle. This coordination ensures that one head of kinesin remains tightly bound to the microtubule at all times, facilitating long run lengths, important for processivity.

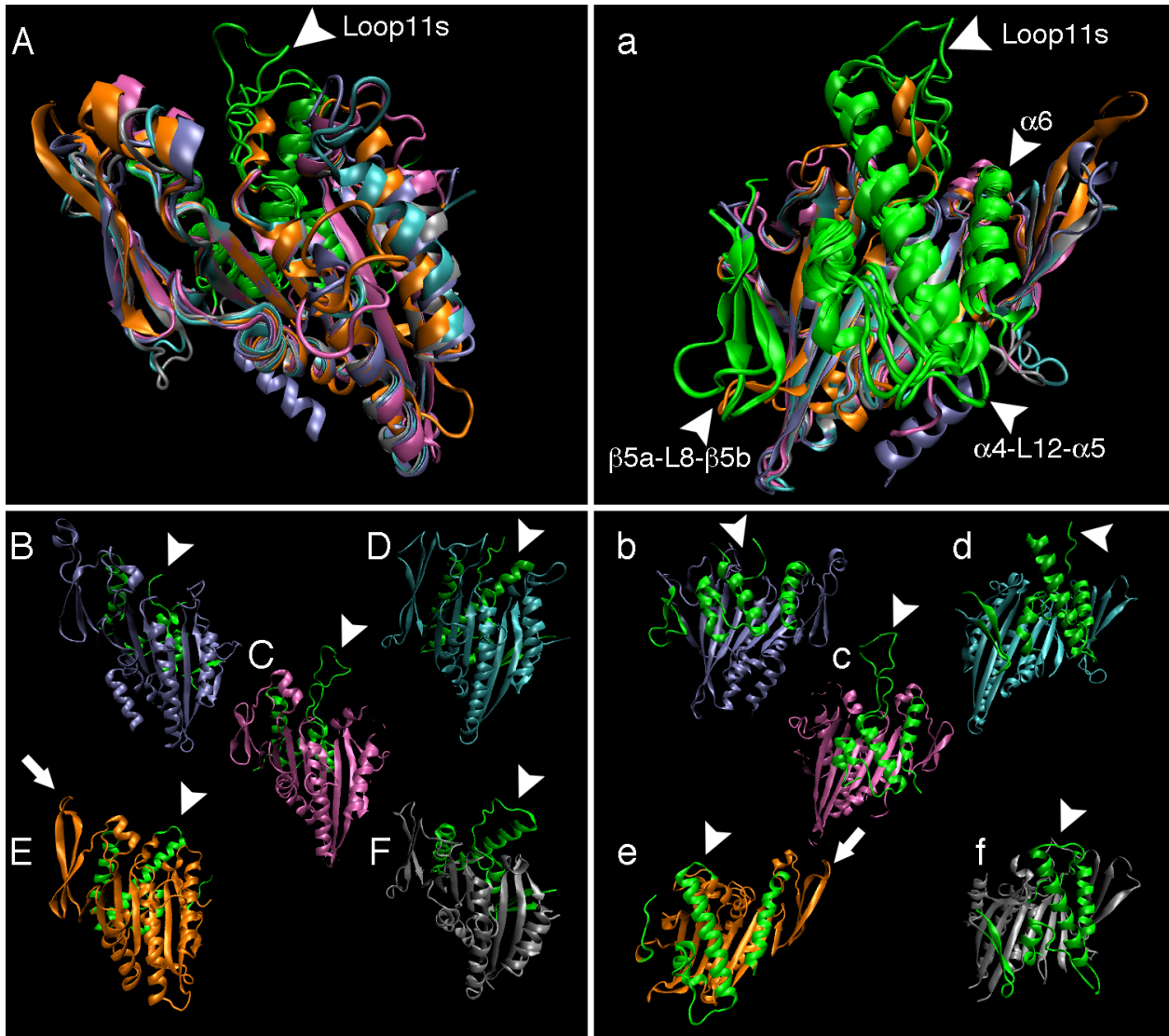


Figure 4. Five Kinesin Structures Show Differences in Loop 11

1.6.4 Figure 4 Legend

The Differences Found on the Kinesin•Microtubule Interface

The crystal structures of Kinesin-14, Ncd (2NCD), conventional Kinesin-1 (KHC) (1BG2), Kinesin-14, Kar3 (3KAR) a Kinesin-13, pKinI (1RY6) and a Kar3 R598A mutant (1F9V) discussed in this work are presented here. The RSCB PDB (www.pdb.org) numbers are in parentheses. The proteins in the left panels represent the nucleotide binding faces of the kinesins, and those on the right, the microtubule binding faces. A, a show overlays of the structures, illustrating the remarkable structural similarity of the nucleotide binding (A) and the microtubule binding faces of the different kinesins (a). The microtubule interacting residues are highlighted in green and labeled. The microtubule binding Loop 11 is the region among kinesin crystals that exhibits the most variability (arrowheads) [141]. The kinesin residues at the microtubule interface are labeled in (a) and include β 5a-Loop 8- β 5b, Loop 11, α 4-Loop 12- α 5, and α 6 [130, 140, 227], and are all highlighted in green in the structures. In most kinesin crystal structures Loop 11 is disordered (ALL arrowheads) [142], and is thought to become ordered upon kinesin binding to the microtubule [142]. For visualization purposes, Loop 11 was modeled in on the conventional kinesin structure (C,c arrowhead) to show where the loop should be, or is missing (arrowheads) in Ncd (B,b, blue) and Kar3 (D,d cyan). Interestingly KinI (E,e orange) displays a very short, very ordered Loop 11 (arrowhead). The Loop 11 residues are Kinesin-13 class-specific and the amino acid sequence of GAVDT is highly conserved [98, 99, 228]. The white arrow points out Loop 2, elongated in Kinesin-13s, containing the Kinesin-13 class-conserved KVD residues crucial to depolymerization. This Loop is hypothesized to bind to the $\alpha\beta$ -tubulin intradimer face and as such facilitate microtubule depolymerization. The mutant Kar3 R598A has an ordered Loop 11 (F,f arrowhead) showing the intermediate Loop 11 length as compared to KHC or KinI. These proteins were obtained from the PDB at www.pdb.org and rendered using VMD software available at the site.

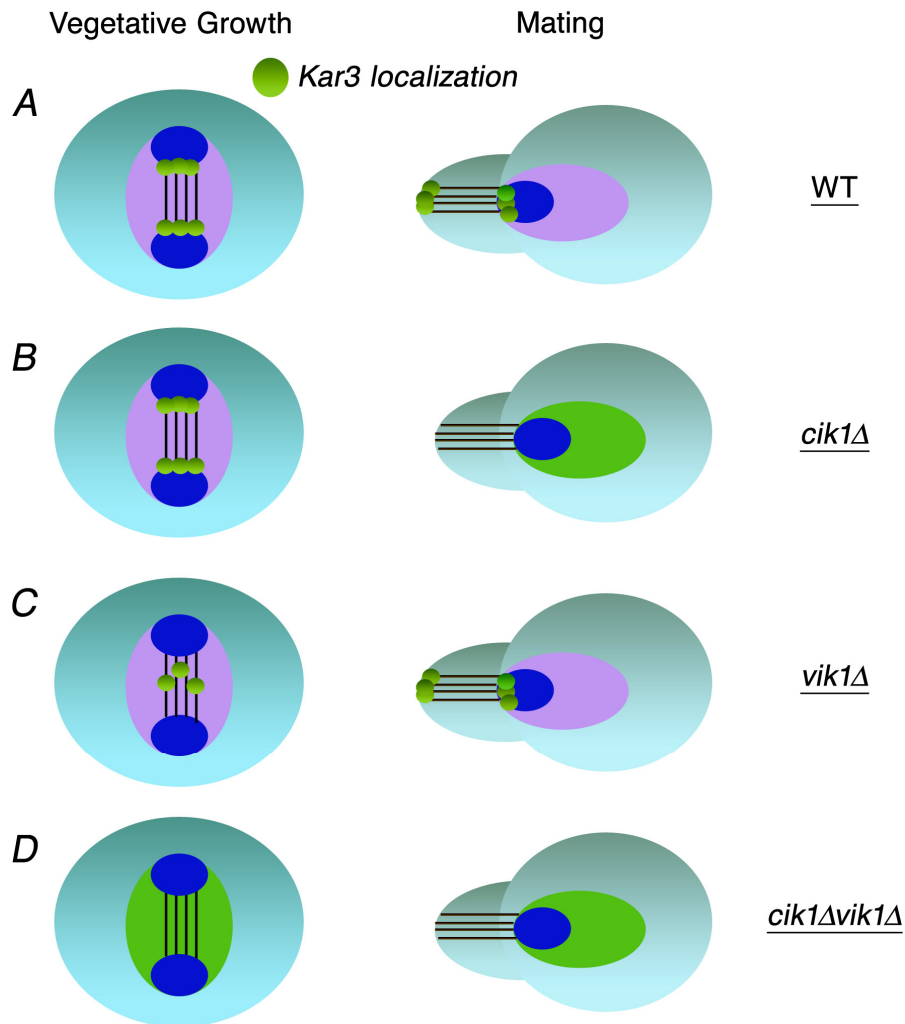


Figure 5. Kar3 Requires Cik1 and Vik1 *in vivo*, adapted from ref. [229]

1.6.5 Figure 5 Legend

Kinesin-14 Kar3 Requires Cik1 and Vik1 For *in vivo* Function and Localization

Kar3 (green) requires Vik1 or Cik1 for proper localization and function during vegetative growth (mitosis) and mating (A). If Cik1 is deleted (B), mating is blocked because Kar3 cannot localize outside the nucleus. Mitosis proceeds similar to wild-type. If Vik1 is deleted (C) Kar3 cannot bind to the spindle poles for proper mitotic function, and is found on the spindle microtubules. Mating proceeds like wild-type because Vik1 does not participate. If both Cik1 and Vik1 are deleted (D), Kar3 cannot bind microtubules. Kar3 cannot be transported out of the nucleus, and therefore remains diffusely nuclear. Mating is blocked, and mitosis is aberrant.

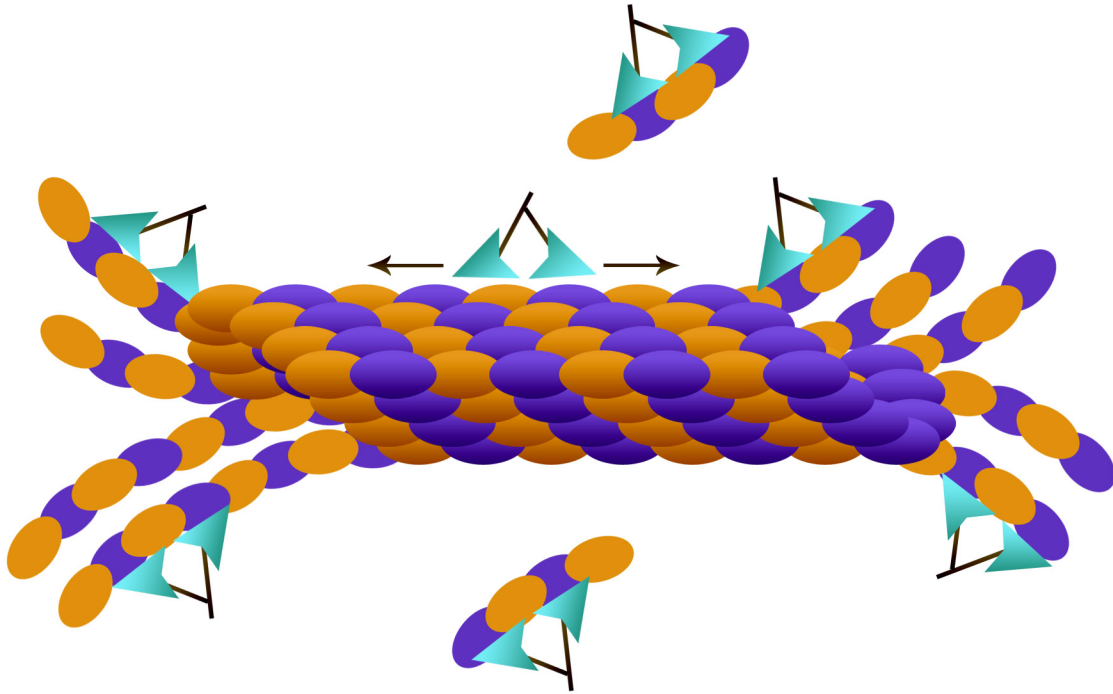


Figure 6. Microtubule•MCAK Interaction

1.6.6 Figure 6 Legend

Kinesin-13s (MCAK) Induce Microtubule Catastrophe By Binding To the Ends

MCAK (cyan) moves to the microtubule ends by 1D-diffusion in either direction in a nucleotide independent manner. MCAK binds to the microtubule ends where it induces an ATP-dependent conformational change on the microtubule end, such that the ends curl and are destabilized, promoting microtubule catastrophe. MCAK releases from the microtubule ends in a high affinity association with the tubulin heterodimers and/or small protofilament fragments [68, 83].

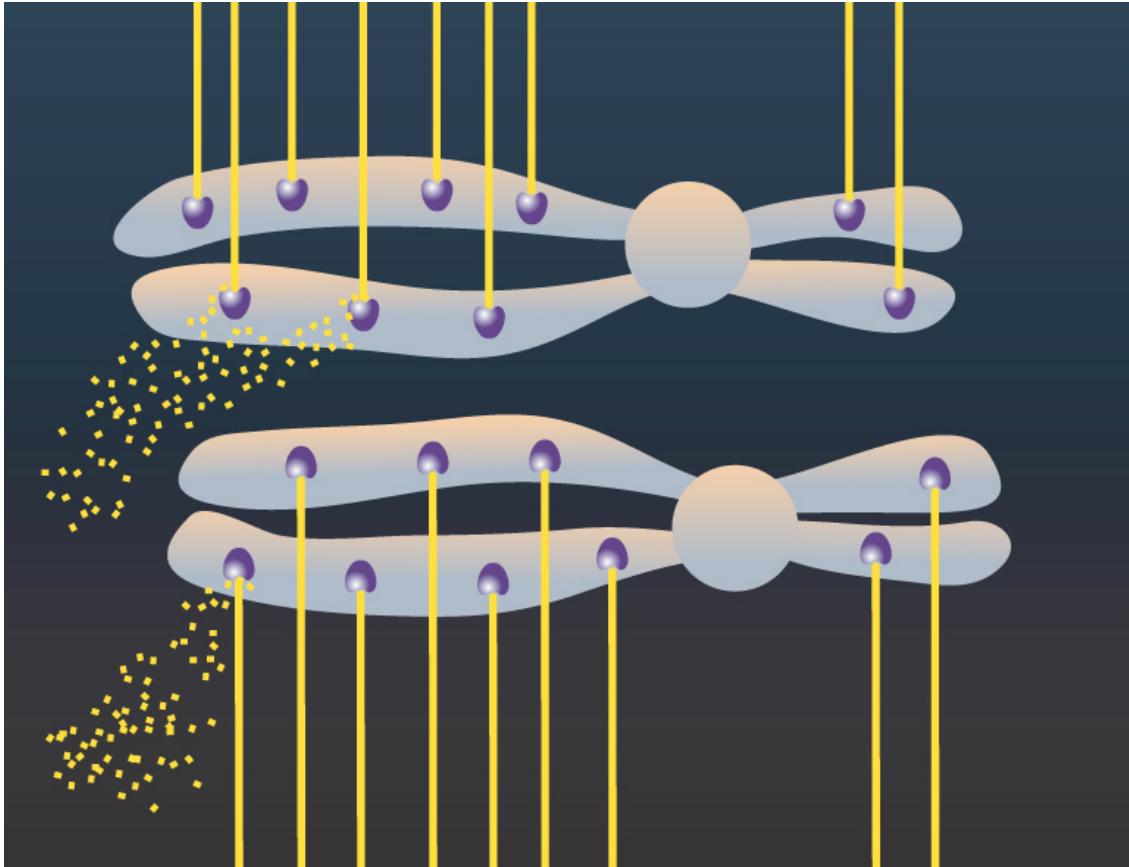


Figure 7. Model: Nod Exerts a Polar Ejection Force To Align Chromosomes in Metaphase

1.6.7 Figure 7 Legend

Nod Exerts a Polar Ejection Force At Microtubule Plus Ends

Nod (purple) binds along the arms of the chromosomes in *Drosophila* meiosis using its C-terminal DNA binding domains. Nod associates with microtubule (yellow rods) plus ends using its conserved kinesin motor domain. We propose that Nod prevents excessive poleward movement or loss of the chromosomes by facilitating microtubule polymerization at the microtubule plus end. Nod may act as a microtubule-stabilizing protein, holding the microtubule in a conformation competent for polymerization. Through a cycle of microtubule detachment and re-association, tubulin subunits (small yellow squares) are added onto the rapidly growing plus end.

2.0 MATERIALS AND METHODS

This chapter describes the experimental techniques used in the mechanistic analysis of four kinesin molecular motors: *Saccharomyces cerevisiae* Kar3Cik1 and Kar3Vik1 as well as *Drosophila melanogaster* Ncd and Nod.

2.1 BUFFERS AND EXPERIMENTAL CONDITIONS

The following buffers were used in the experimental procedures outlined in this chapter.

Lysis Buffer: 10 mM sodium phosphate, pH 7.2, 50 mM NaCl, 2 mM MgCl₂, 1 mM EGTA, 1 mM dithiothreitol (DTT), 2 mM phenylmethylsulfonyl fluoride (PMSF).

ATPase Buffer: 20 mM Hepes, pH 7.2, 5 mM magnesium acetate, 0.1 mM EDTA, 0.1 mM EGTA, 50 mM potassium acetate, 1 mM DTT, 5% sucrose.

PME Buffer: 10 mM PIPES, pH 6.9, 5 mM MgCl₂, 1 mM EGTA.

A.1.1

Oxygen Scavenging Mix (OSM), Containing per 500 μ l: 100 μ l of 5X PME, 7.5 μ l of 100 mM ATP or AMPPNP, 3.8 μ l of 200 mM magnesium acetate (1.5 mM MgAXP final), 100 μ l of 5.0 mg/ml BSA (1.0 mg/ml final), 10 μ l of 10 mg/ml glucose oxidase (0.2 mg/ml final), 1.75 μ l of 10 mg/ml catalase (35 μ g/ml final), 12.5 μ l of 1 M glucose (4.5 mg/ml final), and Taxol (1.5 μ M for depolymerization of Kar3Cik1_L or \geq 3 μ M for all other assays) as described.

ATP Regeneration System: 0.3 $\mu\text{g}/\mu\text{l}$ creatine phosphokinase + 2 mM phosphocreatine.

A.1.2

Ni-NTA Buffer: 10 mM sodium phosphate, pH 7.2, 2 mM MgCl_2 , 200 mM NaCl.

A.1.3

TBSTX: 10 mM Tris, pH 7.4, 100 mM NaCl, 0.1% Triton X-100.

2.2 MOLECULAR MOTORS

Table 1 presents the molecular motors used for the *in vitro* characterization of unconventional kinesins. The constructs, the predicted relative molecular mass (M_r) based on amino acid sequence, and purification affinity tags.

Table 1. The Motors Analyzed for the Studies Presented in Chapters 2-6.

Protein	Oligomeric State	M_r (Da)	Tags
Kar3MD	monomer	38, 888	No Tag
Kar3Cik1 _L	heterodimer	104, 281	His ₆
Kar3Cik1	heterodimer	95, 878	His ₆
Kar3Vik1	heterodimer	101, 395	His ₁₀
Vik1MHD	monomer	34, 564	His ₆ , Removed
K401	dimer	90,158	No Tag
Ncd (MC1)	dimer	114, 712	No Tag
Nod _{FL-GFP}	ND*	102, 498*	FLAG, His ₆
Nod ₃₁₈	monomer	63,648	FLAG, His ₆
Nod _{318-GFP}	monomer	35,326	FLAG, His ₆

* Oligomeric state of Nod_{FL-GFP} is **Not Determined**, as such the M_r is reported for a monomeric motor.

2.3 CONSTRUCT DESIGN

2.3.1 Kar3Cik1_L

To study the Kar3Cik1_L heterodimer (Chapter Three), Kar3 and Cik1 were amplified from yeast genomic DNA (generous gift of Dr. Michael Snyder, Yale University) by PCR using the following primers:

Kar3 N-terminal primer: 5' - CGGGGTACCATGGTGAACGAT-3'

Kar3 C-terminal primer: 5' - CGCGGATCCGCGATTTCATTTTCTACT-3'

Cik1 N-terminal primer: 5' -TTCCATATGGAAGTAGAAAATTTGAAACC-3'

Cik1 C-Terminal primer: 5' - GCGTCACAAGATCTGGATCCTTCTTA-3'

The Kar3 N-terminal primer contains an NcoI site, while the C-terminal primer contains a BamH1 site to be used for ligation into the pET-24d plasmid (Novagen). Cik1 was cloned into pET-15b (Novagen) using the upstream NdeI site (N-terminal primer) and downstream BamH1 site (C-terminal primer).

2.3.2 Kar3Vik1 and Kar3Cik1

A smaller version of Kar3Cik1 (Chapter Five) was engineered to be similar to the Kar3Vik1 motor in N-terminal coiled-coil length for optimal heterodimer formation. Kar3, Cik1, and Vik1 were amplified from cDNAs (a gift from Dr. Michael Snyder, Yale University) by PCR using the following primers:

1. Kar3Cik1 heterodimer for biochemistry and microscopy:

Kar3 N-terminal primer:

5'- CCAATCCATGGGGAAAAAGGATATAGAGC -3'

Kar3 C-terminal primer:

5'- GCTCGAATTTCGGATCCGCGTCATTTTCTACTAACC -3'

Cik1 N-terminal primer:

5'-GGACAAGAAATTCGAGCATATGAAGAAAGTTAAGAACGATGCTAG
AATTG-3'

Cik1 C-terminal primer:

5'- GGGCTTGGATCCCAGCCGGATCCTTCTTAATCTAGC -3'

2. Kar3Vik1 heterodimer for biochemistry and microscopy:

Kar3 N-terminal primer:

5'- CCAATCCATGGGGAAAAAGGATATAGAGC -3'

Kar3 C-terminal primer:

5'- GCTCGAATTCGGATCCGCGTCATTTTCTACTAACC -3'

Vik1 N-terminal primer:

5'- GATAGCATATGTTAAAATCCATGGAAAATTGACAAAC -3'

Vik1 C-terminal primer:

5'- CGATAATGGATCCGAGCTTAAGTGAGC -3'

Kar3 cDNA was cloned into pET-24d (Novagen, kanamycin selection) using Nco1, (N-terminal primer) and the BamH1 site (C-terminal primer). This plasmid when expressed yields amino acid residues MetGly-Lys²⁶⁸-Lys⁷²⁹ with a predicted molecular mass M_r of 52,819 Da. Cik1 cDNA was amplified to express residues Lys²⁵²-Asp⁵⁹⁴ and cloned into pET-15b (ampicillin selection) at Nde1 (N-terminal) and Bam H1 (C-terminal) sites. Cik1 when expressed yields residues MGSSH₆SSGGLVPRGSHMet-Lys²⁵²-Asp⁵⁹⁴ with predicted M_r = 43,059 Da. Vik1 was engineered for expression of Leu²⁵³-Thr⁶⁴⁸. The amplified sequence was inserted into pET-16b (ampicillin selection) at Nde1 (N-terminal) and BamH1 (C-terminal) cloning sites. Vik1 is expressed as MGH₁₀SSGHIEGRHM-Leu²⁵³-Thr⁶⁴⁸ with a predicted M_r = 58,796 Da.

2.4 PROTEIN EXPRESSION AND PURIFICATION

2.4.1 Kar3Cik1_L, Kar3Cik1, Kar3Vik1

The appropriate Kar3 plasmid was coexpressed with either Cik1 or Vik1 plasmids in *E.coli* BL21 Codon Plus™ (Stratagene). Ten ml of Luria Broth (LB) plus 7.5 µl of 100 mg/ml ampicillin, 2 µl of 50 mg/ml chloramphenicol, and 30 µl of 10 mg/ml kanamycin, were inoculated with one colony of bacteria and grown at 37 °C, shaken at 250 rpm for 3-4 hours until the LB was visibly cloudy. Two ml of this bacterial culture was added to one of five aliquots of 100 ml of LB plus 75 µl of 100 mg/ml ampicillin, 20 µl of 50 mg/ml chloramphenicol, and 300 µl of 10 mg/ml kanamycin, and grown at 37 °C for 3-4 more hours. The culture shook at 250 rpm until the A₆₀₀ was ~ 0.2 and/or visibly cloudy. The 100 ml cultures were added to one of five two liters of LB medium plus 1.5 ml of 100 mg/ml ampicillin, 400 µl of 50 mg/ml chloramphenicol, and 6 ml of 10 mg/ml kanamycin, and grown at 37 °C, 250 rpm to reach an A₆₀₀ of 0.4. Protein expression was induced by the addition of 0.075 mM isopropyl-beta-D-thiogalactopyranoside (IPTG). The cells were continuously grown at 20 °C, shaken at 125 rpm overnight. The cells were harvested at 7,000 rpm for 20 minutes at 4 °C, and the bacterial pellets were resuspended at 1 g/3 ml in Lysis Buffer and stored at -80 °C.

For purification the cells were thawed and further diluted to 1 g/10 ml in Lysis Buffer + 0.1 mg/ml lysozyme (Roche). Bacterial lysate was obtained from three rounds of freeze-thaw cycles and two clarifying spins at 18,000 and 50,000 rpm. The 50,000 rpm supernatant was loaded onto a 50 ml S-Sepharose column (Sigma) equilibrated with Lysis Buffer. The S-Sepharose column selects for the charged residues found on the surface of kinesins, and therefore Kar3, as detailed in [230]. The protein was eluted from the column using a linear gradient of 0.05 – 0.6 M NaCl. The protein eluted between 0.15 – 0.22 M NaCl. The protein was collected and dialyzed into nickel-nitrilotriacetic acid (Ni-NTA) buffer. The Ni-NTA buffer contained 0.2 M NaCl to stabilize the heterodimers. The eluted protein was clarified at 40,000 rpm and then loaded onto a 5 ml Qiagen Ni-NTA Agarose column to select for Cik1 or Vik1 containing a His tag.

The protein was eluted as > 99% pure from the column using Ni-NTA buffer plus 0.2 M imidazole and was checked by SDS-PAGE stained with Coomassie Blue (See Figures 9A and 13C). The protein was subsequently dialyzed into ATPase Buffer plus 0.2 M NaCl, and aliquots were frozen in liquid N₂ and stored at -80 °C.

Kar3Cik1_L contains the Kar3 motor protein (Met²⁴⁴-Lys⁷²⁹) with predicted *M_r* of 55,706 Da. Leucine residue at position 245 of Kar3 was mutated to valine during the cloning process. This change is in the hinge region and did not affect dimerization or mechanochemistry. The engineered Cik1_L clone resulted in an additional 21 N-terminal amino acid residues: MGSSH₆SSGLVPRGSHM followed by Glu²⁰⁰-Asp⁵⁹⁴ of Cik1, predicted *M_r* of 48,575 Da [202].

The smaller Kar3Cik1 motor contains amino acid residues MetGly-Lys²⁶⁸-Lys⁷²⁹ of Kar3 with a relative *M_r* of 52,819 Da. Cik1 was amplified to express residues Lys²⁵²-Asp⁵⁹⁴ with a His₆ tag for purification. The protein expresses as MGSSH₆SSGGLVPRGSHM-Lys²⁵²-Asp⁵⁹⁴ with a *M_r* of 43,059 Da. The complementary Kar3Vik1 uses the same Kar3 plasmid, while the Vik1 plasmid was engineered to express Leu²⁵³-Thr⁶⁴⁷. The plasmid construction adds 22 amino acids 5' to the start of the Leu²⁵³-Thr⁶⁴⁷ Vik1, including a His tag for motor purification. The protein expresses as: MGH₁₀SSGHIEGRHM followed by Leu²⁵³-Thr⁶⁴⁷ of Vik1 with a *M_r* of 58,796 Da. Kar3Cik1 and Kar3Vik1 heterodimers were purified as described for the Kar3Cik1_L above, with a final step of selection for the pure heterodimers by gel filtration (See Figure 17a).

2.4.2 Kar3MD

The Kar3MD clone was the generous gift of Dr. Sharyn A. Endow of Duke University [96]. The Kar3MD construct in pMW/Kar3 was previously described [96], and it encodes residues Met³⁸³-Lys⁷²⁹ of the conserved motor domain. Leu³⁸³ was changed to Met during plasmid construction. The predicted *M_r* = 38,888 Da.

2.4.3 Vik1MHD and SeMetVik1MHD

The Vik1MHD and SeMetVik1MHD were provided by collaborators Drs. John Allingham and Ivan Rayment, University of Wisconsin-Madison, and were designed to express the C-terminal globular domain predicted to lie close to the Kar3MD following dimerization through coiled-coil stalks [188]. Vik1MHD contains amino acid sequence Thr³⁵³-Thr⁶⁴⁷. The SeMetVik1MHD is identical in sequence except that selenomethionine replaced methionine in the Vik1MHD, this construct was used to determine the X-ray crystal structure of Vik1MHD. These proteins contained N-terminal His-Tags and were purified by Ni-NTA affinity chromatography. The His-tags were removed following purification by rTEV proteolytic digestion. The Vik1MHD has a M_r of 34,564 Da, based on amino acid sequence (Table 1).

2.4.4 Nod_{FL}-GFP, Nod₃₁₈, and Nod₃₁₈-GFP

The Nod_{FL}-GFP, Nod₃₁₈, and Nod₃₁₈-GFP constructs were designed and purified by our collaborators Drs. Wei Cui and R. Scott Hawley, at the Stowers Institute as described [224].

2.4.5 Ncd, K401, KHC_R, Kinesin-1

Dimeric Ncd and conventional kinesin K401 have been characterized previously by our group [200, 230]. KHC_R was purchased from Cytoskeleton, Inc. It is a short recombinant fragment of the kinesin heavy chain used as a control for motility. Native heterotetrameric squid conventional Kinesin-1 was the generous gift of Dr. Steven M. Block, (Stanford University).

2.4.6 Tubulin

Microtubules used in the experiments were assembled from tubulin that was purified from bovine brain according to the method of Borisy [231]. Rhodamine-labeled tubulin was purchased from Cytoskeleton, Inc. Microtubules were cold depolymerized and clarified the morning of each experiment as described [230]. The microtubules were assembled with Taxol (paclitaxel - Sigma) at 34 °C. The microtubules were collected by centrifugation, and the microtubule pellet was resuspended in ATPase buffer plus Taxol to stabilize the microtubules. The amount of Taxol used to stabilize the microtubules varied with the assay and is specified for each experiment.

2.5 ANTIBODIES

We generated rabbit polyclonal antibodies (Cocalico Biologicals) to identify the Kar3 motors. The antibodies are to the Kar3MD (UPT142), and to the Vik1MHD (UPT162). The antibodies were affinity purified as needed, by binding to, and release from, the antigen bound to activated CNBR Sepharose beads from Amersham™ adapted from ref. [232]. Representative Coomassie gels and complementary Western Blots in Figures 9A and 13C demonstrate the specificity of the antibodies.

2.6 GEL FILTRATION AND STOKES RADII CALCULATIONS

Purified proteins were analyzed using a Superose-6 HR 10/30 gel filtration column (Amersham Biosciences) equilibrated at 25 °C in ATPase buffer, using the System Gold® high-pressure liquid chromatography system (Beckman Coulter, Inc.) using intrinsic fluorescence for protein detection. The Stokes radii of Kar3MD, Kar3Cik1_L, Kar3Vik1, Kar3Cik1, and dimeric K401 were calculated as described previously [233]

using five protein standards: ovalbumin, 3.1 nm; thyroglobulin, 3.1 nm; aldolase, 4.8 nm; catalase, 5.2 nm; and ferritin, 6.1 nm.

2.7 STEADY STATE ANALYSIS OF MOTOR PROTEINS

The steady state ATPase kinetics of the motors examined in these studies were measured monitoring the hydrolysis of [$\alpha^{32}\text{P}$] ATP to [$\alpha^{32}\text{P}$] ADP•P_i as described previously [234]. The steady-state kinetics as a function of microtubule or soluble tubulin concentration (Figures 9E and 14B) were fit to the quadratic equation 1:

$$\text{Rate} = 0.5 * k_{cat} * [(E_0 + K_{1/2,MT} + MT_0) - [(E_0 + K_{1/2,MT} + MT_0)^2 - (4E_0MT_0)]^{1/2}] \quad (\text{Eq. 1})$$

where Rate is the amount of product formed per second per site, k_{cat} is the maximum rate constant of product formation at saturating substrate, E_0 is the motor concentration, $K_{1/2, MT}$ is the steady-state Michaelis constant, and MT_0 is the microtubule concentration (μM tubulin polymer). The data as a function of MgATP concentration were fit to the Michealis-Menten equation.

For the longer Kar3Cik1_L, steady-state turnover was examined under conditions where Kar3Cik1_L promoted microtubule depolymerization. Because the amount of Taxol used varied with the amount of tubulin used in the experiments where Kar3Cik1_L promoted microtubule depolymerization, on each day of the experiment, duplicate samples of stable and Kar3Cik1_L depolymerizing microtubules were centrifuged and analyzed by SDS-PAGE to confirm that the microtubules were either stable or being depolymerized in the presence of Kar3Cik1_L.

2.8 MICROTUBULE COSEDIMENTATION ASSAYS

2.8.1 Microtubule Depolymerization Solution Assay

Soluble tubulin was adjusted to 1 mM MgGTP or 1 mM MgGMPcPP (Jena Biosciences), cold depolymerized, clarified, and cycled each morning of the experiment. Kar3Cik1_L at 50 nM was incubated with microtubules (500 nM tubulin), which were stabilized with either 20 μ M Taxol for stable microtubule conditions or 3 μ M Taxol for the experiments where Kar3Cik1_L-dependent depolymerization was observed. Assays were performed at 25 °C in PME buffer at a final volume of 150 μ l. The reactions were initiated by the addition of 1 μ M MgATP or 1 μ M MgAMPPNP and incubated for varying times, followed by centrifugation. The reactions were terminated by the addition of the non-hydrolysable analog AMPPNP followed directly by centrifugation. The supernatant and pellet at equal volume were analyzed by SDS-PAGE with Coomassie blue staining. NIH Image (v1.62) was used to quantify tubulin that partitioned either to the supernatant or to the microtubule pellet.

2.8.2 Microtubule Polymerization Solution Assay

For the sedimentation assays to assess microtubule polymerization, tubulin was treated as described above. Soluble tubulin at 3 μ M was incubated with 1.5 μ M Taxol, 1.5 μ M MgATP, and 1.5 μ M MgGTP in the presence or absence of Nod_{FL}-GFP or Nod₃₁₈ (0.15 μ M of Nod_{FL}-GFP and 0.3 μ M of Nod₃₁₈) at 34 °C for 0-10 minutes, and then the solution was centrifuged in the Airfuge (Beckman Coulter, Inc.) at 100,000 x g for 30 minutes. The resulting supernatant and pellet for each reaction were analyzed by SDS-PAGE followed by Coomassie Brilliant Blue staining. The density of the protein bands was measured using Scion Image (NIH). To verify that the pellets represented microtubules, we used rhodamine-labeled and unlabeled tubulin at the ratio of 1 to 15 and repeated the sedimentation assay. We resuspended the labeled microtubule pellets in PME buffer and evaluated the suspension by fluorescence microscopy.

2.8.3 Microtubule•Motor Equilibrium Binding Assays

Soluble tubulin was adjusted to 1 mM MgGTP, cold depolymerized, clarified, and cycled each morning of the experiment. All concentrations reported are final after mixing. Reactions of 150 μ l microtubules (0-3 μ M tubulin) were incubated with 50 nM motor for 10 minutes at room temperature in PME Buffer. MgAMPPNP or MgADP (2 mM final) or 0.1 U/ml apyrase were then added, and the reactions were incubated for 30-60 min to reach equilibrium. The microtubules and associated proteins were sedimented at 100,000 x *g* for 30 min at 34 °C (Beckman Coulter TLX Ultracentrifuge). Supernatant fractions were analyzed by SDS-PAGE, followed by staining with Sypro Ruby® (Invitrogen). To quantify the motor or Vik1MHD that cosedimented with microtubules, a standard curve was used with the corresponding protein within a range of concentrations where Sypro Ruby-staining was linear. The protein was quantified using Image J. The data were plotted as the fraction of motor in the pellet as a function of microtubule concentration and fit to quadratic equation 2:

$$[\text{MT}\cdot\text{E}] / [\text{E}_0] = 0.5 \left[\left([\text{E}_0] + K_d + [\text{MT}_0] \right) - \left[\left([\text{E}_0] + K_d + [\text{MT}_0] \right)^2 - 4([\text{E}_0][\text{MT}_0]) \right]^{1/2} \right]$$

(Eq. 2)

where MT•E is the fraction of motor or Vik1MHD sedimenting with the microtubule pellet, E₀ is the total motor or Vik1MHD, and K_d is the dissociation constant.

2.9 MICROSCOPY ASSAYS OF KINESIN MOTORS

2.9.1 Preparation of Polarity-Marked Fluorescent Microtubules

Rhodamine-labeled microtubules were assembled using rhodamine tubulin (Cytoskeleton, Inc.) and unlabeled native bovine brain tubulin. The tubulin was thawed, adjusted to 1 mM GTP, clarified and cycled for each microscopy experiment. Rhodamine-labeled microtubules were polymerized using a ratio of one part rhodamine-labeled tubulin (4 μ l of 20 μ M) per four parts native bovine tubulin (16 μ l of 20 μ M) in PME buffer plus 1 mM MgGTP at 34 °C. The microtubules were subsequently stabilized with either 1.5 or \geq 3 μ M Taxol in PME, dependent upon the assay. For polarity-marked microtubules, highly fluorescent seeds were assembled at a 1:1 ratio of rhodamine-labeled tubulin (6 μ l of 20 μ M) to native bovine tubulin (6 μ l of 20 μ M) at 34 °C, followed by stabilization with 6 μ M Taxol. The microtubules were sheared using a 23.5 gauge needle and mixed with the 1:4 rhodamine-tubulin:unlabeled-tubulin mix. Microtubules were extended from the seeds at 34 °C and stabilized with 1.5 or \geq 3 μ M Taxol. The fluorescence microscopy assays were performed in OSM.

2.9.2 Motility of Kinesin Motor Proteins

For motility assays, acid washed microscopy perfusion chambers were used. The microtubule•motor complex (1 or 2 μ M Motor, 300 nM tubulin, \geq 3 μ M Taxol) was preformed in the presence of 1 mM MgAMPPNP in OSM. The microtubule•motor + AMPPNP complex (8 μ l) was flowed into the chamber, and incubated for three minutes. The chamber was rinsed with 8 μ l of OSM + 1 mM MgAMPPNP to remove unattached microtubules. Three-to-four image frames were collected of the stationary microtubules, and the reaction was initiated by 1.5 mM MgATP plus an ATP regeneration system in OSM. Images were collected every 20 seconds over 20 minutes. Microtubules were analyzed using Adobe Photoshop based on the following criteria: microtubules exhibited continuous movement in one direction for $t > 1$ minute, microtubules did not contact

other microtubules, scored microtubules were completely in the field of view, and were $\geq 2.5 \mu\text{m}$ in length. Slides were viewed with an Olympus BX60 epifluorescence microscope using a 100X oil immersion objective. Digital images were captured with a Hamamatsu 4742 CCD-cooled camera in conjunction with QED In Vivo™ imaging software.

2.9.3 Microtubule Shortening Promoted by Kinesin Motor Proteins

For the Kar3Cik1_L assays the coverslip was coated with poly-L-Lysine, followed by the addition of the microtubule-binding-protein GST-XCTK2-NM [235] (generous gift of Dr. Claire E. Walczak, Indiana University) at 10 nM in a volume of 8 μl . GST-XCTK2-NM binds to the poly-L-Lysine and to microtubules, thus acting as a scaffold to lift the microtubules away from the coverslip. Excess GST-XCTK2-NM was removed, and the remaining poly-L-Lysine sites blocked by 8 μl of 1.0 mg/ml BSA. The preformed microtubule•motor + AMPPNP complex in OSM was flowed into the perfusion chamber followed by 8 μl of OSM to remove unattached microtubules. The field of view was imaged at time 0, and the depolymerization reaction was initiated with 1.5 mM MgATP in OSM plus an ATP regeneration system. The microtubule scoring criteria used were: microtubules that did not contact other microtubules, microtubules that were completely in the field of view, and were $\geq 2.5 \mu\text{m}$ in length.

Control experiments were performed in which the microtubule seed was less fluorescent with extension from the seed with a higher concentration of rhodamine-labeled tubulin. These microtubules with the more highly fluorescent plus-end were also shortened with the same kinetics, illustrating that the plus end microtubule shortening was motor-specific rather than a function of the possible stabilization of the microtubule minus end by the higher concentration of rhodamine-tubulin used to form the polarity-marked microtubules.

Because our rates of microtubule shortening were significantly slower than observed for karyogamy *in vivo*, 0.05 $\mu\text{m}/\text{min}$ (Figure 2D) *versus* $0.23 \pm 0.07 \mu\text{m}/\text{min}$ [196] we tested the hypothesis that the GST-XCTK2-NM microtubule binding protein

[235] was stabilizing the microtubule lattice. For this experimental design, the microtubule·Kar3Cik1/Kar3Vik1 + MgAMPPNP complex was added directly to the perfusion chamber and N-terminal motor tails with His-tags were allowed to interact directly with the coverslip.

2.9.4 Microtubule·Motor Immunolocalization

Reactions of 10 μ l were formed containing the microtubule·motor complex (500 nM tubulin, \geq 3 μ M Taxol) in the presence of 1 mM MgAMPPNP. The reactions were fixed in 10 volumes of 1% glutaraldehyde in PME (3 μ l of the original 10 μ l reaction plus 30 μ l of 1% glutaraldehyde). The 30 μ l was then diluted with 800 μ l of PME. An aliquot of 50 μ l of this dilution was centrifuged through a 10% glycerol cushion onto round 1 mm poly-L-Lysine coated glass coverslips. The microtubule-bound coverslips were treated with -20 °C methanol for five minutes and washed with TBSTX. The coverslips were blocked with 2% BSA-TBSTX and processed for immunofluorescence. The purified primary polyclonal Kar3 or Vik1 antibodies generated to the native Kar3MD and Vik1MHD respectively. The Kar3 antibodies were used to localize the Kar3MD, Kar3Cik1_L and Kar3Cik1, whereas the Vik1MHD antibodies were used to localize Kar3Vik1 and Vik1MHD binding to the microtubule. The AKIN01 antibody (Cytoskeleton, Inc.) was used to localize Ncd and conventional kinesin K401 on the microtubule. Alexa 488 goat anti-rabbit (Molecular Probes) was used as the secondary antibody. The Nod motors were expressed with GFP tags; ergo the direct fluorescence of Nod·GFP was used to determine microtubule·Nod interactions. Motor binding was scored without knowledge of the sample and classified as motor binding to the microtubule end, the microtubule lattice, both the microtubule end and microtubule lattice, or saturating the microtubule lattice. The binding events on polarity marked microtubules were scored for plus end or minus end binding.

For the real-time microtubule binding assays, Nod_{FL}-GFP or Nod₃₁₈-GFP proteins were allowed to bind to microtubuls in the presence of 1 mM MgAMPPNP in PME, and

8 μ l of the microtubule•Nod complexes were flowed into perfusion chambers (Cytoskeleton, Inc). After the microtubule•Nod complexes settled onto the coverslip, unattached microtubules were removed by washing with 8 μ l of OSM. The microtubule•Nod complexes were imaged by fluorescence microscopy, and the resulting data were deconvolved using the Softworx package (Applied Precision). The two controls for this experiment are denoted as “no motor” and “GFP”. The no motor control consists of assaying the microtubules in the absence of any added Nod protein. The GFP control consisted of adding recombinant green fluorescent protein (rGFP) to microtubules. The rGfP plasmid was purchased from BD Biosciences and expressed in *E. coli* and purified.

2.9.5 Analysis of Microtubule Polymerization by Fluorescence Microscopy

For qualitative analysis of the polymerization of microtubules, both rhodamine-labeled and unlabeled tubulin were thawed, adjusted to 1 mM MgGTP, cold depolymerized, and clarified by centrifugation for 15 minutes at 14,000 rpm at 4 °C. The soluble tubulin was mixed to obtain a final ratio of 1:10 rhodamine-labeled:unlabeled tubulin and adjusted to 20 μ M tubulin. Nod at 0 or 50 nM protein was mixed with 3 μ M soluble tubulin in the presence of 1 mM MgATP (or MgAMPPNP), 1mM MgGTP, and 1.5 μ M Taxol in PME. The final volume of the reaction was 150 μ l. Reactions were initiated by the addition of soluble tubulin to the mix. At the pre-determined time points, 8 μ l was taken from the tube and perfused into the observation chamber. Five fields per time point (15 minute intervals) were then imaged on an Olympus BX60 epifluorescence microscope using a 100X oil immersion objective. Digital images were captured with a Hamamatsu 4742 CCD camera in conjunction with QED In Vivo™ imaging software.

2.9.6 Error Calculations

For Chapters Three, Five, and Six all error reported is the standard error of the mean (SEM). The significance between controls and experimental samples was determined using the Microsoft Excel Student T-test where noted.

3.0 KAR3CIK1, A NOVEL KINESIN DEPOLYMERASE

3.1 ABSTRACT

Kar3, a *Saccharomyces cerevisiae* Kinesin-14, is essential for karyogamy and meiosis I, but also has specific functions during vegetative growth [12, 169, 170, 172, 174, 185, 193]. For its various roles during the yeast life cycle, Kar3 forms a heterodimer with either Cik1 or Vik1, both of which are non-catalytic polypeptides [186-189]. Here, we present the first biochemical characterization of Kar3Cik1, the kinesin motor which is essential for karyogamy [186-189]. Kar3Cik1 depolymerizes microtubules from the plus end and promotes robust minus end directed microtubule gliding (2.4 $\mu\text{m}/\text{min}$). Immunolocalization studies show that Kar3Cik1 binds preferentially to one end of the microtubule, while the Kar3 motor domain, in the absence of Cik1, exhibits significantly higher microtubule lattice binding. Kar3Cik1-promoted microtubule depolymerization requires ATP turnover, and the kinetics fit a single exponential function ($k_{obs} = 0.07 \text{ s}^{-1}$). The disassembly mechanism is not microtubule catastrophe like that induced by the MCAK Kinesin-13s [14, 59, 83, 98, 99, 154-156]. Soluble tubulin does not activate the ATPase activity of Kar3Cik1, and there is no evidence of Kar3Cik1•tubulin complex formation as observed for MCAK [14, 59, 83, 98, 155, 156]. These results reveal a novel mechanism to regulate microtubule depolymerization. We propose that Cik1 targets Kar3 to the microtubule plus end. Kar3Cik1 then uses its minus end directed force to depolymerize microtubules from the plus end with each tubulin subunit release event tightly coupled to one ATP turnover.

3.2 INTRODUCTION

Kar3 is one of six kinesin-related genes in budding yeast [169, 181, 189]. Like *Drosophila* Ncd, Kar3 is classified as a Kinesin-14 because its motor domain is at the carboxy terminus, and it promotes minus-end directed microtubule gliding *in vitro* [169, 192, 193]. However, Kar3 is the only Kinesin-14 in *S. cerevisiae*, and there are specific roles for Kar3 motor activity in both the cytoplasm and the nucleus. The cellular localization is modulated in part by Cik1 and Vik1 to either the cytoplasm or nucleus [186-189]. During conjugation in response to mating pheromone, Cik1 targets Kar3 to astral microtubules and to the spindle pole bodies [186-189]. Mating cells that lack either Kar3 or Cik1 fail to interdigitate their microtubules and pull nuclei together after cell fusion [169, 186-188] (Figure 8). During vegetative growth, Kar3 regulates microtubule dynamics which affects both spindle size and spindle position [174, 183]. Because both Kar3Cik1 and Kar3Vik1 function during vegetative growth [185, 189, 190], it is difficult to distinguish Kar3 functions driven by Kar3Vik1 from those due to Kar3Cik1.

Initial *in vitro* studies using GST-Kar3 revealed that this C-terminal kinesin promoted minus end directed microtubule gliding but also microtubule shortening from the minus end [192]. Historically, it was thought that Kar3 motored to the minus end of the microtubule and then switched its catalytic activity to microtubule depolymerization [174, 177, 192]. Subsequent studies with green fluorescent protein fused to α -tubulin (GFP-tubulin) showed that the microtubule dynamics in yeast appear to occur only at the microtubule plus ends [196, 236]. Recently, Maddox *et al.* reported that during mating, GFP-Kar3 couples the microtubule plus-ends to the cortical shmoo tip during microtubule depolymerization and the Bim1-Kar9 complex maintains attachment of the microtubule plus ends during microtubule polymerization [165]. Bim1 is the EB1 homolog (microtubule plus end tip protein), and Kar9 is the microtubule linker-cortex attachment protein [237, 238].

Budding yeast is an excellent model system to dissect the roles of kinesin motor associated proteins for regulation of motor activity and microtubule dynamics. Because Kar3Cik1 is essential for karyogamy and Kar3Vik1 is not involved [188], our questions

are framed around the role of Kar3Cik1 for karyogamy (Figure 8). At least 3 hypotheses can account for the observations in the literature:

1) After cell fusion, microtubules interdigitate, and Kar3Cik1 slides microtubules relative to one another to bring the nuclei together.

2) Microtubules interdigitate, but only Kar3Cik1-promoted microtubule depolymerization is required.

3) Nuclear fusion requires both Kar3Cik1-promoted microtubule sliding and microtubule depolymerization.

For our *in vitro* studies, we have addressed the role of Cik1 for Kar3 mechanochemistry. We used the Kar3Cik1_L motor described in Chapter 2, Table 1. We propose that Cik1 may modulate the catalytic activity of the Kar3 motor domain comparable to a myosin light chain, Cik1 may modulate the Kar3 interaction with the microtubule directly or indirectly, and/or Cik1 may target Kar3 to the microtubule plus end.

3.3 RESULTS

3.3.1 Expression and Purification

We co-expressed truncated genes of Kar3 and Cik1 (Figure 9). The Kar3 motor domain (Kar3MD) and dimeric *D. melanogaster* Ncd MC1 [200, 201] were used as comparative C-terminal kinesins. The Coomassie-stained gel (Figure 9B) shows that the expressed Kar3Cik1 proteins purified with an apparent stoichiometry of one Kar3 per Cik1, and the analytical gel filtration analysis (Figure 9C) reveals that Kar3Cik1 migrates ahead of dimeric kinesin K401 [230, 239]. These data indicate that the truncated Kar3Cik1 motor is a stable heterodimer.

3.3.2 Kar3Cik1 Promotes Robust Microtubule Gliding

We used both polarity-marked and unmarked rhodamine-labeled 20 μM Taxol-stabilized microtubules to show that Kar3Cik1, like GST-Kar3 [192], was able to promote microtubule gliding *in vitro* ([Supplemental Movie S1](#)). Figure 9D illustrates one example of a polarity-marked microtubule that moved with its plus end leading, indicating minus end directed motion. Microtubule polarity was confirmed using conventional kinesin, a well-characterized plus end directed motor. The rate of Kar3Cik1 microtubule gliding was $2.40 \pm 0.06 \mu\text{m}/\text{min}$. This rate was slightly faster than the $1.3 \pm 0.1 \mu\text{m}/\text{min}$ reported previously for GST-Kar3 [192].

3.3.3 Kar3Cik1-Promoted Microtubule Depolymerization Requires ATP Turnover

The phenotypes of the *kar3 Δ* strain and *kar3-1* rigor mutant suggest that Kar3 motor function acts to limit both microtubule length and number during vegetative growth and karyogamy [165, 169, 174]. To analyze the Kar3Cik1 depolymerase activity, we developed both a solution assay (Figure 10) and a real time microscopy assay (Figure 11). The microtubule•Kar3Cik1 complex was preformed using different microtubule-stabilized substrates, and the addition of MgATP initiated depolymerization (Figure 10). The results for Kar3Cik1 were compared to the kinetic profile of MCAK depolymerases [14, 59, 98, 99, 154-156, 163]. Kar3Cik1 was unable to depolymerize 20 μM Taxol-stabilized or 1 mM MgGMPcPP-stabilized microtubules (Figure 10A). Both can be rapidly destabilized by MCAK [14]. Kar3Cik1 was able to depolymerize microtubules stabilized with 3 μM Taxol (Figure 10B,C). In the absence of Kar3Cik1, the 3 μM Taxol-stabilized microtubules showed only trace amounts of soluble tubulin in the supernatant. Upon addition of Kar3Cik1 plus MgATP, there was an exponential increase in tubulin partitioning to the supernatant as a function of time ($k_{obs} = 0.07 \text{ s}^{-1}$). Experiments were performed with 1 mM MgAMPPNP to ask whether ATP binding was sufficient to induce Kar3Cik1-promoted depolymerization as observed for MCAK [14, 98, 99, 154, 156]. No evidence of microtubule depolymerization by Kar3Cik1 with

MgAMPPNP was observed (Figure 10A). MgAMPPNP is a non-hydrolyzable ATP analog, which acts to lock kinesin motors on the MT in a tightly bound state, preventing translocation or force transduction. These results demonstrate that Kar3Cik1-promoted microtubule depolymerization requires ATP turnover. In contrast to MCAK, ATP binding is not sufficient for Kar3Cik1 to destabilize microtubules. The kinetics of MCAK-promoted depolymerization are sigmoid, which is characteristic of a microtubule catastrophe mechanism [159]. However, the Kar3Cik1-promoted microtubule depolymerization kinetics best fit a single exponential function (Figure 10C). These data indicate that Kar3Cik1 does not promote microtubule catastrophe, which is characterized by microtubule destabilization followed by rapid microtubule shortening as the polymer falls apart. Rather, the Kar3Cik1 results suggest a mechanism of sequential release of tubulin subunits from the microtubule polymer with each release event tightly coupled to one ATP turnover.

3.3.4 Kar3Cik1 Steady-State ATPase Is Only Stimulated by Microtubules

We examined the ATPase properties of Kar3Cik1 to compare with Kar3MD [240] dimeric Ncd [200, 201] and MCAK [155, 156]. Traditionally, kinesins in the absence of microtubules exhibit a very low ATPase activity, and microtubules greatly enhance this rate. Kar3Cik1 exhibited this behavior (Figure 9E-G). For MCAK, soluble tubulin subunits also activate steady-state ATP turnover, and MCAK can form a stable complex with a tubulin heterodimer *in vitro* [14, 59, 98, 99, 154-156]. These observations for MCAK have led to a proposed mechanism in which the MCAK•tubulin complex detaches from the microtubule, and ATP turnover is used to liberate the motor from the tubulin heterodimer [98, 99, 154-156]. We pursued experiments to test this type of mechanism for Kar3Cik1. In the absence of microtubules, the Kar3Cik1 steady-state ATPase was 0.014 s^{-1} (Figure 9E inset, green circle). When Kar3Cik1 was added to soluble tubulin, there was no activation of this rate by soluble tubulin (Figure 9E inset, red triangles), yet there was dramatic activation of the steady-state ATPase when microtubules were used at the same tubulin concentrations (Figure 9E inset, black circles). In addition, there was no evidence of complex formation between soluble

tubulin and Kar3Cik1 when analyzed by gel filtration (data not shown). Our results suggest that Kar3Cik1 does not detach from the microtubule in association with a tubulin heterodimer.

The Kar3Cik1 steady-state ATPase was activated by stable microtubules (25 μM Taxol) and microtubules that depolymerized (15 μM Taxol) in the presence of Kar3Cik1 (Figure 9E-G). Note that the concentration of Taxol used for Kar3Cik1-promoted microtubule depolymerization in the different experiments varied. The concentration required was determined in each case experimentally using co-sedimentation assays and SDS-PAGE. The steady-state ATPase kinetics reveals a slightly higher k_{cat} at conditions where Kar3Cik1 promoted motility (0.37 s^{-1}) as compared to conditions for Kar3Cik1-promoted microtubule depolymerization (0.26 s^{-1}). The two functional activities of Kar3Cik1 exhibited different relative affinities for MgATP: $K_{m, ATP} = 8.2 \mu\text{M}$ for stable microtubules and $71 \mu\text{M}$ for depolymerizing microtubules. At this time, we do not know the mechanistic significance of the differences in the steady-state parameters for the two activities—microtubule depolymerization *versus* microtubule gliding.

3.3.5 Kar3Cik1 Promotes Plus-to-Minus End Microtubule Shortening

We visualized Kar3Cik1-promoted microtubule depolymerization using rhodamine-microtubules immobilized by the microtubule-binding protein GST-XCTK2-NM [235] which acted as a scaffold to hold the microtubules away from the glass coverslip. The microtubules were imaged, and the reaction initiated by MgATP (Figure 11). Figure 11A-C shows time 0, 60 min, and the overlay of the two images. The red tipped microtubules reflect shortening during the reaction. The microtubules generally shorten from only one end (Figure 11C, Table 2). Microtubule shortening depended upon the addition of Kar3Cik1 plus MgATP. No change in microtubule length was observed in the absence of motor or in the presence of Kar3Cik1 plus MgAMPPNP (Figure 11, Table 2). These experiments were consistent with our solution studies where Kar3Cik1-promoted microtubule depolymerization required ATP turnover (Figure 10).

The use of polarity-marked microtubules showed Kar3Cik1-promoted shortening from the microtubule plus end (Figure 11D-F). We also evaluated dimeric Ncd to determine whether microtubule depolymerization was characteristic of other C-terminal kinesins. Dimeric Ncd also promoted microtubule shortening from the plus to the minus end (Figure 11G-I). The rates of motor-promoted depolymerization were similar for Kar3Cik1 (45 nm/min) and Ncd (53 nm/min). In contrast, MCAK promoted microtubule shortening from both ends and at rates significantly faster (> 800 nm/min) [156].

For the polarity-marked microtubules, we saw no examples in which Kar3Cik1-promoted microtubule shortening specifically from the minus end although some microtubules showed shortening from both ends for Kar3Cik1 and Ncd (Figure 11, Table 2). In contrast, conventional kinesin K401 was not observed to shorten microtubules (Figure 11P-R). We do not know whether the depolymerase activity of Ncd is biologically relevant because there are no genetic or cellular studies reported to date which implicate Ncd in regulating microtubule dynamics. However, our results document the ability of Ncd to shorten microtubules with characteristics similar to Kar3Cik1 *in vitro*. These observations suggest that this depolymerase activity may be common to the Kinesin-14 C-terminal kinesins.

3.3.6 Kar3Cik1 Has a Higher Affinity for the Microtubule End than Kar3MD

To determine whether Cik1 modulates the binding of Kar3 to the microtubule, we localized Kar3 on rhodamine-microtubules using polyclonal antibodies to the Kar3MD. The affinity-purified Kar3 antibodies recognize both the Kar3MD and the Kar3 subunit of Kar3Cik1 but not tubulin or Cik1 as shown by Western blot (Figure 9B). We localized both Ncd and K401 using an antibody to a conserved sequence in the kinesin catalytic core. In the absence of motor, there was very little non-specific binding resulting in low background fluorescence (Figure 12A-C). Figure 12D-F illustrates an example of a polarity-marked microtubule with Kar3Cik1 localized to the plus-end, Figure 12G-I shows Kar3MD bound to the microtubule lattice, Figure 12J-L demonstrates Ncd binding to the lattice, while Figure 12M-O shows conventional kinesin coating the microtubule. Table 3 summarizes the localization results for the Kar3MD, Kar3Cik1,

dimeric Ncd, and dimeric K401. Very few localization events were scored in the absence of motor, and very few binding events were evident at 50 nM Kar3MD in comparison to 50 nM Kar3Cik1, 50 nM Ncd, or 50 nM K401. These results indicate that the Kar3Cik1 heterodimer shows a higher affinity for microtubules than the monomeric Kar3MD. For the Kar3MD at 100 nM, 21.7% of scored microtubules showed end binding, 72.9% with lattice-binding, and 5.3% with lattice and end binding. In contrast, at both 50 nM and 100 nM Kar3Cik1, 48% of the microtubules exhibited end binding, 27% lattice-binding, and 25% lattice and end binding. These data indicate that there is a high affinity site at the microtubule end for Kar3Cik1 resulting in microtubule end binding in preference to microtubule lattice binding. In contrast, the Kar3MD binds more often to the microtubule lattice. The results for Ncd are more similar to the Kar3MD results, and conventional kinesin K401 shows no preference for the microtubule ends.

3.4 DISCUSSION

We provide the first *in vitro* characterization of Kar3Cik1 mechanochemistry. Our results reveal that C-terminal kinesins exhibit a depolymerase activity quite distinct from the MCAK depolymerases. *In vitro* Kar3Cik1 binds preferentially to one end of the microtubule and promotes slow, directed microtubule shortening that occurs from only the plus end of microtubules. This mechanism is novel and critical for the hypothesized roles of Kar3Cik1 during karyogamy, meiosis, and mitosis [12, 165, 169-172, 174, 177, 183, 185-190, 193, 229]. *In vivo*, most kinesin depolymerases appear to facilitate dynamic instability catalyzing the rapid microtubule fluctuations associated with chromosome “search and capture” during mitosis [9, 151, 241]. To date, all of these kinesins have been MCAK Kinesin-13s, but other types of microtubule depolymerization events occur in the cell such as the very specific unidirectional microtubule depolymerization that leads to karyogamy. It is plausible to argue that a C-terminal kinesin, possessing minus end directed force makes an attractive candidate to ensure directed, coordinated shortening of the microtubule from the plus end to carry out

events where microtubule shortening must be temporally and spatially exact. Kar3Cik1 is the first example of a motor used in such a specialized cellular event.

We propose that Cik1 targets Kar3 to the plus end of microtubules in the shmoo tip for microtubule shortening, and Kar3Cik1-promoted depolymerization acts to pull the nucleus into the shmoo tip (Figure 8). Once the two shmoo cytoplasms become confluent, our results would suggest that Kar3Cik1 uses both its microtubule gliding activity to slide anti-parallel microtubules and its depolymerase activity to shorten the astral microtubules for nuclear fusion. Our *in vitro* data provide a mechanism to explain the role of Cik1 for Kar3Cik1 function in karyogamy, but unresolved questions remain. First, Kar3Cik1 appears to be tethered to the cortex much like Bim1-Kar9 for microtubule polymerization [165] and our *in vitro* analysis shows that it is the C-terminal domain of Kar3Cik1 that tracks with the shortening microtubules. Therefore, our results suggest that it is the N-terminal domain of Kar3Cik1 that binds to a cortex partner yet to be identified. Lastly, we do not yet know if other microtubule and/or Kar3Cik1 associated proteins participate to regulate Kar3Cik1-promoted microtubule depolymerization during karyogamy.

3.5 FIGURES AND FIGURE LEGENDS

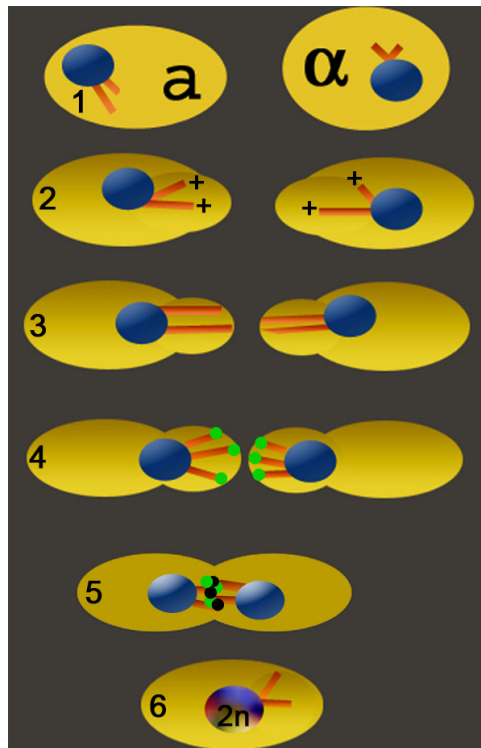
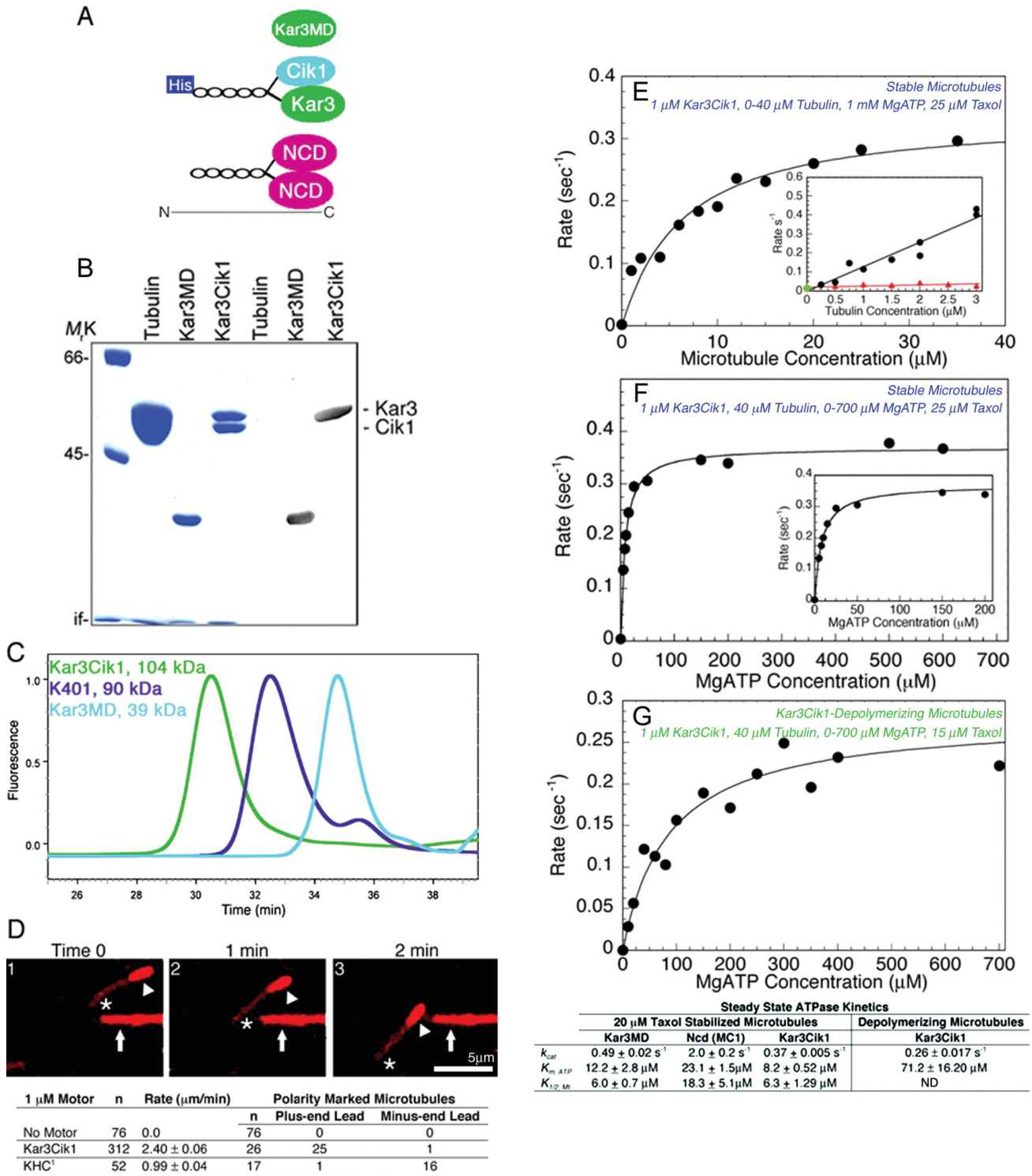


Figure 8. Model for Kar3Cik1 Function during Karyogamy

3.5.1 Figure 8 Legend

Model for Kar3Cik1 Function during Karyogamy

1. Mating-specific pheromones induce Kar3 and Cik1 expression as well as the formation of the rounded cell protrusions or “shmoos”. 2-3. The astral microtubules are highly dynamic, and the microtubule plus ends become associated with the cortex. 4. For microtubule shortening, Kar3Cik1 motors (green spheres) are targeted to the microtubule plus ends. Kar3Cik1-promoted microtubule depolymerization shortens the microtubules to pull each nucleus into its shmoo. 5. Localized cell wall breakdown allows cytoplasm fusion, resulting in interdigitating microtubules of opposite polarity. Bik1 (black) and Kar3Cik1 are found at the plus ends of the interdigitating depolymerizing microtubules. 6. Kar3Cik1 can now use its minus end directed force for both microtubule sliding and microtubule shortening to form the diploid nucleus.



¹Recombinant Kinesin Heavy Chain Motor Domain from Cytoskeleton, Inc.

Figure 9. Kar3Cik1 Characterization

3.5.2 Figure 9 Legend

Kar3Cik1 Characterization

(A) The three motors used: monomeric Kar3MD, Kar3Cik1 heterodimer, and dimeric *D. melanogaster* Ncd MC1. (B) Coomassie-stained gel (2M Urea, 8% SDS-PAGE) and Western blot showing protein purity and antibody specificity. (C) Analytical gel filtration of Kar3Cik1, dimeric conventional kinesin K401, and Kar3MD with MW based on amino acid sequence. Stokes radius of Kar3Cik1 = 4.0 nm, K401 = 3.8 nm, and Kar3MD = 3.4 nm. (D) Kar3Cik1 minus end directed microtubule motility in the presence of MgATP. Arrowheads denote the bright microtubule minus end and the asterisks, the dim microtubule plus end. Scale bar = 5 μm . (E-G) The steady-state ATPase kinetics of Kar3Cik1 as a function of microtubules (E) and MgATP (F-G). Both E & F were performed at 25 μM Taxol, where the microtubules were stable and resistant to Kar3Cik1-promoted depolymerization. (E) Final concentrations: 1 μM Kar3Cik1, 1-40 μM tubulin, 25 μM Taxol, 1 mM Mg [$\alpha^{32}\text{P}$] ATP. Steady-state parameters: $k_{cat} = 0.35 \pm 0.02 \text{ s}^{-1}$; $K_{1/2,MT} = 6.3 \pm 1.3 \mu\text{M}$. *Inset*, Kar3Cik1 was incubated with increasing concentrations of tubulin as microtubules (black), soluble tubulin heterodimer (red), or in the absence of tubulin (green circle), and the reactions were initiated with MgATP. Final concentrations: 0.5 μM Kar3Cik1, 0-3 μM tubulin, $\pm 3 \mu\text{M}$ Taxol, 100 μM Mg [$\alpha^{32}\text{P}$] ATP. The ATPase rate in the absence of tubulin (green) was $0.014 \pm 0.006 \text{ s}^{-1}$, soluble tubulin (red) = $0.015 \pm 0.002 \text{ s}^{-1}$. (F) Steady-state ATPase at stable microtubule conditions. Final concentrations: 1 μM Kar3Cik1, 40 μM tubulin, 25 μM Taxol, and 1-700 μM Mg [$\alpha^{32}\text{P}$] ATP. Kar3Cik1: $k_{cat} = 0.37 \pm 0.005 \text{ s}^{-1}$, $K_{m,ATP} = 8.2 \pm 0.53 \mu\text{M}$. *Inset*, Initial phase at 1-200 μM MgATP. (G) The steady state ATPase at microtubule depolymerizing conditions. Final concentrations: 1 μM Kar3Cik1, 40 μM tubulin, 15 μM Taxol, 1 mM Mg [$\alpha^{32}\text{P}$] ATP. Kar3Cik1: $k_{cat} = 0.26 \pm 0.017 \text{ s}^{-1}$, $K_{m,ATP} = 71.2 \pm 16.2 \mu\text{M}$. (Table) The steady-state parameters of Kar3Cik1 in comparison to Kar3MD [240], and dimeric Ncd MC1 [200], ND, not determined.

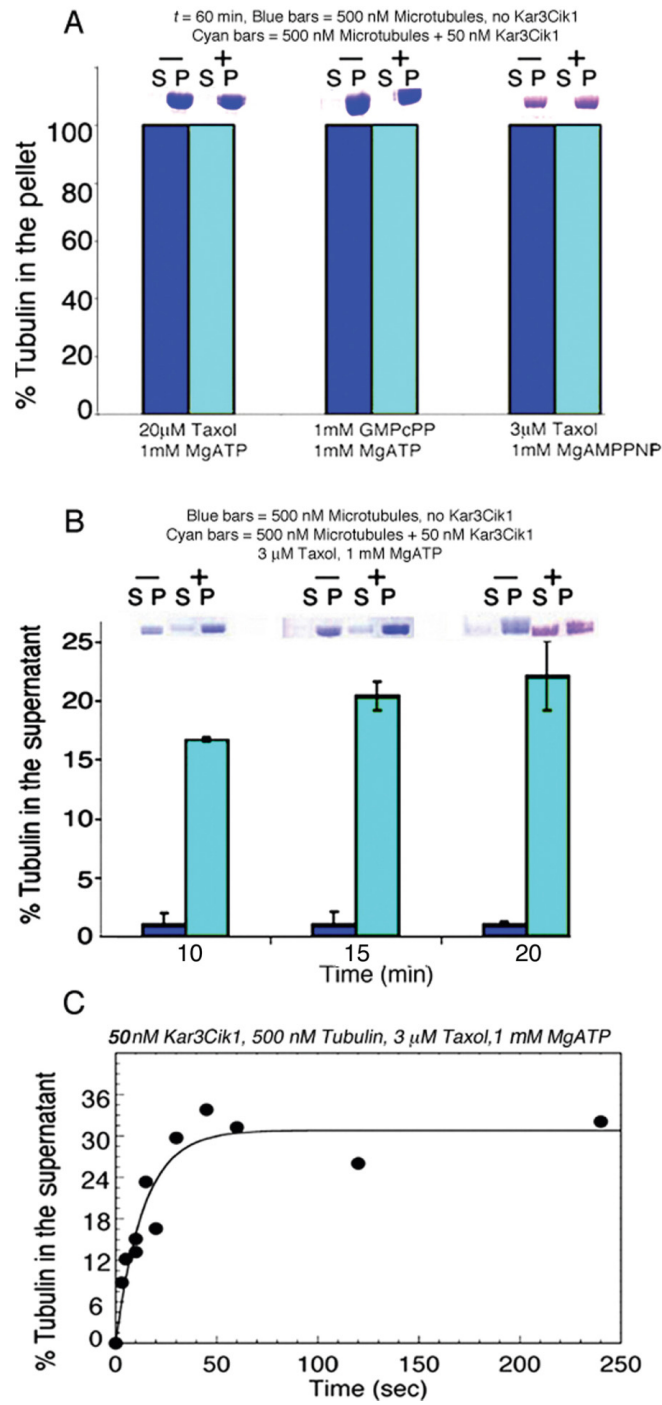


Figure 10. Solution Assays of Microtubule Depolymerization

3.5.3 Figure 10 Legend

Solution Assays of Microtubule Depolymerization

(A & B) Representative gel slices above each set of bars show tubulin partitioning to either the supernatant (S) or to the microtubule pellet (P). Each bar is the mean of three replicates, and the error bars report standard error. Microtubules in the presence (cyan bars) or absence (blue bars) of Kar3Cik1 were incubated with different nucleotides and microtubule stabilizing agents to determine the substrates for Kar3Cik1 depolymerization. Final concentrations: \pm 50 nM Kar3Cik1, 500 nM tubulin, 3 or 20 μ M Taxol or 1 mM MgGMPcPP, and 1 mM MgATP or 1 mM MgAMPPNP. (B & C) Microtubules stabilized with 3 μ M Taxol were incubated with Kar3Cik1 in the presence of 1 mM MgATP. The reactions were terminated at specific times with 2 mM MgAMPPNP, followed by centrifugation and analysis by SDS-PAGE. The percent of tubulin partitioning to the supernatant was plotted as a function of time, and the data were fit to a single exponential function with $k_{obs} = 0.07 \pm 0.01 \text{ s}^{-1}$.

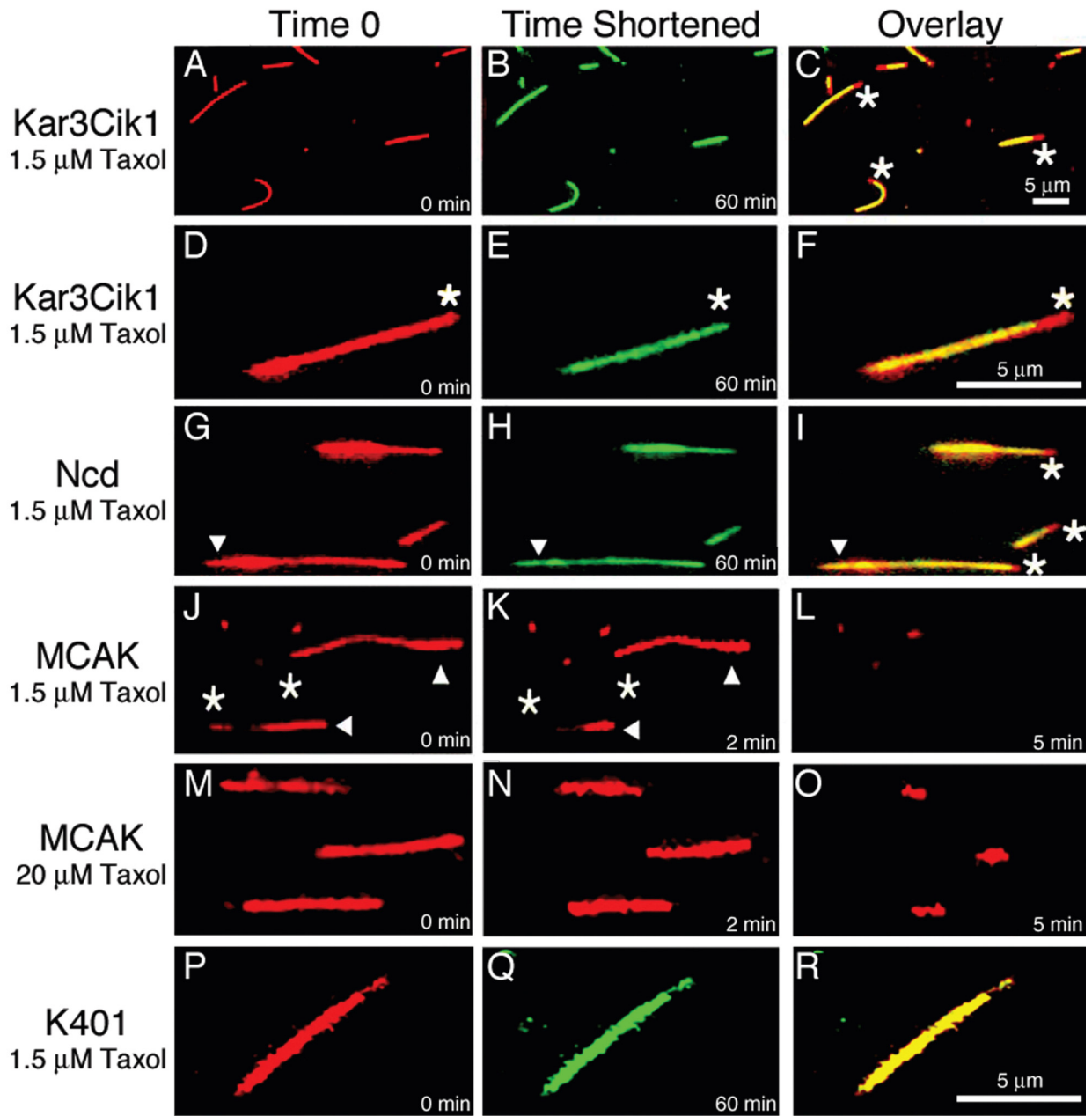


Figure 11. Microtubule Shortening Promoted by Kar3Cik1, Ncd, and MCAK

3.5.4 Figure 11 Legend

Microtubule Shortening Promoted by Kar3Cik1, Ncd, and MCAK

Microtubule•motor complexes were formed in the presence of MgAMPPNP and imaged at $t = 0$. MgATP plus an ATP regeneration system initiated microtubule depolymerization. (C, F, I) Merge of time 0 and 60 min to show microtubule shortening (yellow) compared to the original length (red). (C) The microtubules exhibited shortening from only one end in the presence of Kar3Cik1 plus 1.5 mM MgATP. Scale bar = 5 μ m. (F) Microtubule shortening from the plus end (*) of the microtubule in the presence of Kar3Cik1 and 1.5 mM MgATP. Scale bar = 5 μ m. Panels D-R are at the same magnification. (G-I) Microtubule shortening from the plus end (*) of microtubules in the presence of dimeric Ncd and 1.5 mM MgATP, the microtubule seed (\blacktriangledown) denotes the microtubule minus end. (J-O) Microtubule shortening from both ends promoted by *Xenopus* MCAK. (P-R) Conventional kinesin K401 did not promote microtubule shortening. The microtubule shortening rate is reported as nm/min \pm the standard error.

Table 2. Summary of Motor-Microtubule Depolymerization

Motor	Nucleotide	Taxol (μ M)	Microtubules n	Rate nm/min	Polarity Marked Microtubules			
					Microtubules n	Plus-End n	Minus-End n	Both Ends n
Kar3Cik1	ATP	≥ 3.0	269	0.0	0	0	0	0
Kar3Cik1	ATP	1.5	165	45.4 \pm 1.7	43	39	0	4
Ncd	ATP	≥ 3.0	51	0.0	0	0	0	0
Ncd	ATP	1.5	101	53.2 \pm 4.1	48	33	0	15
No Motor	ATP	≥ 3.0	76	0.0	0	0	0	0
No Motor	ATP	1.5	82	0.0	0	0	0	0
Kar3Cik1	AMPPNP	1.5	50	0.0	0	0	0	0
Ncd	AMPPNP	1.5	50	0.0	0	0	0	0
MCAK	ATP	20.0	27	812 \pm 540	27	0	0	27
MCAK	ATP	1.5	7	869 \pm 169	7	1	0	6
K401	ATP	≥ 3.0	50	0.0	0	0	0	0
K401	ATP	1.5	50	0.0	0	0	0	0

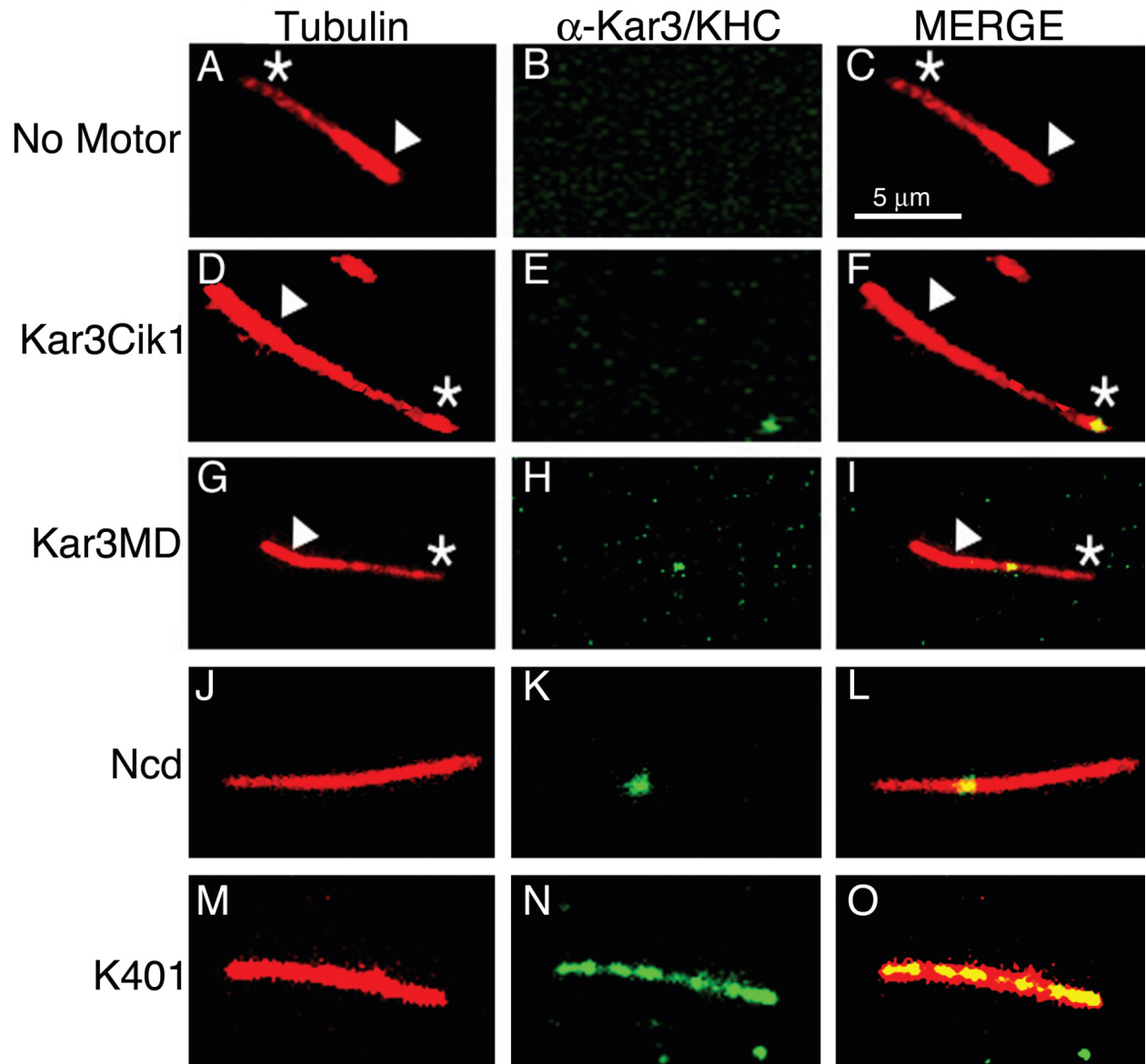


Figure 12. Immunolocalization of Kar3MD, Kar3Cik1, and Ncd

3.5.5 Figure 12 Legend

Immunolocalization of Kar3MD, Kar3Cik1, and Ncd

Microtubule•motor complexes were preformed in solution in the presence of MgAMPPNP, followed by glutaraldehyde fixation, and centrifugation through a glycerol cushion onto coverslips. The coverslips were processed for immunofluorescence. Final concentrations: 50 nM or 100 nM motor, 500 nM tubulin, 3 μ M Taxol, 1 mM MgAMPPNP. All panels represent the same magnification. Scale bar = 5 μ m. The microtubule seed (\blacktriangledown) marks the microtubule minus end, and (*) denotes the microtubule plus end extended from the seed. (A, D, G, J, M) Rhodamine-labeled tubulin. (B, E, H, K, N) Anti-Kar3/Kinesin fluorescence. (C, F, I, L, O) Merge of the two channels to show microtubule•motor co-localization.

Table 3. Summary of Motor•Microtubule Binding

[Motor]	Microtubules n	% Microtubules Bound (n)	% Localization Events on the Microtubule (n)		
			End	Lattice	Lattice and End
50 nM Kar3MD	420	6.0 (25)	20.0 (5)	80.0 (20)	0.0 (0)
100 nM Kar3MD	410	50.5 (207)	21.7 (45)	72.9 (151)	5.3 (11)
50 nM Kar3Cik1	797	37.4 (298)	48.0 (140)	26.5 (79)	25.5 (79)
100 nM Kar3Cik1	931	45.3 (422)	48.6 (205)	27.7 (117)	23.7 (100)
50 nM Ncd	251	46.6 (117)	29.9 (35)	49.6 (58)	20.5 (24)
100 nM Ncd	187	66.3 (124)	17.7 (22)	46.0 (57)	36.3 (45)
50 nM K401	51	66.7 (34)	2.9 (1)	20.6 (7)	76.5 (26)
100 nM K401	58	36.2 (21)	4.8 (1)	23.8 (5)	71.4 (15)
No Motor	291	4.8 (14)	21.4 (3)	64.3 (9)	14.3 (2)

4.0 CHAPTER THREE *ADDENDUM*:

4.1 **KAR3CIK1 AND BIK1, RESPONSIBLE FOR COORDINATING MICROTUBULE DEPOLYMERIZATION FROM THE PLUS ENDS DURING KARYOGAMY**

At the end of our study, detailed in Chapter Three, conflicting models existed to explain nuclear congression [167]. The simplest model was referred to as a “sliding cross-bridge” mechanism that arose from genetic and biochemical analysis of karyogamy [242]. The model postulates that after cellular fusion, anti-parallel microtubules slide past one another, overlapping and elongating at the plus ends, producing a bridge of microtubules of opposite orientations that interdigitate and possibly slide over the opposite nuclei. Kar3 (in complex with Cik1) was hypothesized to cross-link the microtubules and coordinate the microtubules sliding past one another, using its minus end directionality. Kar3 depolymerized the microtubules at the minus ends at the spindle poles, while at the same time sliding microtubules in a Kar3-dependent manner as the nuclei came together. This model had not been tested for minus end depolymerization of the microtubules. In addition, the ability to visualize the anti-parallel microtubule interactions has only recently existed. An unexplained tenet of this model was the mechanism by which the Kar3-dependent sliding and depolymerization are coordinated. However, as new imaging technology became available, these were hypotheses that could be resolved.

Though the “sliding cross bridge model” drew from genetics and biochemical *in vivo* and *in vitro* observations, there were inconsistencies between the model and reports of Kar3 in the literature. For example, the hypothesis that Kar3 was shortening microtubules only at the minus ends during karyogamy came from *in vitro* work showing Kar3 simultaneously gliding toward and destabilizing microtubules at the minus ends

[192]. However, earlier Kar3 localization *in vivo* showed the predominant localization of Kar3 was at the shmoo tip during karyogamy, which is where microtubule plus ends localize [169, 187]. These reports were published more than five years before a key publication by Maddox *et al.* that showed that microtubule polymerization and depolymerization occur primarily at the microtubule plus end in all tested stages of the life cycle of budding yeast [196]. This evidence combined with the early *in vivo* localization challenged the idea that Kar3Cik1 promoted minus end only depolymerization in karyogamy. Maddox *et al.* also found that the shmoo tip localization of Kar3 was specific to depolymerizing microtubule plus ends [165], suggesting Kar3 may play a role in microtubule shortening from the plus ends *in vivo*. Complementing this, our *in vitro* data characterized the interaction of Kar3Cik1 with the microtubule and showed Kar3Cik1, the motor responsible for karyogamy, to be targeted to the microtubule plus ends where it then shortens microtubules toward the minus ends [167]. This was in contrast to the Kar3 motor domain in the absence of Cik1 [167]. Our *in vitro* observation of Kar3Cik1-dependent microtubule shortening from the plus to the minus end, further suggests that localization to the microtubule plus ends at the shmoo tip may regulate the microtubule dynamics. This hypothesis was extremely viable in light of the multiple levels of regulation being discovered for microtubule plus end binding proteins [69, 243-246]. The conflicting results for Kar3 combined with better live cell imaging technology allowed the “sliding cross bridge model” to be tested, and led to consideration of alternative hypotheses to account for nuclear fusion.

Following our publication of Cik1 targeting Kar3 to the microtubule plus end *in vitro* [167], an elegant study by Molk *et al.* was published detailing the mechanism of how nuclei fuse in karyogamy. This mechanism characterized previously unknown roles for microtubule plus end binding proteins in facilitating karyogamy [168]. The work validated our *in vitro* observations *in vivo* during karyogamy. The authors showed that microtubule plus end interactions drive the nuclear fusion event (Figure 8, steps 5 & 6) [168]. To accomplish the study, Molk *et al.* examined a different model, the “plus end model” which predicts that following cell fusion the linkage of microtubules between the two nuclei is a product of the anti-parallel microtubule plus ends interacting at a discrete site with little to no sliding overlap (Figure 8, step 5). This interaction is thought

to be driven by the plus end binding proteins from the original two shmooing cells coming into close proximity with each other as a result of the oppositely oriented microtubules and forming complexes (Figure 8, steps 4 & 5). Support for this hypothesis came from the fact that several proteins that bind to the plus ends of microtubules were essential for karyogamy. These proteins include Kar3, Bim1, Bik1, and Kip2 [168, 242, 245, 247, 248]. Bim1 is the EB1 homolog that in yeast is found on microtubule plus ends. Bim1 is required because it links the polymerizing microtubules to the cortical actin cytoskeleton [16, 165, 238, 249]. The actin cytoskeleton forms the shmoo and orients the nucleus for cell and nuclear fusion in the shmoo tip. Bik1, the Clip-170 orthologue in yeast is a plus end tracking protein, important for microtubule stability and growth into the shmoo tip, found in yeast to localize to both polymerizing and depolymerizing microtubule plus ends [245, 248, 250-253]. Bik1 is loaded onto the plus end via transport to the plus end by orphan kinesin Kip2 [248, 254]. To define the mechanism of nuclear congression *in vivo*, microtubules and plus end binding proteins were analyzed in mating *Saccharomyces cerevisiae* [168].

The study found that prior to nuclear fusion, the microtubule plus end proteins Kar3 (Kinesin-14), Bik1 (CLIP-170 orthologue), and Kip2 (orphan kinesin) were required at the plus end to anchor the microtubule plus ends to the shmoo tip. In yeast, Kar3 is found to target the plus ends of microtubules in a Cik1-dependent manner [167, 187, 188]. Following cell fusion it was found that the plus ends interacted near the site of cell wall fusion and that Bik1 and Kar3 were found to colocalize at this site (Figure 8, step 5 and ref. [168]). The positions of the microtubule plus ends, Bik1, and Kar3 remained unchanged as the nuclei congressed to fuse. Here the authors used cell lines expressing Bik1-3XGFP, Kar3-GFP, and CFP- or GFP-Tub1. When the authors visualize the plus ends, they see localization of Bik1, Kar3 and Tub 1 to a “discreet” site of interaction. However, one must remember that the resolution limit of the light microscope is theoretically ~ 200 nm, and with GFP fluorescence ~ 300-500 nm. Thus, the proposed site of plus end interactions could cover as much distance, suggesting that the colocalizations may not be exact, and that microtubule overlap could occur over this distance. In fact in the paper published by Molk *et al.* the site of Bik1-3XGFP corresponds to approximately 1 μm in length as estimated by their scale bar (Figure 5B,

in ref. [168]) The authors examined the hypothesis that microtubules slide past one another to form an anti-parallel array by assaying GFP-tubulin fluorescence between the two nuclei. The authors speculate that if the anti-parallel plus ends overlapped and slid past one another to a great extent (over 1 μm in this case), an increase in GFP-Tubulin fluorescence would be observed between the nuclei, however if the overlap was minimal or just at the very plus end, no increase in fluorescence would be observed. No dramatic increase in fluorescence was observed in wild-type cells expressing GFP-Tubulin, suggesting that the microtubules do not significantly overlap or slide past one another. Instead, they seem to interact at the plus ends only, with possible overlap of 0.3 - 1 μm (Figure 6C, in ref. [168]), at the site where bands of Kar3 and Bik1 fluorescence colocalize *in vivo* [168].

Deleting Kar3 did cause the anti-parallel microtubule plus ends to slide past one another, as an increase in GFP-tubulin fluorescence between the nuclei was observed in *kar3 Δ* cells in contrast to wildtype cells [168]. In addition, the nuclear fusion step was blocked [168]. Microtubules were longer than wild-type, and no depolymerization was observed (Figure 9A, Video 9, in ref. [168]). These results suggest that Kar3 is required to both initiate oppositely oriented microtubule plus end interactions and to drive microtubule depolymerization while promoting persistent plus end interactions. This result also suggests that anti-parallel microtubule sliding is insufficient to fuse nuclei, and microtubule depolymerization is the essential driving force. Deletion of Bik1 resulted in shorter microtubules that underwent rapid depolymerization and failed to fuse their nuclei as a result [168]. Bik1 is delivered to the microtubule plus end via Kip2. In Kip2 deleted cells Bik1 localization is diminished greatly at the shmoo tip and microtubules do not maintain persistent attachment to the shmoo tip, yet karyogamy can occur [168]. In addition, the linkage between the anti-parallel microtubule plus ends following cell fusion was aberrant in Kip2 deleted cells [168]. Therefore, the role of Bik1 was found to promote shmoo tip attachment by stabilizing microtubule growth during karyogamy and to promote persistent microtubule plus end interactions to facilitate depolymerization leading to nuclear fusion. This study showed that the minimal components necessary for nuclear fusion were wildtype microtubules, Kar3, and Bik1 [168].

The current model for karyogamy is that Kar3 is targeted to the microtubule plus ends, where Kar3 then uses its motor activity to effectively cross-link the microtubule plus ends following cell fusion. Molk and colleagues propose that Kar3 may slide the microtubules over a very short distance ($\sim 1 \mu\text{m}$) before initiating coordinated depolymerization. Kar3 then coordinates depolymerization, and, along with Bik1, promotes persistent microtubule interactions. This study provides a novel mechanism for karyogamy, based on an in-depth view that was previously technically impossible. Here nuclear fusion is driven by plus end binding proteins and microtubule based motors via persistent interaction of depolymerizing plus ends [168]. It may be that Kar3Cik1 and Bik1 form a complex at the plus ends to promote depolymerization of the microtubules to fuse the nuclei, analogous to the Dam1 ring used in mitosis [255]. Unfortunately, the study did not take into account the role of Cik1 in complex with Kar3 found at the plus end, though genetic data argue that Cik1 must be present for Kar3 to interact with cytoplasmic microtubules [187, 188]. Our *in vitro* data argue that Cik1 aids directly in targeting Kar3 to the microtubule plus ends [167]. As Kar3Cik1 shows a marked affinity for the microtubule plus end (Chapter Three, Figure 12) [167], Cik1 in a heterodimeric complex with Kar3 may play an important role in initiating the primary interaction site of the oppositely oriented microtubule plus ends. As *in vivo* imaging improves, the exact role of Cik1 for karyogamy can be examined further.

4.2 KAR3 AT THE KINETOCHORE, BIK1 TOO

In addition to the Molk *et al.* study, Tytell and Sorger [164] published a study examining kinesin function at kinetochores. By looking at GFP-Kar3 during mitosis, Tytell and Sorger find that Kar3 functions specifically at a subset of kinetochores on which microtubule attachments are slow to form, or improperly attached [164]. They report that the major kinetochore motor inducing depolymerization is the Kinesin-8, Kip3 [164]. Subsequent to this report, Gupta *et al.* detailed the mechanism of Kip3 finding it to be a plus-end directed motor, different from Kar3, but like Kar3, a plus-end specific depolymerase [256]. In addition, the Gupta analysis showed that Kip3 behaves similar

to Kinesin-13s in that it binds to and is stimulated by soluble tubulin [256]. Therefore, based on these findings we predict the Kar3 role at the kinetochore to be different from that of Kip3 and the Kinesin-13 kinetochore motors. At the kinetochore, Kar3 may play an important role in specifying the correct microtubule attachments, similar to the coordination of the anti-parallel microtubule interactions in karyogamy, as observed by Molk et al. [168]. Bik1 is also required for mitosis and is essential for a subset of kinetochore microtubules [245, 251, 253, 257, 258]. Bik1 may be essential for the same subset of microtubules that Kar3 associates with at the kinetochore. The interaction of Kar3 and Bik1 at kinetochores has not been examined. Here, Kar3 and Bik1 may also interact to coordinate proper or persistent attachment and depolymerization at those kinetochores that are slow to attach, or improperly attached. Future work will involve examining the role of these two together at kinetochores. Our data, combined with genetics, predict that it is Kar3Cik1 at this subset of kinetochores while Kar3Vik1 is acting at microtubule minus ends at the spindle poles [167, 187, 188]. Again, this study did not take into account Cik1, and thus a look at Cik1 and Kar3 at the kinetochore will help to better define the roles of Kar3Cik1 separate from those of Kar3Vik1 *in vivo*.

5.0 KAR3VIK1, A KINESIN-14 THAT USES A “DEAD” HEAD TO BIND THE MICROTUBULE AND GENERATE FORCE

5.1 ABSTRACT

The Kar3 Kinesin-14, found in *Saccharomyces cerevisiae*, forms one of two heterodimers with non-catalytic proteins Cik1 and Vik1 for function *in vivo*. Kar3Vik1 is the predominant Kar3 motor that functions during mitosis and vegetative growth. In this study, we present the first *in vitro* characterization of the Kar3Vik1 heterodimer. We compare Kar3Vik1 to Kar3Cik1, the Kar3MD, and to the Vik1MHD. We show that Kar3Vik1 can robustly glide microtubules like Kar3Cik1 with minus end directionality. Unlike Kar3Cik1, Kar3Vik1 exhibits weak depolymerizing capability. In contrast to Kar3Cik1, which targets the microtubule plus end, Kar3Vik1 exhibits microtubule saturation by cooperatively binding to a subset of microtubules while not binding at all to others. Our data show that the Vik1MHD binds the microtubule in the absence of the Kar3 motor, and the Vik1MHD can saturate the microtubule lattice. The affinity of Vik1MHD for the microtubule is tight ($K_{d, MT} = 43$ nM). Both Kar3Vik1 and Kar3MD exhibit weaker binding to the microtubule in the presence of AMPPNP, which mimics the ATP-bound state. Interestingly, under conditions of MgADP we find Kar3Vik1 has an affinity for the microtubule like the Vik1MHD in the absence of Kar3 ($K_{d, MT} = 38$ nM). In contrast, the Kar3MD in the absence of Vik1 has a very weak affinity ($K_{d, MT} = 223$ nM). The results suggest that Kar3Vik1 is a non-processive Kinesin-14 like Ncd. We propose a model in which Kar3Vik1 motors toward the spindle poles to crosslink and focus the microtubule minus ends for bipolar spindle stability.

5.2 INTRODUCTION

Kinesin motor proteins are subject to many levels of regulation and modulation *in vivo*; these regulations and modulations for kinesins determine the specific cellular functions [24, 259-261]. For the *Saccharomyces cerevisiae* kinesin motor Kar3, different roles are determined in part by the complex that Kar3 forms during the yeast life cycle [167, 187-189, 262]. *In vivo*, the Kar3 motor forms a heterodimer with either Cik1 or Vik1 for localization and function [167, 187-189, 262]. *In vitro*, the Kar3 motor domain has been shown to be a minus end directed motor [192, 193] with the ability to destabilize microtubules predominantly from the plus ends [167, 192, 262]. Genetic studies show that the Kar3 and Cik1 genes are both essential for meiosis I and karyogamy, the nuclear fusion event that occurs during mating yeast (Figure 8) [169-172, 186, 187, 189, 190]. In contrast, it is Kar3 and Vik1 that play the predominant roles during vegetative growth [188]. Both Kar3 and Cik1 are proteins whose expression is increased approximately 20-fold upon exposure to mating pheromone [169, 186]. Both genes contain pheromone response elements located upstream of their exons [169, 186]. The Vik1 gene lacks response elements, thus protein expression does not increase in the presence of pheromone, and Vik1 has not been shown to participate in karyogamy [188].

The genetic data suggest that the role of Kar3Vik1 is distinct from that of Kar3Cik1 [188]. While the Kar3 and Cik1 deletion phenotypes are identical for karyogamy, they differ for vegetative growth [169, 186, 187]. In addition, during mitosis, BimC/Kinesin-5 subfamily members, Cin8 and Kip1, are responsible for establishing and maintaining the mitotic spindle in yeast. These Kinesin-5 motors are functionally redundant, but the double deletion results in spindle collapse [12, 173]. However, deleting Kar3 can suppress the deletion phenotype of these plus end directed kinesins [12, 173]. These results suggest that the balance of forces within the spindle is maintained by kinesins with opposing directionalities. Cik1-deleted strains exhibit temperature sensitive growth and a severe chromosomal loss defect [186]. However, a *cik1* Δ cannot suppress the spindle collapse phenotype of *cin8* Δ *kip1* Δ [187, 188]. Furthermore, the vegetative localization of Kar3 in wildtype cells is predominantly at the

SPB, with faint localization on spindle and cytoplasmic microtubules [187, 188]. Deleting *Cik1* does not change the predominant *Kar3* localization pattern at the SPB, but the spindle and cytoplasmic microtubule localization is lost [187, 188]. These genetic and indirect immunofluorescence results suggested that *Kar3* had *Cik1* independent mitotic functions, and perhaps *Kar3* formed a complex with another protein.

A database search of the yeast genome for proteins with amino acid sequence homology to *Cik1* yielded an open reading frame with significant sequence homology to the *Cik1* protein [188]. The gene was cloned and named *Vik1* for vegetative interaction with *Kar3* [188]. The *Vik1* protein showed 24% sequence identity and 37% similarity to *Cik1* [188]. *Vik1* also shared predicted structural homology to *Cik1* and was tested as a candidate for *Kar3* complex formation during vegetative growth [188]. Immunoprecipitation of *Kar3* or *Vik1* found the two in complex [188]. Genetic experiments examining *Vik1* contrasted with those of *Cik1*. Deletion of *Vik1* resulted in loss of *Kar3* localization at the SPB, and an increase in spindle microtubule localization that was dependent upon *Cik1* [188]. Moreover, both spindle pole body and spindle microtubule localization is lost in the *cik1Δvik1Δ* double deletion. These phenotypes suggest that it is *Vik1* that is required to restrict *Kar3* localization to the SPB [188]. Microtubules in *vik1Δ* cells look like wildtype, whereas those in *cik1Δ* are shorter in the spindle and longer in the cytoplasm [186-188]. Deletion of *Vik1*, like *Kar3*, can suppress the *cin8Δkip1Δ* phenotype, providing more evidence that the *Kar3* mitotic role to counter balance the forces of the microtubule plus end directed motors in the spindle requires *Vik1* [188]. These genetic experiments showed that *Cik1* and *Vik1* are not redundant and likely confer different microtubule-based roles to *Kar3* [188].

Because both *Vik1* and *Cik1* are expressed during vegetative growth, participate in mitosis, and form heterodimers with *Kar3*, dissecting the roles of microtubule interaction of *Kar3Vik1* from *Kar3Cik1* has been challenging [188]. To complicate matters further, *Saccharomyces cerevisiae*, unlike higher eukaryotic organisms, undergoes closed mitosis, meaning that the nuclear membrane in fungi remains intact during the life cycle. Because of the small size of the yeast cell, one cannot easily resolve the individual microtubules at the spindle pole body or those within the spindle.

Our previous work with Kar3Cik1 focused on questions surrounding the events in karyogamy, which are restricted to Kar3Cik1 function, and tested *in vivo* observations about the microtubule•Kar3Cik1 interaction *in vitro* to reveal how the Kar3Cik1 complex specifically interacted with the microtubule [167]. We took a similar approach to understand Kar3Vik1, comparing Kar3Vik1 function *in vitro* to Kar3Cik1.

In the *in vitro* studies presented here, we have determined the specific Kar3Vik1 interactions with the microtubule to compare with Kar3Cik1, the Kar3MD, and Vik1 in the absence of Kar3. We characterized the unique interactions each motor has with the microtubule to test the hypothesis that the distinct cellular functions of Kar3Vik1 and Kar3Cik1 can be explained by their intrinsic heterodimeric mechanochemical properties. This is also the first study to define the properties that two separate accessory polypeptides confer to the same kinesin motor domain. We find that Vik1 modulates the kinesin motor Kar3 and its interaction with the microtubule in a very different manner as compared to Cik1. We show that the mechanism of microtubule•Kar3Vik1 interaction is novel for a kinesin and in contrast to the plus end targeting we observed for Kar3Cik1 on the microtubule (Chapter Three and ref. [167]).

5.3 RESULTS

5.3.1 Kar3Vik1 is a Minus End Directed Motor

To pursue structural studies, a smaller Kar3Cik1 heterodimer was designed as described in Materials and Methods. This heterodimer is slightly smaller than the Kar3Cik1_L studied in Chapter Three. We engineered a similar Vik1 construct to heterodimerize with the same Kar3 motor as described in Materials and Methods, Chapter Two. The smaller Kar3 motor was engineered for minimal heterodimer formation, as compared to the longer Kar3 expressed in the Kar3Cik1_L heterodimer used in Chapter Three [167]. The Kar3 motor was co-expressed with either Cik1 or Vik1 to form heterodimers through N-terminal coiled-coil interaction. Kar3Cik1, Kar3Vik1, the Vik1MHD and the Kar3MD were purified for comparison (Figure 13). The

proteins elute as > 99% pure from the gel filtration columns as heterodimers with 1:1 stoichiometry (Figure 13C). The C-terminal globular domain of Vik1 was predicted to be in close proximity to the Kar3 catalytic domain [188]. The Vik1 small globular domain shares overall structural identity with kinesin motor domains (our unpublished results in collaboration with Drs. John Allingham and Ivan Rayment), and will be referred to as the Vik1 Motor Homology Domain (Vik1MHD). The heterodimers are retained in the gel filtration column as dimeric kinesin proteins of the expected size (Figure 13B).

To verify the motor activity of Kar3Vik1 and Kar3Cik1, polarity-marked microtubule gliding was assayed in the presence of 1.5 mM MgATP. Kar3Vik1 and Kar3Cik1 both robustly glide microtubules (Supplemental Movies S1 and S2), (Figure 14A). Kar3Vik1 glides microtubules at a rate of $3.14 \pm 0.05 \mu\text{m}/\text{min}$, while Kar3Cik1 glides microtubules at a rate of $2.94 \pm 0.05 \mu\text{m}/\text{min}$. Both motors promote microtubule movement of polarity-marked microtubules with the plus ends leading, indicative of minus end directionality as published for both GST-Kar3 [192] and for Kar3Cik1 [167, 262] (Figure 14A, Table). Figure 14A demonstrates an example of minus end directionality where a polarity-marked microtubule glides over time relative to stationary microtubules, with the dim plus end leading in the presence of Kar3Vik1 and MgATP.

5.3.2 Kar3Vik1 Steady State ATPase

The steady state ATPase kinetics of Kar3Vik1 and Kar3Cik1 (Figure 14B) were examined as a function of either microtubule [Figure 14B (upper panel)] or MgATP [Figure 14B (lower panel)] concentration. Both Kar3Vik1 and Kar3Cik1 have faster steady-state k_{cat} rate constants at 3.7 s^{-1} , and 2.8 s^{-1} compared to the Kar3MD at 0.49 s^{-1} [240], and exhibit tighter apparent microtubule affinity at 2.0 and 1.7 μM for Kar3Vik1 and Kar3Cik1 respectively, compared to 6.0 μM for the Kar3MD. These data are indicative of Kar3 motor modulation by Vik1 and Cik1. The following studies were designed to provide further insight into the roles that Vik1 and Cik1 have on the microtubule•Kar3 interaction.

5.3.3 Kar3Cik1 is a More Robust Microtubule Depolymerase than Kar3Vik1

To determine if Kar3Vik1, like GST-Kar3 [192] and Kar3Cik1 [167, 262] could depolymerize microtubules, time-lapse microscopy of microtubules in the presence of Kar3Vik1 and Kar3Cik1 was performed under depolymerizing microtubule conditions. The assay was changed from that used to image Kar3Cik1_L depolymerization in Chapter Three [167], as detailed in the Materials and Methods in Chapter Two, such that the depolymerization was performed in the absence of a microtubule tether to the glass through poly-L-Lysine coating. Instead, the MT•Kar3Vik1 or MT•Kar3Cik1 complexes in the presence of MgAMPPNP were flowed into observation chambers, and the N-terminal tails of the heterodimers containing His-tags (See Figure 13) were allowed to interact with the glass. Complexes that failed to interact with the glass were washed away, and microtubule depolymerization was initiated by flowing in MgATP. Kar3Vik1, like Kar3Cik1 [167] shortens microtubules in the presence of MgATP (Figure 14C). No microtubule shortening was observed in the presence of MgAMPPNP (*data not presented*). The rates observed for Kar3Vik1 *versus* Kar3Cik1 differ significantly. The rate observed for Kar3Vik1 (0.25 $\mu\text{m}/\text{min}$) is slower than that observed for Kar3Cik1 at 0.69 $\mu\text{m}/\text{min}$ by more than a factor of two. The rate observed for Kar3Cik1 accounts for the fast rates observed for karyogamy *in vivo* [168], a process primarily dependent on Kar3Cik1-promoted microtubule depolymerization [168]. Both motors shorten microtubules from the microtubule ends; however, the plus-end specificity is most pronounced for Kar3Cik1 (Figure 14C, Table). The Kar3Vik1 results are similar to the results observed for Ncd depolymerization reported in Chapter Three [167]. Both motors seem to depolymerize non-specifically from both microtubule ends, whereas Kar3Cik1 clearly prefers to depolymerize from the microtubule plus-end. No direct role for Kar3Vik1-promoted microtubule depolymerization has been observed *in vivo* [179, 184, 188, 190], and the weaker depolymerizing ability it retains *in vitro* may be a capability that is intrinsic to Kar3 [167, 168, 193], but one that is inhibited when in complex with Vik1, and/or down regulated *in vivo*.

5.3.4 Kar3Vik1 Cooperative Binding Inhibits Microtubule Depolymerization

Both Kar3Vik1 (Figure 16, Table) and Kar3Cik1 [167] (Figure 16, Table) have the ability to bind the microtubule lattice. Kar3Vik1 exhibits cooperative binding for microtubule saturation, in that it will completely coat a few microtubules in a field, while leaving most microtubules free of motor (Figure 16A-F, J-O and Table). This behavior is indicative of cooperative microtubule binding and was not observed for either the Kar3MD or Kar3Cik1 (Figure 16, Table, and ref.[167]). To determine if the cooperative binding leads to microtubule stabilization against microtubule shortening, we assayed microtubule shortening at three different motor concentrations for both Kar3Cik1 and Kar3Vik1. The rates and the percentages of microtubule shortening in the presence of increasing motor concentrations are plotted in Figure 14D. Both the rate and the percentage of microtubules shortened decreased as motor concentration increased. However, it should be noted that in all cases Kar3Cik1 retained the ability to shorten microtubules more robustly than Kar3Vik1.

5.3.5 Kar3Vik1 Microtubule Binding Properties – Cosedimentation Experiments

To examine the microtubule binding affinity of Kar3Vik1, microtubule co-sedimentation assays were performed looking at the microtubule affinity of Kar3Vik1, the Kar3MD, and the Vik1MHD. The Vik1MHD and the SeMetVik1MHD are both monomeric and both bind the microtubule very tightly (Figure 15), as compared to the Kar3MD under all conditions examined (Figure 15A and Table). Kar3Vik1 also binds the microtubule tightly (Figure 15B and Table); the tightest microtubule affinity is exhibited when 2 mM MgADP is present. In contrast, the Kar3MD exhibits the weakest microtubule affinity under these conditions. Please note that most of the Kar3Vik1 and Kar3MD is bound to the microtubule in the presence of 2 mM MgAMPPNP or Apyrase treatment, to achieve a nucleotide-free state. However, the overall percentage of binding for both Kar3Vik1 and the Kar3MD in the presence of 2 mM MgADP is reduced. For Kar3Vik1, only 54 % of the motor partitions with the microtubules at 2 mM MgADP, yet approximately 94 %

bound to the polymer under nucleotide-free conditions or in the presence of AMPPNP. Kinesins normally exhibit weak microtubule binding with MgADP at the active site [200, 263]. Therefore, the increased affinity of Kar3Vik1 for the microtubule under MgADP conditions is atypical, suggesting that the tight affinity observed is governed by Vik1. The Kar3Vik1 + MgADP K_d is very similar to the K_d of the Vik1MHD and the SeMetVik1MHD. The fact that not all motors bind under these conditions suggests that cooperative interactions within the heterodimer between Kar3 and Vik1 are being governed by the MgADP bound at the Kar3 active site. The ADP-bound state weakens the Kar3 affinity for the microtubule, resulting in a similar decrease in percentage of Kar3 binding to the microtubule as observed for the Kar3MD + 2 mM MgADP (Figure 15A).

5.3.6 Immunolocalization of Kar3Vik1 on the Microtubule

To determine if Kar3Vik1 or the Vik1MHD has a higher affinity for a microtubule end versus the microtubule lattice like Kar3Cik1, we performed immunolocalization experiments. The microtubule-motor complex was performed in the presence of AMPPNP to trap the collision complex. Glutaraldehyde was added immediately to fix the microtubule-motor complexes followed by centrifugation through a glycerol cushion onto coverslips. The coverslips were then processed for immunofluorescence using affinity-purified antibodies to either native Kar3MD or Vik1MHD (Figure 13C – Western Blot). We find that Kar3Vik1 binds microtubules cooperatively (Figure 16A-F,J-O, and Table), saturating the microtubule lattice, whereas Kar3Cik1 targets microtubule ends [ref. [167] and Figure 16, Table], and the Kar3MD shows a binding preference for the microtubule lattice [ref. [167] and Figure 16, Table]. The Vik1MHD exhibited unique microtubule binding properties, in that at low Vik1MHD concentrations, Vik1MHD exhibited punctate microtubule binding with an end preference (Figure 16P-R, and Table). However, as the Vik1MHD concentration increased, the microtubule lattice became saturated with Vik1MHD (Figure 16S-X, and Table).

5.4 DISCUSSION

5.4.1 Kar3Vik1 and Kar3Cik1: Two Distinct Kinesin-14 Motors

Our data provide the first *in vitro* characterization of the Kar3Vik1 heterodimeric Kinesin-14. We show that Kar3Vik1 is a motor and that its ATPase is stimulated by microtubules (Figure 14B). Both Kar3Vik1 and Kar3Cik1 have a faster ATPase than the Kar3MD, suggesting that interaction with the Vik1 and Cik1 polypeptides provides a more effective ATPase. Kar3Vik1 has a higher steady-state k_{cat} , as compared to Kar3Cik1. These complexes are functionally distinct *in vivo*, and the differences we observe *in vitro* are likely linked to their unique *in vivo* roles. Like GST-Kar3 and Kar3Cik1, Kar3Vik1 can glide microtubules, exhibiting minus end directionality (Figure 14A). The *in vivo* localization of Kar3Vik1 is restricted to the SPB where the minus ends of microtubules are localized. Therefore, the minus end directionality may be relevant for the specific *in vivo* localization and function of Kar3Vik1 at the spindle poles. We show that Kar3Vik1 depolymerizes microtubules *in vitro*, but unlike Kar3Cik1, it does not show a plus end preference for depolymerization (Figure 14C). Another difference is in the rate of microtubule shortening. Kar3Vik1 depolymerization is much slower than Kar3Cik1 (Figure 14C, Table). The rate difference may reflect the fact that the modulation of the Kar3 motor by Vik1 is different from the way in which Kar3 and Cik1 interact. As there is no direct *in vivo* evidence for Kar3Vik1 to depolymerize microtubules, this slower rate may indicate Vik1 inhibition of the Kar3 motor depolymerizing capabilities. Support for this hypothesis is evidenced by our experiments showing inhibition of Kar3Vik1-promoted microtubule shortening as the concentration of Kar3Vik1 binding to the microtubule increased (Figure 14D). The Kar3Vik1 immunolocalization on the microtubule differed greatly from the Kar3Cik1 immunolocalization previously discussed [Chapter Three and ref.[167]]. While Kar3Cik1 accumulates on the plus ends of microtubules *in vitro* and *in vivo* [164, 165, 167, 169, 184, 185, 193], Kar3Vik1 was found to saturate the microtubule at all concentrations (25 nM -100 nM) examined (Figure 16, Table). This binding behavior was similar to the

microtubule interactions previously described for Kinesin-14 homodimeric *Drosophila* Ncd [264].

5.4.2 The Vik1MHD Binds Microtubules in the Absence of Kar3

To test the hypothesis that Vik1 was directly interacting with the microtubule to enhance the binding of the Kar3 motor and to promote the cooperative binding we observed for Kar3Vik1, we examined the microtubule localization of the Vik1MHD (Figure 17). At low concentrations, the Vik1MHD displays a preference for binding to a subset of microtubule ends, in a given field, with binding observed predominantly at one end. However, as the Vik1MHD concentration was increased, the binding became cooperative, saturating the lattice of a few microtubules in the field, similar to Kar3Vik1. We propose that the Kar3Vik1-promoted microtubule saturation binding observed is driven by Vik1. These results indicate that Cik1 and Vik1 differentially modulate Kar3 interactions with the microtubule.

5.4.3 Kar3Vik1 Exhibits Strain Dependent Cooperativity

Further evidence for Vik1 modulation of Kar3 by its intrinsic microtubule binding is shown by our equilibrium binding experiments in Figure 15. The Vik1MHD and the SeMetVik1MHD both bind the microtubule with greater affinity than either the Kar3MD or Kar3Vik1 with apyrase treatment or with MgAMPPNP bound (Figure 15A & B). However, Kar3Vik1 with MgADP bound exhibits tight affinity like the Vik1MHD for the microtubule (compare Figure 15A & B), yet not all motors are bound under these conditions. This result suggests that the tight affinity for the microtubule displayed by approximately 50% of the Kar3Vik1 motors in the presence of 2 mM MgADP is dependent upon the Vik1 subunit. However, the Kar3 subunit with ADP bound at the active site has a weak affinity for the microtubule (examine the Kar3MD + ADP, Figure 15A). These results suggest that the Vik1 subunit would be tightly bound to the microtubule, tethering the detached Kar3 motor that points toward the minus end of the microtubule as observed for Ncd [264]. However, it is difficult to reconcile how a force

generating mechanism would begin from this intermediate to generate minus end directed movement because the microtubule affinity of the Vik1 subunit cannot be modulated through ATP turnover like Kar3, as it lacks an active site.

Rather, we present the following non-processive model (Figure 17) for Kar3Vik1 translocation along a microtubule. We propose that Kar3Vik1 may be similar to Ncd, a non-processive dimeric Kinesin-14, that moves a microtubule cargo along an adjacent microtubule. After its ATPase cycle both heads detach from the microtubule [200, 201, 264-266]. Ncd focuses minus ends at spindle poles by bridging two parallel microtubules using N-terminal microtubule binding sites in addition to the microtubule interface found on the C-terminal kinesin head [267, 268]. We propose that like Ncd, Kar3Vik1 contains a microtubule-binding site within the N-terminus that is not nucleotide dependent, and this site binds another microtubule as its cargo. Similar sites have been proposed for Kar3, and provide another explanation for Kar3Vik1 minus end localization and microtubule focusing [169, 187, 188]. In our model (depicted in Figure 17), the collision of the Vik1MHD with the microtubule (Figure 17A) results in a series of structural transitions that are communicated to the Kar3MD, promoting its binding to the microtubule at a β -tubulin site 16 nm away from Vik1 (Figure 17B). ADP is rapidly released from Kar3 leading to a tightly bound Kar3Vik1 intermediate. ATP binding by Kar3 results in an approximate 90° rotation of the neck-stalk domain, generating additional strain between the two heads (Figure 17C). This action pulls Vik1 off the microtubule and displaces the microtubule cargo. Hydrolysis of ATP generates the weak binding state of Kar3Vik1, and it detaches from the microtubule competent to begin another cycle. There are two requirements for this model: 1) The neck-stalk domain between the two heads must melt or unzip sufficiently to allow for binding to two β -tubulin subunits along the same protofilament. 2) The rotation that we propose for the neck-stalk must be non-reversible toward the minus end of the microtubule to prevent back binding of the Vik1 head that would lock the motor in a tightly bound, non-productive state. While this may be an attractive hypothesis for how Kar3Vik1 accumulates at the spindle pole as motors translocate toward the minus ends of the microtubules we propose that this must be inhibited along the lattice if Kar3Vik1 is translocating microtubule cargoes to the minus ends. In this model, we assume that

there are multiple Kar3Vik1 motors working in concert; therefore, a need for processivity as observed for conventional Kinesin-1 may not exist. However, if future studies reveal that Kar3Vik1 is processive, we predict this motor to be an excellent candidate for movement by an “inchworm mechanism [269].” As an alternative to our model, we must also suggest that Kar3Vik1 may be the best candidate of a kinesin motor that binds side by side protofilaments using the two heads. In this case, one would assume the neck-stalk would remain more rigid and not unzip or melt as proposed above for the translocation along a single protofilament.

The accumulation of Kar3Vik1 at the spindle poles may simply occur because the motors reach the minus end of the microtubule where there are no free microtubule binding sites. In this case, Kar3Vik-ADP would be the predominant intermediate, remaining tightly bound to the microtubule and acting to cross-link and focus the microtubules at the spindle pole bodies.

5.4.4 Functional Role of Kar3Vik1 in Mitosis

Our *in vitro* findings parallel the Kar3Vik1 mitotic phenotypes observed *in vivo*. We show that Kar3Cik1 and Kar3Vik1 are very different motors, and our results suggest that Kar3Vik1 is more similar to the Kinesin-14 Ncd than Kar3Cik1, consistent with the yeast genetics. We observe Kar3Vik1 saturating the microtubules using immunofluorescence; these data support the intense *in vivo* localization seen for Kar3Vik1 at microtubule minus ends early in mitosis. The localization is thought to focus and stabilize the yeast microtubule minus ends at the spindle pole body for bipolar spindle formation [8, 12, 173-175]. The cooperative binding we observe may account for this stabilization. Loss of Vik1 leads to loss of Kar3 at the spindle poles [188], and a Kar3 deletion leads to an increase in inviable cells with a mitotic block and to an overproduction of cytoplasmic microtubules [8, 169, 173, 174, 187, 188]. In *Schizosaccharomyces pombe*, two Kar3 homologs exist, Pkl1 and Klp2 (**P**ombe **k**inesin like 1 & **K**inesin like protein 2) [270]. These proteins are predicted to form homodimeric Kinesin-14s [270]. Interestingly, Pkl1 seems to perform the functions of Kar3Vik1, while Klp2 is more similar to Kar3Cik1 in function [270]. Overexpression of Kar3 or Pkl1, the Kar3Vik1 homolog found in *S.*

pombe, results in splayed, V-shaped spindle poles [12, 271]. These are phenotypes similar to those observed for the minus-end directed motor, Ncd, when a null allele is used, or loss of function alleles for the Kinesin-5 subfamily members are examined [7, 8, 272-277].

The role of Ncd in *Drosophila* meiosis and mitosis is to slide and focus microtubule minus ends for proper spindle formation [212, 272, 278, 279]. Ncd has been shown to oppose the Kinesin-5 subfamily member KLP61F; similarly Kar3Vik1 opposes the forces of Kinesin-5s, Cin8 and Kip1, contributing to spindle stability [12, 173, 175, 187, 188, 280]. In the absence of Cin8 and Kip1, the spindle collapses [7, 8, 274]. This phenotype can be suppressed with either a *kar3Δ* or a *vik1Δ* [173, 188]. In this manner, Kar3Vik1 may act like the *Drosophila* Ncd, sliding and focusing microtubule minus ends in the spindle. In addition, Ncd and Kar3Vik1 both display similar cell cycle-dependent spindle pole mitotic functions. Both are required early in mitosis [7, 8, 188, 272]. Recent work with Ncd has suggested that only one head of Ncd has to be catalytic and interactive with the microtubule for Ncd force generation, suggesting more similarity between the two motors [281, 282]. The tight lattice binding, displayed by both Kar3Vik1, and Vik1MHD, combined with the depressed microtubule depolymerizing activity of Kar3Vik1 we observed, complements the *in vivo* Kar3Vik1 genetic and localization data. Kar3Vik1 is a motor very unlike Kar3Cik1. As such, we propose that Kar3Vik1 uses cooperative microtubule binding and the robust gliding properties to properly transport microtubules and focus microtubule minus ends at the spindle pole body, in a manner more like the Ncd Kinesin-14 motor, and less like Kar3Cik1, more similar to the depolymerizing kinesins Kip3 and MCAK.

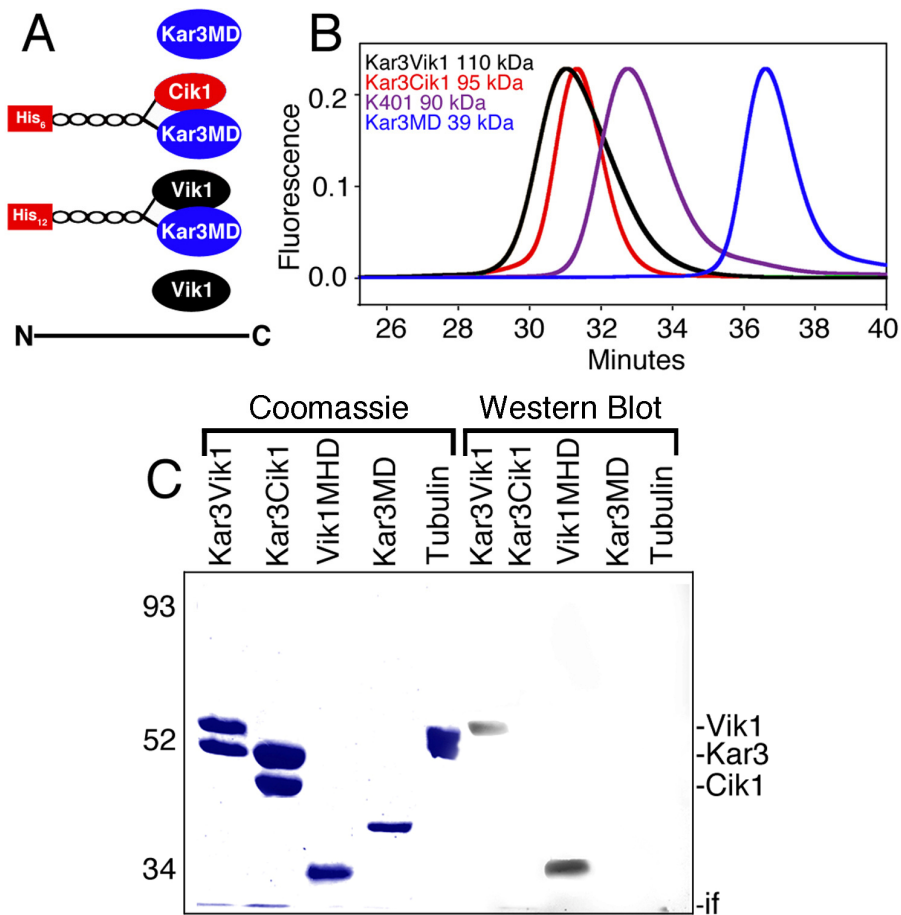
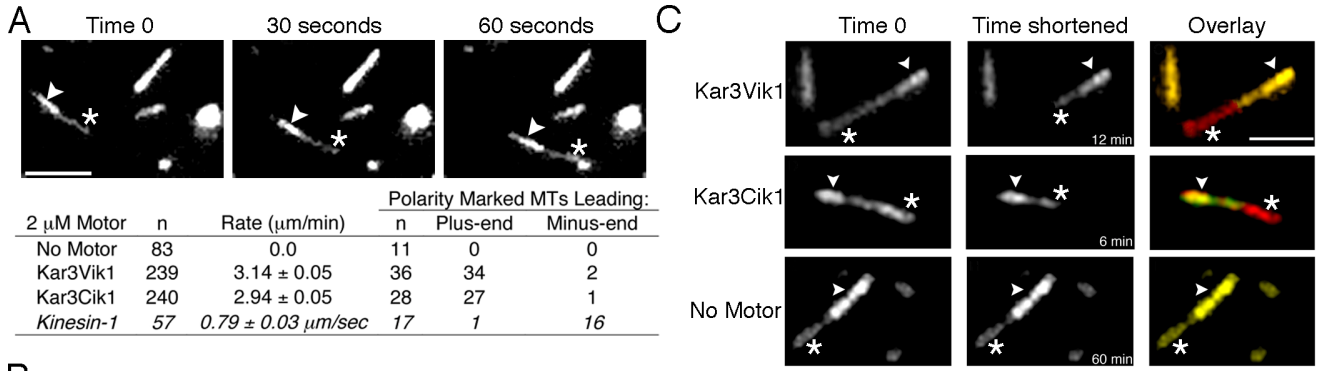


Figure 13. Purification of the Heterodimeric Kar3Vik1, Kar3Cik1 and Monomeric Kar3MD

5.4.5 Figure 13 Legend

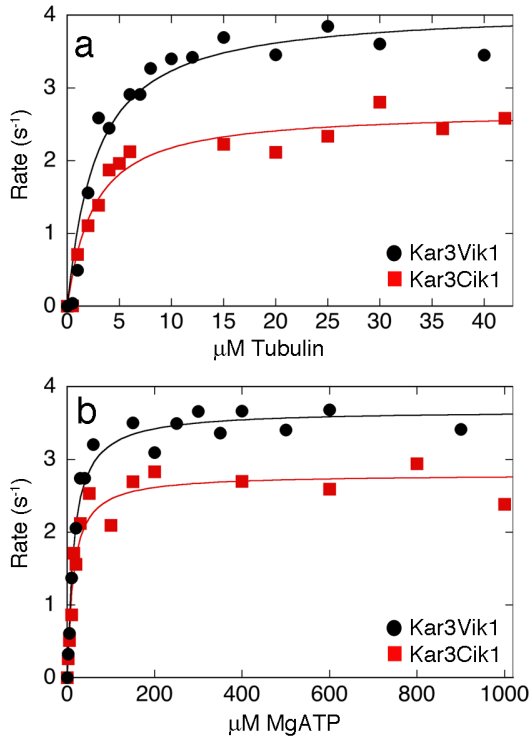
Characterization of Motor Proteins Used In the Study

(A) Schematic of the four motors used: Kar3MD (monomer), Kar3Cik1 and Kar3Vik1 heterodimers, and the monomeric Vik1MHD. (B) Analytical gel filtration of Kar3Vik1, Kar3Cik1, dimeric conventional kinesin K401, and Kar3MD with the M_r predicted based on amino acid sequence. Stokes radius of Kar3Vik1 = 4.1 nm, Kar3Cik1 = 3.9 nm, K401 = 3.8 nm, Kar3MD = 3.4 nm. (C) Coomassie-stained gel (2M Urea, 10 % SDS-PAGE) and Western Blot showing protein purity and the Vik1 antibody specificity.



2 μ M Motor	n	Rate (μ m/min)	Polarity Marked MTs Leading:		
			n	Plus-end	Minus-end
No Motor	83	0.0	11	0	0
Kar3Vik1	239	3.14 ± 0.05	36	34	2
Kar3Cik1	240	2.94 ± 0.05	28	27	1
<i>Kinesin-1</i>	57	$0.79 \pm 0.03 \mu$ m/sec	17	1	16

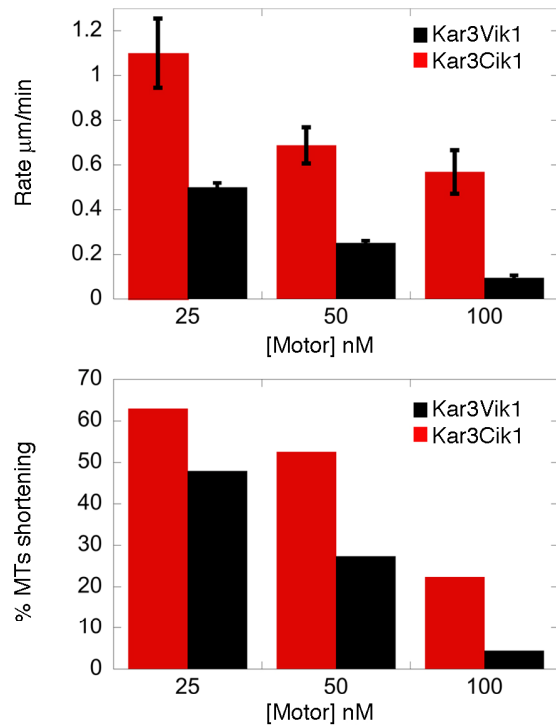
B



Steady State ATPase Kinetics			
	Kar3MD	Kar3Cik1	Kar3Vik1
k_{cat}	$0.49 \pm 0.0 \text{ s}^{-1}$	$2.8 \pm 0.1 \text{ s}^{-1}$	$3.7 \pm 0.0 \text{ s}^{-1}$
$K_{m,ATP}$	$12.2 \pm 2.8 \mu\text{M}$	$18.6 \pm 3.0 \mu\text{M}$	$15.0 \pm 0.7 \mu\text{M}$
$K_{1/2,MT}$	$6.0 \pm 0.7 \mu\text{M}$	$2.0 \pm 0.4 \mu\text{M}$	$1.7 \pm 0.3 \mu\text{M}$

50 nM Motor	[Taxol]	MTs (n)	Rate (nm/min)	Shortened Polarity Marked Microtubules:			
				MTs n	Plus-end n	Minus-end n	Both n
Kar3Vik1	5 μ M	555	250 ± 11.1	77	40	15	22
Kar3Cik1	5 μ M	352	687 ± 81.3	37	35	2	0
No Motor	5 μ M	37	0.0	17	0	0	0

D



Motor Concentration Dependent Microtubule Shortening							
[Motor] nM	Kar3Cik1			Kar3Vik1			
	Rate (μ m/min)	% Shortened (n)	Total # MTs Observed	Rate (μ m/min)	% Shortened (n)	Total # MTs Observed	
25	1.10 ± 0.16	62.9 (124)	197	0.50 ± 0.05	47.9 (147)	307	
50	0.69 ± 0.08	52.6 (185)	352	0.25 ± 0.01	37.3 (207)	555	
100	0.57 ± 0.10	22.3 (23)	103	0.10 ± 0.01	4.4 (26)	587	

Figure 14. Kar3Vik1 is a Kinesin-14 Heterodimeric Motor

5.4.6 Figure 14 Legend

Kar3Vik1, A Kinesin-14

Kar3Vik1 is a Kinesin-14 heterodimeric motor. (A) Kar3Vik1 minus end-directed motility in the presence of MgATP. Arrowheads denote the bright microtubule minus end, and the asterisks (*), the dim, leading microtubule plus end. Scale bar = 5 μm . The table compares the microtubule gliding promoted by Kar3Vik1, Kar3Cik1, and squid Kinesin-1. (B) The steady-state ATPase kinetics of Kar3Vik1 and Kar3Cik1 as a function of microtubule and MgATP concentrations. Upper panel final concentrations: 0.82 μM Kar3Vik1 or 1.1 μM Kar3Cik1, 0–42 μM tubulin polymer, 40 μM Taxol, and 1 mM [$\alpha^{32}\text{P}$] MgATP. Lower panel final concentrations: 0.85 μM Kar3Vik1 or 1 μM Kar3Cik1, 20 μM tubulin polymer, 40 μM Taxol, and 0-1 mM [$\alpha^{32}\text{P}$] MgATP. The table shows the steady-state parameters of Kar3Vik1 and Kar3Cik1 in comparison to the Kar3MD [240]. (C) ATP-dependent Kar3Vik1 and Kar3Cik1 promoted microtubule shortening. Microtubule•motor complexes were preformed in the presence of 1 mM MgAMPPNP and imaged at $t = 0$, Column 1. MgATP at 1.5 mM plus an ATP regeneration system initiated microtubule shortening [167]. Column 3 is the merge of $t = 0$ and the elapsed time (middle column) to show microtubule shortening (yellow) in comparison to the original length. Polarity-marked microtubules were identified from microtubule•motor populations at both 25 and 50 nM motor incubated with 500 nM microtubules in the presence of MgATP. (D) Increased motor binding to microtubules stabilizes the microtubule lattice against shortening. Upper panel: Kar3Cik1 and Kar3Vik1 rates of microtubule shortening plotted as a function of increasing motor concentration. Lower panel: The percentage of microtubules that showed Kar3Cik1 or Kar3Vik1-promoted ATP-dependent shortening plotted as a function of motor concentration.

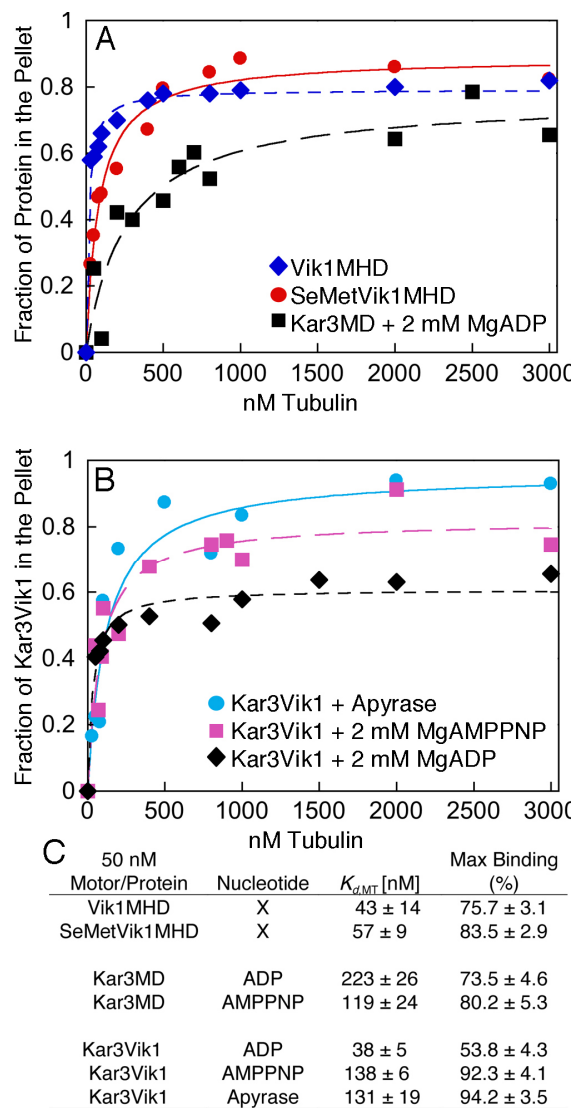
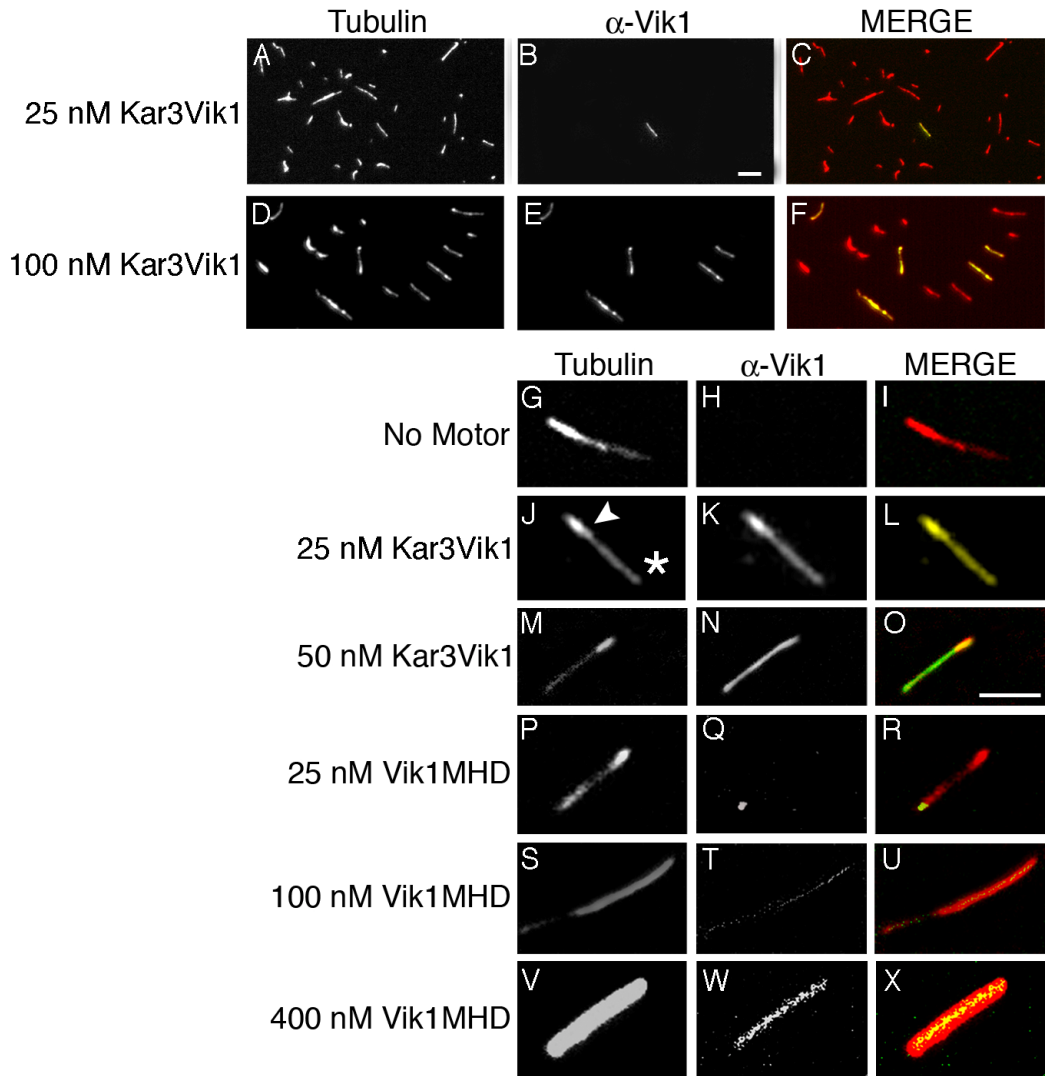


Figure 15. Microtubule binding by Vik1MHD, SeMetVik1MHD, Kar3MD, and Kar3Vik1.

5.4.7 Figure 15 Legend

The Microtubule Binding of Kar3Vik1 and the Vik1MHD

(A & C) Microtubule•motor cosedimentation was performed to compare the binding of 50 nM Vik1MHD, SeMetVik1MHD, Kar3MD, and (B & C) Kar3Vik1 at three different nucleotide conditions. The data were plotted as the fraction of motor partitioning to the pellet as a function of microtubule concentration and fit to quadratic equation 2, providing the constants in C. Error is reported as SEM. Final concentrations: 0-3 μ M tubulin polymer, 40 μ M Taxol, and \pm 0.1U/ml Apyrase, or 2 mM MgAMPPNP, or 2 mM MgADP.



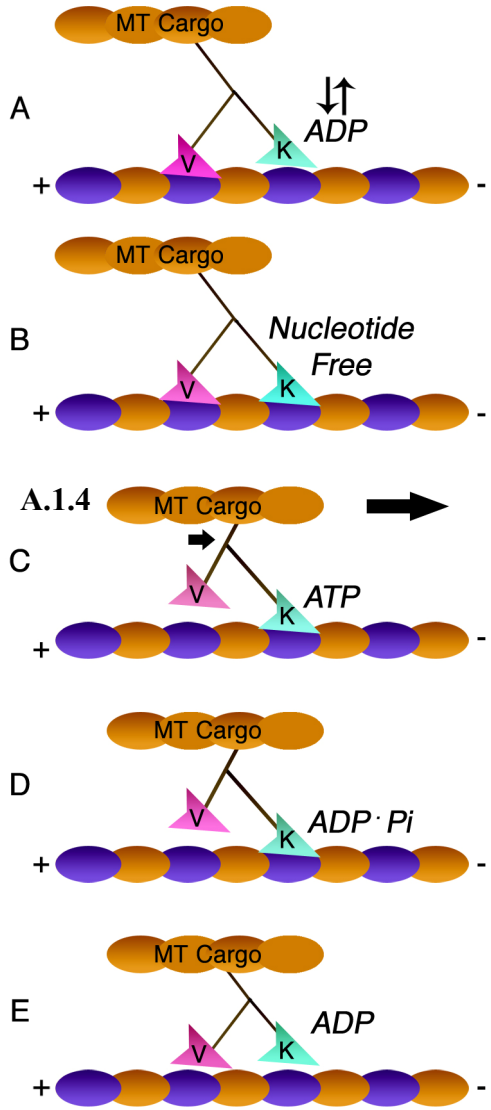
[Motor]	Microtubules n	% Microtubules Bound (n)	% Localization Events on the Microtubule (n)			
			Lattice	End	Both	Saturated
25 nM Kar3MD	108	7.4 (8)	50.0 (4)	0.0 (0)	50.0 (4)	0.0
50 nM Kar3MD	476	6.1 (29)	86.2 (21)	20.7 (6)	6.9 (2)	0.0
100 nM Kar3MD	695	49.9 (347)	47.0 (163)	15.0 (52)	38.0 (132)	0.0
25 nM Kar3Cik1	1939	16.0 (310)	35.8 (111)	43.6 (135)	20.6 (64)	0.0
50 nM Kar3Cik1	901	10.1 (91)	19.8 (18)	34.0 (31)	46.2 (42)	0.0
100 nM Kar3Cik1	1003	18.7 (188)	39.9 (75)	43.1 (81)	17.0 (32)	0.0
25 nM Kar3Vik1	861	23.3 (201)	7.0 (14)	3.0 (6)	2.5 (5)	90.0 (176)
50 nM Kar3Vik1	959	9.9 (95)	1.0 (1)	5.3 (5)	0.0	93.7 (89)
100 nM Kar3Vik1	605	10.7 (65)	1.5 (1)	0.0 (0)	0.0	98.5 (64)
25 nM Vik1MHD	1096	12.3 (135)	45.2 (61)	48.1 (65)	6.7 (9)	0.0
50 nM Vik1MHD	1235	14.2 (176)	33.0 (58)	55.1 (97)	11.9 (7)	0.0
100 nM Vik1MHD	964	13.8 (133)	44.3 (59)	38.3 (51)	17.3 (23)	0.0
200 nM Vik1MHD	1523	12.6 (192)	22.9 (44)	32.3 (62)	0.0	44.8 (86)
400 nM Vik1MHD	1201	15.1 (181)	20.4 (37)	31.5 (57)	0.0	48.1 (87)
No Motor	643		---	---	---	---

Figure 16. Immunolocalization of Kar3Vik1, Kar3Cik1, Kar3MD, and Vik1MHD

5.4.8 Figure 16 Legend

Kar3Vik1 Cooperatively Binds Microtubules

Microtubule-motor complexes were preformed in the presence of MgAMPPNP. Final concentrations: 500 nM tubulin polymer, 40 μ M Taxol, and 1 mM MgAMPPNP. Rows 1 and 2 represents magnification of a section of the field, whereas the remaining rows show individual microtubules at a higher magnification (scale bars = 5 μ m). The microtubule seed (arrowhead) marks the microtubule minus end and (*) denotes the dim microtubule plus end. The first column of each row shows the rhodamine-labeled microtubules, and the second column, the immunofluorescence of affinity-purified Vik1MHD antibodies. The third column is the merge of the two channels to show the colocalization. The table presents the summary of microtubule localization events scored for the three motors using affinity-purified antibodies to the Kar3MD or the Vik1MHD.



Kar3Vik1 with a MT cargo bound at the N-terminus collides with the microtubule via the Vik1MHD. Kar3 is in the weak binding state with ADP on the active site. The neck-stalk is oriented toward the microtubule plus end, with the Kar3MD oriented toward the minus end.

The Vik1 tight binding to the microtubule promotes Kar3 motor binding to the microtubule. This causes rapid ADP release. Both heads are bound with Kar3 in the nucleotide free state.

ATP rapidly binds to the Kar3 motor. This induces a strain dependent rotation of the neck-stalk that pulls Vik1 off the microtubule and moves the MT cargo toward the microtubule minus end. The neck-stalk is now oriented toward the microtubule minus end.

ATP is hydrolyzed, which produces the weak binding state of Kar3Vik1.

Kar3Vik1 detaches from the motor, the neck-stalk reorients toward the microtubule plus end, and the motor is ready to repeat the cycle.

Figure 17. A Proposed Mechanism for Kar3Vik1 Transport of a Microtubule Cargo

5.4.9 Figure 17 Legend

A Non-Processive Model of Kar3Vik1 Transport of a MT Cargo

A model for Kar3Vik1 minus end directed MT cargo transport. (A-B) Kar3Vik1 binds the microtubule tightly with the Vik1 (**V**) subunit. The Vik1 binding induces a conformational change that promotes Kar3 (**K**) collision with the microtubule and release of ADP from the active site. (B) Both heads of Kar3Vik1 bind the microtubule. (C) Kar3 in the no nucleotide state, rapidly binds ATP [283]. ATP binding promotes rotation of the neck coiled coil toward the minus end of the microtubule. This serves two purposes, strain dependent release of Vik1 from the microtubule lattice, and translocation of a MT cargo toward the microtubule minus end. (D) ATP hydrolysis occurs, generating the Kar3Vik1 weakly bound intermediate to the microtubule. (E) This action returns the motor to the Kar3Vik1•ADP solution state, able to rebind the microtubule and repeat the ATPase cycle.

6.0 DROSOPHILA NOD PROTEIN BINDS PREFERENTIALLY TO THE PLUS ENDS OF MICROTUBULES AND PROMOTES MICROTUBULE POLYMERIZATION *IN VITRO*

6.1 ABSTRACT

Nod, a non-motile kinesin-like protein, plays a critical role in segregating achiasmate chromosomes during female meiosis. In addition to localizing to oocyte chromosomes, we show that functional full-length Nod-GFP (Nod_{FL}-GFP) localizes to the posterior pole of the oocyte at stages 9-10A, as does Kinesin Heavy Chain (KHC), a plus end directed motor. This posterior localization is abolished in *grk* mutants that no longer maintain the microtubule gradient in the oocyte. To test the hypothesis that Nod binds to the plus ends of microtubules, we expressed and purified both full-length Nod (Nod_{FL}) and a truncated form of Nod containing only the motor-like domain (Nod₃₁₈) from *E. coli*, and assessed their interactions with microtubules *in vitro*. Both Nod_{FL} and Nod₃₁₈ demonstrate preferential binding to the ends of the microtubules, displaying a strong preference for binding to the plus ends. In an experiment in which Nod₃₁₈-GFP•microtubule collision complexes were trapped by glutaraldehyde fixation, the preference for binding to plus ends versus minus ends was 17:1. Nod_{FL} and Nod₃₁₈ also promote microtubule polymerization *in vitro* in a time-dependent manner. The observation that Nod is preferentially localized to the plus ends of microtubules, and stimulates microtubule polymerization suggests a mechanism for its function.

6.2 INTRODUCTION

In *Drosophila melanogaster* female meiosis, the controlled movement of achiasmate chromosomes on the meiotic spindle is dependent on Nod, a 666 amino acid kinesin-like protein that localizes along the arms of meiotic chromosomes [210, 219, 220] (Figure 18B). In the absence of functional Nod protein, achiasmate chromosomes dissociate from the main chromosome mass immediately after nuclear envelope breakdown (NEB) by migrating off the ends of the developing spindle [213]. Both genetic and cytological studies suggest that Nod functions to hold chromosomes at or near the metaphase plate, opposing the poleward force exerted by the kinetochores [213, 223]. Given that the microtubules in the oocyte spindle are arranged with their plus ends at or near the metaphase plate [284], these results initially suggested that Nod acted as a plus end directed motor that pushes chromosomes toward the metaphase plate [223]. A function of Nod in pushing chromosomes arms toward the metaphase plate has also been demonstrated in *Drosophila* mitotic cells by Goshima and Vale [285]. These authors have shown that in cells in which Nod RNAi ablates function, the arms of most chromosomes were extended along the spindle axis toward one of the two poles rather than being held at or near the metaphase plate.

However, several lines of evidence show that the motor-like domain of Nod lacks the capacity for vectorial transport [221]. First, Nod lacks three major structural elements that are found in virtually all kinesins (the neck, the neck-interactor region, and a crucial salt bridge) and are required for movement [286, 287]. Second, although the motor-like domain of Nod is 34% identical to the prototypical human kinesin heavy chain protein (HsKHC) motor domain, when one considers only residues that are strongly conserved within the KHC super-family, 12 of the 62 fully conserved amino acids are changed in Nod, and 6 of the 51 strongly similar amino acids are different in Nod [221]. Similarly, with respect to the ten residues in HsKHC that are most critical for microtubule binding [130], seven of these amino acids are altered in Nod. Third, although microtubules activate the ATPase activity of Nod over 2000-fold [221], this ATPase activity is not coupled to motor activity (i.e. Nod does not produce microtubule gliding *in vitro*) [221]. Fourth, the substitution of a single amino acid in the ATP-binding motif of

Drosophila KHC with the analogous amino acid from Nod results in a drastic inhibition of motility [221]. Thus, Nod's ability to hold chromosomes on the meiotic spindle is unlikely to result from any innate ability to move chromosomes along microtubule tracks. Although the ability of Nod to hold chromosomes in position might reflect an ability to bridge chromosome arms to the plus ends of non-kinetochore microtubules in the spindle and hold them in place, microtubule tread-milling would presumably draw chromosomes to the poles of the meiotic spindle rather than pushing them toward the metaphase plate.

To better understand how Nod can generate poleward force, it would be helpful to understand how the Nod protein interacts with both chromosomes and microtubule filaments. In a companion paper [288], Cui and Hawley show that the binding of Nod to the oocyte chromosomes requires the activity of a specific C-terminal motif, referred to as an HhH(2)/NDD domain, which may mediate either Nod:DNA or Nod:protein interactions. In this study, we focus on determining the manner in which Nod interacts with the microtubules. Unfortunately, previous studies of the ability of Nod, or parts of Nod, to localize on microtubule arrays of known polarity within cells have provided confusing results with respect to this question. Clark *et al.* [222] demonstrated that a Nod-KHC- β gal fusion protein containing the Nod motor-like domain fused to the coiled coil domain of KHC and β -galactosidase (see Figure 18A) functions as an *in vivo* reporter for the minus ends of microtubule arrays. However, using a similar *in vivo* assay, we show below that full length Nod-GFP protein, which retains full biological function, localizes in a fashion similar to that exhibited by the plus end directed motor KHC [222, 289].

In order to directly determine whether or not Nod binds to the ends of microtubules, and if so, to which end, we have examined the interactions of purified full length Nod (Nod_{FL}) and the Nod motor-like domain (Nod₃₁₈) with microtubules *in vitro*. We demonstrate that both Nod_{FL} and Nod₃₁₈ bind preferentially to the plus ends of the microtubule and promote polymerization. As discussed below, the observation that Nod localizes preferentially to the plus end of microtubules suggests a mechanism for its function, similar to the clamped-filament elongation model proposed for actin-based motors [290]. This mechanism provides a means for explaining the ability of a protein

like Nod, which lacks the capacity for vectorial transport, to propel chromosomes toward the metaphase plate.

6.3 RESULTS

6.3.1 Functional Nod_{FL}-GFP Localizes to the Posterior Pole of Stage Nine Embryos in a Fashion That Requires a Properly Organized Microtubule Network

When expressed in *nod* mutant oocytes under the control of the germline-specific *nanos-Gal4::VP16* driver, the Nod_{FL}-GFP protein localizes to oocyte chromosomes and fully rescues the defective chromosome segregation phenotype exhibited by *nod* oocytes [288]. We show here that Nod_{FL}-GFP also accumulates at the posterior pole of stage 9 oocytes, as shown in Figure 19. This pattern parallels the localization pattern observed for KHC, a known plus end-directed motor [222, 289], but contrasts with that of a Nod-KHC-βgal fusion protein, which localizes to the minus ends of microtubule [222]. The contradiction between our observations and the localization of Nod-KHC-βgal may be resolved by supposing that some component of the Nod-KHC-βgal fusion protein other than the Nod motor-like domain, perhaps the KHC sequences, is responsible for minus end-directed localization.

To determine whether the localization of Nod to the posterior pole of stage 9 oocytes requires the integrity of the oocyte microtubule network, we localized Nod_{FL}-GFP in *grk^{2B}/grk^{DC}* mutant oocytes. Januschke *et al.* [291] demonstrated that the normal organization of microtubules in stage 9 oocytes is abolished in *grk^{2B}/grk^{DC}* mutants, as visualized using the microtubule-associated protein Tau-GFP. Although cytoplasmic Nod_{FL}-GFP is localized at the posterior pole in *grk* heterozygous stage 9-10A oocytes, this localization was abolished in *grk^{2B}/grk^{DC}* mutant oocytes. Instead, Nod_{FL}-GFP was dispersed throughout the entire egg chamber (Figure 20). These results suggest that Nod_{FL}-GFP accumulation at the posterior pole is dependent on proper microtubule organization within the oocyte.

However, several lines of evidence suggest that interpreting the significance of this localization in terms of the manner in which Nod interacts with microtubules must be done with some caution. First, the minus-end motor dynein also concentrates at the posterior [292], albeit in a manner that depends on the function of KHC [293]. Second, microtubule imaging shows no evidence of microtubules plus ends being concentrated at the posterior pole. Indeed, although minus ends are highly concentrated at the anterior of the oocyte and near the cortex, the posterior pole is relatively free of microtubules [294]. Both Cha *et al.* [294] and Serbus *et al.* [295] have proposed elegant models to explain these discrepancies while still proposing that KHC localizes to the posterior pole because of its capacity to act as a plus end directed motor and thus push away from the minus ends concentrated at the anterior pole and along the cortex. However, these observations at least raise the possibility that the processes that localize Nod to the posterior pole may not be completely dependent on direct interactions of Nod with the microtubule. Indeed, Cui and Hawley [288] have shown that localization of full length Nod to the posterior pole of the oocyte also requires a functional HhH(2)/NDD DNA-binding domain, raising the possibility that this domain mediates the interaction of Nod with at least one other protein. Thus, in order to directly assess the ability of Nod to bind to the plus ends of microtubules we pursued a more direct *in vitro* approach to studying Nod- microtubule interactions.

6.3.2 Nod_{FL} and Nod₃₁₈ Show Preferential Binding to Microtubule Plus Ends *in vitro*

The microtubule-dependent localization of Nod_{FL}-GFP to the posterior pole suggested that Nod might either be moved to or preferentially bind the plus ends of microtubules. To test this possibility, we purified bacterially-expressed Nod_{FL}-GFP and Nod₃₁₈-GFP proteins, incubated them with polarity marked microtubules, and visually assessed the position of Nod binding along the length of the microtubule. Figure 21 shows the expressed and purified proteins used for these *in vitro* assays. Although we were successful in purifying Nod₃₁₈ and Nod₃₁₈-GFP to >99% homogeneity, the purification of the full length Nod construct (Nod_{FL}-GFP) was more problematic. As shown in Figure

21, several additional proteins co-purified with Nod_{FL}-GFP. Based on Western blot analysis (data not shown), the majority of the lower molecular weight bands appear to be the result of breakdown or proteolysis of the Nod_{FL}-GFP protein.

To determine the ability of these proteins to bind to microtubules, we co-incubated Nod_{FL}-GFP and Nod₃₁₈-GFP with rhodamine-labeled microtubules. A substantial fraction of these microtubules were polarity-marked such that the brighter region of fluorescence corresponds to the minus end of the microtubule while the fainter region corresponds to the region including the plus end (see Figure 22A). We then visualized Nod binding to microtubules by measuring the number and position of GFP foci (corresponding to sites of Nod_{FL}-GFP and Nod₃₁₈-GFP binding) along the length of the microtubules by fluorescence microscopy. As expected, no foci were observed in the “no motor” control. Furthermore, binding of GFP protein lacking Nod sequences to microtubules in this assay was rare, even at high concentrations of protein (57.2 nM), and no instances of end-binding to single microtubules were observed. The one example of GFP binding observed involved a GFP focus localized to a site at which the lattices of three microtubules appeared to intersect. However, for both Nod_{FL}-GFP and Nod₃₁₈-GFP, Nod-microtubule complexes were observed and their frequency increased with the concentration of the Nod-GFP protein. Nod₃₁₈-GFP binds to 2.3-6.5 % of microtubules at concentrations of Nod₃₁₈-GFP ranging from 6.1 to 24 nM, while Nod_{FL}-GFP binds to 3.3-24.4% of microtubules at concentrations ranging from 0.19 to 18.9 nM. These observations demonstrate that the Nod-GFP proteins produced in *E. coli* retain their ability to bind microtubules. Moreover, the observation that Nod_{FL}-GFP protein binds to more microtubules at lower concentrations of protein than does Nod₃₁₈-GFP suggests that the full length Nod_{FL}-GFP protein has a higher affinity for microtubules than does the Nod₃₁₈ protein, which carries only the motor-like domain of Nod.

We categorized the binding of Nod-GFP proteins to microtubules into three classes: *end-binding* (see Figure 22A-C), in which the GFP focus defined the end of the microtubule, *lattice binding* (see Figure 22D-F), in which the GFP focus was positioned somewhere along the length of the microtubule, and *junctions* (Figure 22G-I) in which the GFP focus marks a site of intersection between two microtubules. In those cases in

which the microtubule was polarity marked, end binding events could be further classified as plus or minus end bindings (see below). Although the images in Figure 22 portray microtubule-binding events for the Nod_{FL}-GFP protein, microtubule binding data for both Nod_{FL}-GFP and Nod₃₁₈-GFP are summarized in the table embedded in Figure 22. In the case of Nod₃₁₈-GFP, the majority of microtubule-binding events involved single microtubules at all three concentrations tested, while for Nod_{FL}-GFP junction events involving two microtubules were the most frequently observed class of Nod-microtubule interaction at all concentrations tested. I will first discuss the cases in which Nod_{FL}-GFP or Nod₃₁₈-GFP interacts with a single microtubule and then Nod interactions with microtubule junctions.

Figure 23 displays the microtubule binding events for both Nod_{FL}-GFP and Nod₃₁₈-GFP as a histogram of Nod-GFP localization along the microtubules. We separated the position of the Nod-GFP focus along the microtubule into seven 'bins' to denote their position. The first bin, labeled 'Tip', denotes those cases in which the Nod-GFP focus was located at a point between 0 and 7% of the length of the microtubule, the second bin denotes those cases where the focus fell between 8 and 14% of the length of the microtubule, and so on. The last bin, labeled 'Center', includes those GFP foci mapping close to or at the center of the microtubule. Because we are always measuring the distance from the GFP focus to the nearest end, the position of the focus cannot exceed 50% of the length of the microtubule. The bin size of seven reflects the fact that for foci denoted as lattice binding events which were close to, but not at, the tip, the distance from focus to tip was at least 7% of microtubule length. Foci less than 7% of microtubule length from the tips were considered end-binding events. Using this binning method to quantitate the position of the GFP focus on the microtubule, we found that both Nod_{FL}-GFP and Nod₃₁₈-GFP show higher binding affinity to the end of the microtubule compared to any other location along the microtubule (see Figure 23). Evidence that the binding of Nod to the microtubule end occurs preferentially at the plus end is provided in the following section.

In addition to binding at the ends or along the lattice of microtubules, Nod_{FL}-GFP or Nod₃₁₈-GFP were often observed to connect two microtubules and form structures we denote as junctions (see Figure 22G-I). The analysis of these junctions further supports

our conclusion that Nod binds preferentially to microtubule ends and suggests that the C-terminal half of Nod also carries a microtubule-binding domain. The conclusion that the Nod binding in junctions is also often mediated by the binding to microtubule ends is based on an analysis of the structure of the junctions themselves. Junctions were observed either between two microtubule ends (with Nod at the junction), between an end and a lattice (as shown in Figure 22G-I) or between two lattices. The ten junctions with Nod₃₁₈-GFP foci may be further classified as 3 end-end junctions, 4 end-lattice junctions, and 3 lattice-lattice junctions. Thus, among the 20 microtubules composing these ten junctions, Nod₃₁₈-GFP is bound at the end of the microtubule in 50% of the cases. For Nod_{FL}-GFP, a total of 52 microtubules were observed as components of 26 junctions. These 26 junction structures may be further classified as 8 end-end junctions, 13 end-lattice junctions, and 5 lattice-lattice junctions, such that of the 52 microtubules involved, Nod_{FL}-GFP was bound to the end of the microtubule in 54.7% of the cases.

The argument that Nod possesses a second microtubule-binding domain within its C-terminus is based on the observation that Nod_{FL}-GFP protein clearly possesses a greater ability to bind to or create microtubule junctions (36-57%) than does the Nod₃₁₈-GFP protein (8-18%). This greater ability of Nod_{FL}-GFP to form or bind to junctions suggests that a second microtubule-binding domain might exist in the C-terminal half of Nod, such that the Nod_{FL}-GFP protein can bind more than one microtubule fiber. Such a secondary microtubule binding domain has been identified in the C-terminal (non-motor) half of the HsKid protein, a human chromokinesin that is similar in structure to Nod [296]. Although the ability of Nod to form junctions might also be explained by an ability to form dimers, chromokinesins like Nod and HsKid lack the coiled coil domain that is believed to essential for dimerization [296].

These data allow two general conclusions. First, both Nod_{FL}-GFP and Nod₃₁₈-GFP bind to microtubules *in vitro*, with a strong preference for the ends of the microtubule. Second, Nod_{FL}-GFP has a higher affinity for microtubule-binding than does Nod₃₁₈-GFP, apparently as a consequence of a greater ability of Nod_{FL}-GFP to inter-connect two microtubules, a property that may reflect a secondary microtubule binding site in the C-terminus of Nod. However, even these junction events are also a

manifestation of Nod's preferential ability to bind microtubule ends, since the majority of junctions involve at least one microtubule end.

6.3.3 Nod Binds Preferentially to the Plus Ends of Microtubules

Using those cases in which Nod_{FL}-GFP or Nod₃₁₈-GFP localized to the end of a polarity marked microtubule, we were able to demonstrate that Nod preferentially binds to the plus ends of microtubules. As shown in Figure 23, we found that Nod bound twice as frequently to the plus versus the minus end of the microtubule for both Nod_{FL}-GFP and Nod₃₁₈-GFP. The ratio of plus end/minus end binding events for Nod_{FL}-GFP was 15/8, and for Nod₃₁₈-GFP the ratio was 8/4. However, because the number of instances in which Nod was bound to the end of a polarity-marked microtubule was small, we repeated these experiments using a different method (glutaraldehyde fixation) for trapping the collision complex between Nod₃₁₈-GFP and polarity marked microtubules. The results of this experiment are presented in Figure 24. In this experiment the frequency with which Nod₃₁₈-GFP bound to the microtubule end (71.8%) was approximately two-fold higher than observed in the experiment presented in Figure 21 in which Nod₃₁₈-GFP was mixed with microtubules only in the presence of AMPPNP. Moreover, the ratio of plus-end (52) to minus end (3) binding events was approximately 17:1. The difference in these two sets of results likely reflects the fact that by mixing Nod₃₁₈-GFP and microtubules in the presence of AMPPNP we are failing to trap the Nod complex at the site of the initial binding and may be allowing Nod to migrate along the length of the microtubule. Evidence in support of this hypothesis will be presented in the following section, in which we demonstrate that both Nod₃₁₈-GFP and Nod_{FL}-GFP stimulate microtubule polymerization in the presence of either ATP or AMPPNP. However, by fixing with glutaraldehyde immediately after mixing, as we do in Figure 23, we are capturing the initial sites of Nod-microtubule interactions. Taken together, both experiments argue strongly that when binding to the microtubule end, Nod has a strong preference for the plus end.

6.3.4 Nod_{FL}-GFP and Nod₃₁₈ Promote Microtubule Polymerization *in vitro*

The preferential binding of Nod to ends, and specifically the plus ends, of microtubules suggested that Nod might play a role in controlling microtubule polymerization. To address this possibility, we set out to test the ability of Nod_{FL}-GFP and Nod₃₁₈ to facilitate this process. In order to test the ability of the Nod motor-like domain to mediate microtubule polymerization, we incubated Nod₃₁₈ with soluble rhodamine-labeled tubulin in the presence of MgATP or MgAMPPNP. At times 0 and 30 minutes, we visualized the presence or absence of polymerization by microscopic examination. As shown in Figure 25, there are many more microtubules formed by 30 minutes in Nod-treated samples than are formed in the no motor control. The observation that Nod-promoted microtubule assembly occurred in the presence of either MgATP or MgAMPPNP suggests that Nod₃₁₈ does not require ATP turnover to promote microtubule polymerization. To control for the possibility that some of the observed microtubule polymerization might be due to the presence of bacterial proteins, we repeated this experiment by performing the microtubule polymerization experiment using extracts from *E. coli* cultures that did or did not express Nod₃₁₈. While a high degree of microtubule polymerization was observed in the presence of Nod₃₁₈ little or no polymerization was observed in the presence of *E. coli* extract alone (see Figure 28).

We used sedimentation analysis to quantify the ability of the Nod motor-like domain (Nod₃₁₈) and full length Nod (Nod_{FL}-GFP) to mediate microtubule polymerization. Soluble tubulin was incubated with or without Nod_{FL}-GFP or Nod₃₁₈, centrifuged, and subjected to SDS-PAGE to determine the fraction of tubulin that remained in the supernatant in comparison to the fraction that sedimented in the pellet. As shown in Figure 26A, both Nod_{FL}-GFP and Nod₃₁₈ result in a statistically significant increase ($p < 0.01$) in tubulin partitioning to the pellet when compared to the no motor controls. Similar results were also obtained using a Nod₃₁₈-GFP construct (data not shown). To confirm that the partitioning of tubulin to the pellets represents Nod-promoted microtubule polymerization, we repeated the sedimentation assay with fluorescently labeled tubulin and resuspended the pellets for direct microscopic

examination. As shown for Nod_{FL}-GFP in Figure 26C, the resuspended pellets are comprised of large numbers of microtubules rather than aggregates of soluble tubulin.

If Nod-promoted microtubule assembly is functionally significant, we would expect there to be a time-dependence to the process. Figure 27 shows Nod₃₁₈-promoted microtubule assembly using the sedimentation assay. The results reveal a significant increase ($p < 0.05$) in the fraction of tubulin that partitions to the pellet over time, whereas no increase in the fraction of tubulin sedimentation was seen in the absence of Nod. Therefore, Nod exerts its ability to stimulate microtubule polymerization in a time-dependent fashion.

6.4 DISCUSSION

The data presented above reveal two critical insights into Nod function: namely that full length Nod localizes to the ends of microtubules *in vitro*, and that Nod promotes microtubule polymerization. Our conclusion that Nod binds preferentially to plus ends *in vivo* is supported by three observations: (1) Nod localizes to the posterior pole of stage 9 oocytes, in a manner similar to the plus-end directed motor KHC; (2) the preferential binding of Nod to microtubule plus ends *in vitro*; and (3) Nod-promoted microtubule polymerization *in vitro*. Given that the microtubules in the oocyte spindle are arranged with their plus ends at or near the metaphase plate [284], these data suggest a straightforward mechanism by which Nod, when bound to the arms of chromosomes, can generate the force required to push chromosome arms towards the metaphase plate [223, 285]. Indeed, we propose that Nod proteins bound along the arms of chromosomes cause the extension of microtubule plus ends by polymerization, and that it is the growth in the microtubules that serves to literally “push” those arms towards the metaphase plates. If correct, this mechanism provides at least one biochemical explanation for the “polar ejection force” [216].

In the experiments presented, Nod promotes polymerization of microtubules in the presence of both MgATP and MgAMPPNP, suggesting that ATP turnover is not required for the addition of tubulin subunits. This observation is perhaps not surprising

given the observation by Matthies *et al.* [221] that the affinity of Nod-ATP for microtubules is similar to, and indeed slightly less than, the affinity of Nod-ADP for microtubules. (Compare this to conventional kinesins in which the affinity of the motor-ATP complex for microtubules is ~40-50 times greater than the affinity of the motor-ADP complex for microtubules.) Nod ATPase activity may not be critical for the microtubule polymerization activity but it is essential for the ability of Nod to faithfully segregate chromosomes [217, 218, 221]. The following model can reconcile this apparent contradiction:

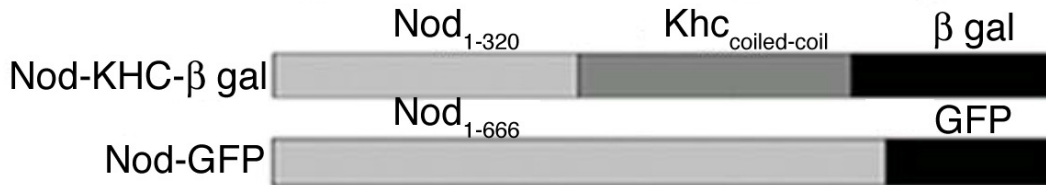
1) Nod microtubule polymerization activity also functions to stabilize the plus ends of growing microtubules. Indeed, plus end binding proteins have this property [297]. *In vivo*, microtubules are highly dynamic structures undergoing fluctuations between growth and rapid shortening; these dynamics are highly regulated by microtubule-binding proteins, which bind to the microtubule ends to facilitate stabilization or destabilization of the microtubule [14, 45, 297]. Nod may act as a stabilizing protein by binding to the chromosomes with its C-terminus and to the microtubule plus end with its N-terminal kinesin motor domain.

2) By stabilizing the plus ends, Nod allows new tubulin dimers to be added to these ends. The addition of a new dimer leads to GTP hydrolysis in the microtubule polymer and a new GTP cap. This GTP cap may then be the new binding site for Nod.

3) ATP turnover by Nod could regulate in part the dynamics at the microtubule plus end by allowing Nod to detach from the elongated microtubule at the appropriate time and allowing re-binding to the plus end. This mechanism of binding the microtubule plus end, stabilizing the plus ends, then allowing subunit addition, would account for the *in vivo* observations that suggest Nod acts to 'push' chromosomes away from the poles during meiotic spindle formation. The various aspects of this model help to explain how Nod, a chromokinesin-like protein that lacks the capacity for vectorial transport, can nonetheless provide the force that maintains achiasmatic chromosomes near the metaphase plate during spindle elongation at prometaphase I of meiosis.

6.5 FIGURES AND FIGURE LEGENDS

A. Structural comparison of Nod-KHC-β gal and Nod-GFP



B. Structure of Nod

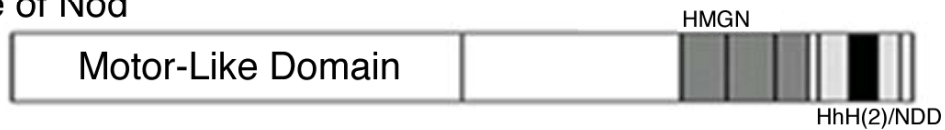


Figure 18. The Structure of the *Drosophila* Nod Kinesin-Like Protein

6.5.1 Figure 18 Legend

The Structure of the *Drosophila* Nod Kinesin-Like Protein

(A) A schematic comparison of the structure of the Nod_{FL}-GFP protein expressed for these studies and the Nod-KHC-γgal fusion protein studied by Clark *et al.* [222]. Light gray blocks denote Nod sequences, dark gray blocks denote the KHC component of the Nod-KHC-βgal fusion protein, and black regions denote the βgal or GFP tags. The motor-like domain of Nod falls entirely within the first 320 amino acids at the N-terminus.

(B) A drawing of the Nod protein indicating the position of the motor domain, the three HMGN domains and the HhH(2)/NDD domain. The HMGN and HhH(2)/NDD domains are involved in binding Nod to chromosomes [219, 288].

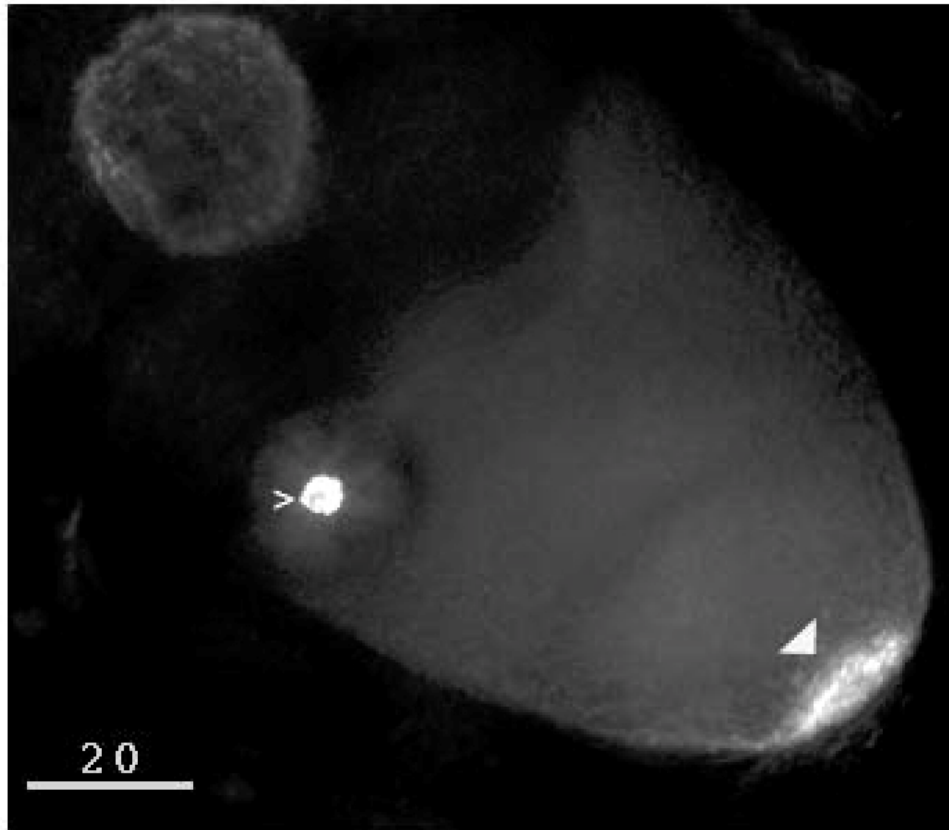


Figure 19. Nod_{FL}-GFP Localizes to both the Oocyte Chromosomes and to the Posterior Pole in Stage 9 Oocytes (Photo by Wei Cui)

6.5.2 Figure 19 Legend

Nod_{FL}-GFP Localizes to Both the Oocyte Chromosomes and to the Posterior Pole in Stage 9 Oocytes

Wildtype oocytes expressing Nod_{FL}-GFP were stained with α -GFP antibody and analyzed by deconvolution microscopy. The open arrowhead indicates Nod_{FL}-GFP localization to the oocyte chromosomes. The filled arrowhead indicates Nod_{FL}-GFP localization to the posterior pole of the oocyte. Scale bar equals 20 μ m.

grk/+

grk^{DC}/grk^{2B}

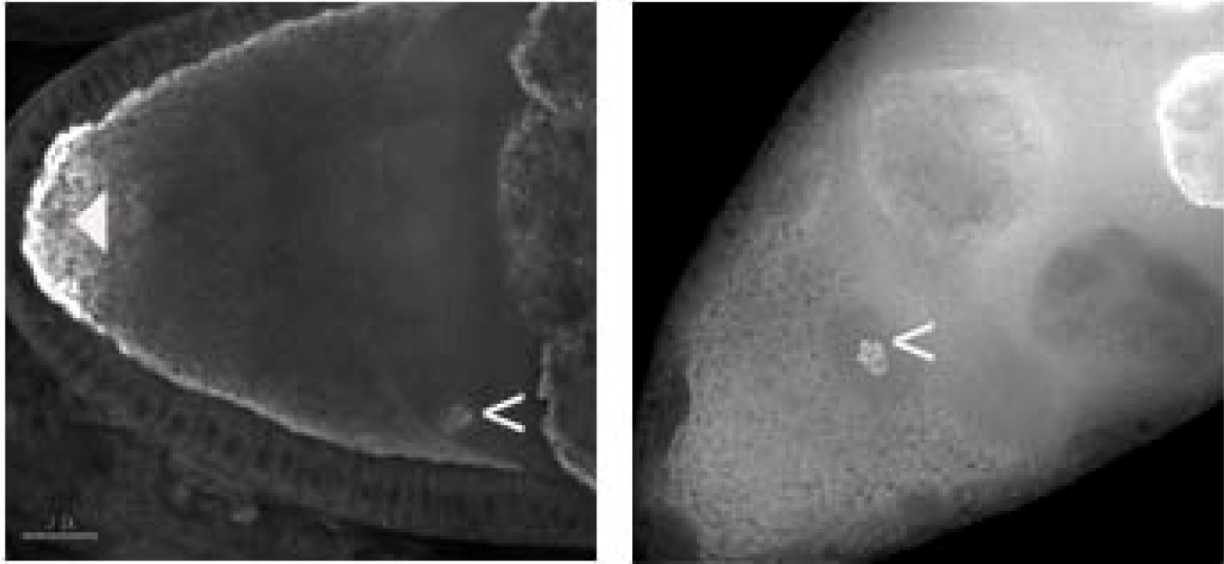


Figure 20. Localization of Nod_{FL}-GFP in Stage 9 Oocytes in Which the Microtubule Organization is Disrupted by Mutations in *grk* (Photo by Wei Cui)

6.5.3 Figure 20 Legend

Localization of Nod_{FL}-GFP in Stage 9 Oocytes in Which the Microtubule Organization is Disrupted by Mutations in *grk*

Normal (*grk/+*) and *grk* (*grk^{DC}/grk^{2B}*) oocytes expressing Nod_{FL}-GFP were stained with anti-GFP antibody (GFP) and analyzed by deconvolution microscopy. The open arrowhead indicates Nod_{FL}-GFP localization to the oocyte chromosomes. The filled arrowhead indicates Nod_{FL}-GFP localization to the posterior pole of the oocyte. Note that Nod_{FL}-GFP localizes to the oocyte chromosomes in both *grk/+* and *grk* oocytes, but only localizes to the posterior pole in *grk/+* oocytes. Scale bar equals 20 μm.

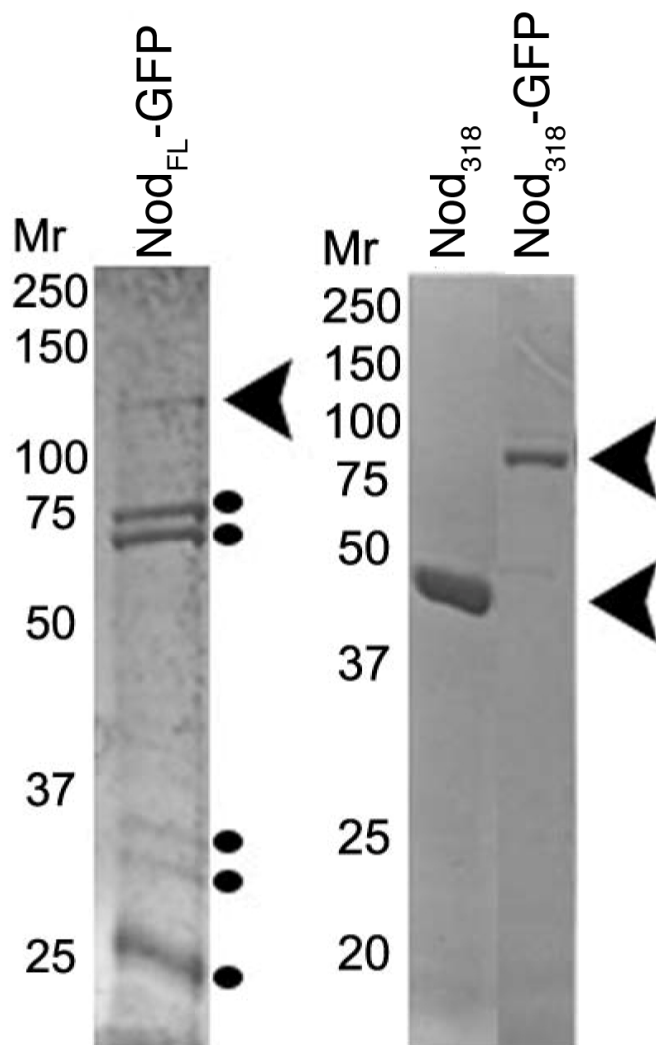


Figure 21. Purification of Nod_{FL}-GFP, Nod₃₁₈, and Nod₃₁₈-GFP From *E. coli*

6.5.4 Figure 21 Legend

Purification of Nod_{FL}-GFP, Nod₃₁₈, and Nod₃₁₈-GFP From *E. coli*

Full length (Nod_{FL}) or motor domain (Nod₃₁₈) constructs were expressed in *E. coli* and purified using Ni-NTA agarose beads. Shown are Coomassie blue-stained SDS-PAGE gels of purified proteins. The (▶) denote the full-length proteins while the (●) indicate breakdown products or contaminants. Based on Western blot analysis (data not shown), the majority of the lower molecular weight bands appear to be the result of breakdown or proteolysis of the Nod-GFP proteins.

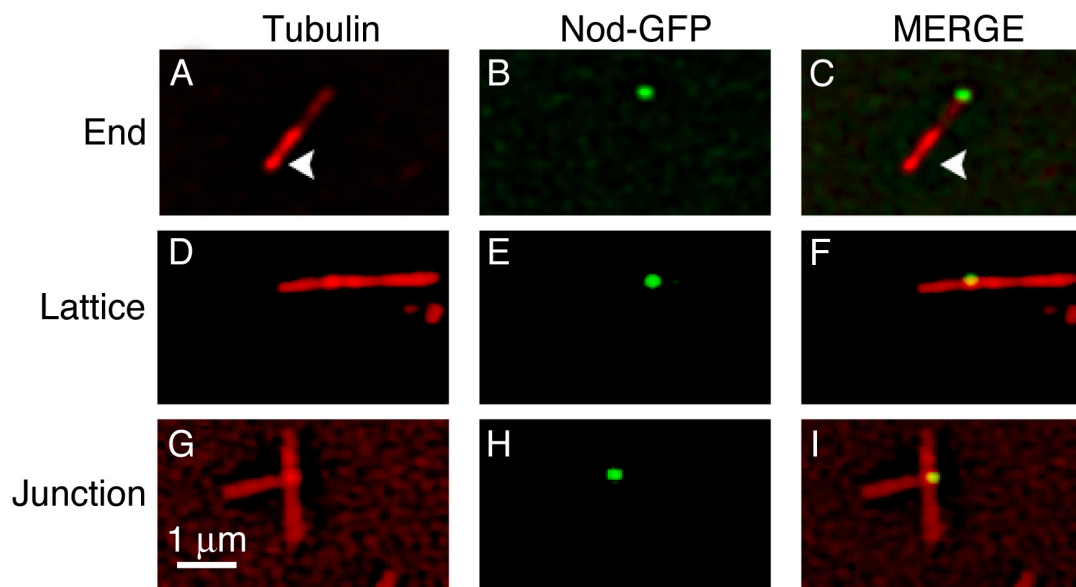


Figure 22. Nod_{FL}-GFP and Nod₃₁₈-GFP Bind to Microtubules *in vitro*

6.5.5 Figure 22 Legend

Nod_{FL}-GFP and Nod₃₁₈-GFP Bind to Microtubules *in vitro*

(A, D and G) Rhodamine-labeled microtubules (red). (B, E and H) Nod_{FL}-GFP localization (green). (C, F and I) Merge of the two channels showing Nod_{FL}-GFP localization on the microtubules. (C) Nod_{FL}-GFP localizes to the plus end of a polarity-marked microtubule. The arrowhead denotes the minus end of the microtubule. (F) Nod_{FL}-GFP localizes to the lattice of a microtubule. (I) Nod_{FL}-GFP localized to the junction between microtubules. The table summarizes microtubule binding scored for Nod_{FL}-GFP and Nod₃₁₈-GFP. Concentrations for Nod_{FL}-GFP and Nod₃₁₈-GFP are listed in the Table; the tubulin concentration = 0.5 μM. As can be seen in Figure 5D-F and G-I, GFP foci were often observed at “bright spots” of rhodamine-tubulin signal along the lengths or at the tips of microtubules. While these associations might indicate a higher concentration of tubulin oligomers at or near the site of Nod binding and the preference for Nod to bind at those sites, we note that “bright spots” are also commonly observed on microtubules that do not have bound Nod protein, and thus they are not likely to be a consequence of Nod binding.

Table 4. Summary of Nod-Microtubule Binding

Nod	[Protein] nM	Total MT	% MT bound (#)	% Binding (#)		
				Lattice	Junction	End
No motor	0.0	335	0.0 (0)	0.0 (0)	0.0 (0)	0.0 (0)
GFP	28.6	535	0.0 (0)	0.0 (0)	0.0 (0)	0.0 (0)
GFP	35.8	423	0.2 (1)	100.0 (1)	0.0 (0)	0.0 (0)
GFP	57.2	763	0.4 (3)	0.0 (0)	100.0 (3)	0.0 (0)
NOD ₃₁₈ -GFP	6.1	1997	2.3 (45)	42.2 (19)	17.7 (8)	40.0 (18)
NOD ₃₁₈ -GFP	12.1	664	3.6 (24)	33.3 (8)	8.3 (2)	58.3 (14)
NOD ₃₁₈ -GFP	24.2	1179	6.5 (77)	54.5 (42)	10.3 (10)	32.4 (25)
NOD _{F1} -GFP	0.2	213	3.3 (7)	14.2 (1)	57.1 (4)	28.4 (2)
NOD _{F1} -GFP	1.0	427	6.3 (27)	22.2 (6)	44.4 (12)	33.3 (9)
NOD _{F1} -GFP	5.7	284	16.5 (47)	25.5 (12)	51.1 (24)	23.4 (11)
NOD _{F1} -GFP	18.9	135	24.4 (33)	27.2 (9)	36.4 (12)	36.4 (12)

* There are end-end, end-lattice and lattice-lattice junctions. All the MTs are counted in the junctions.

Nod Focus Localization

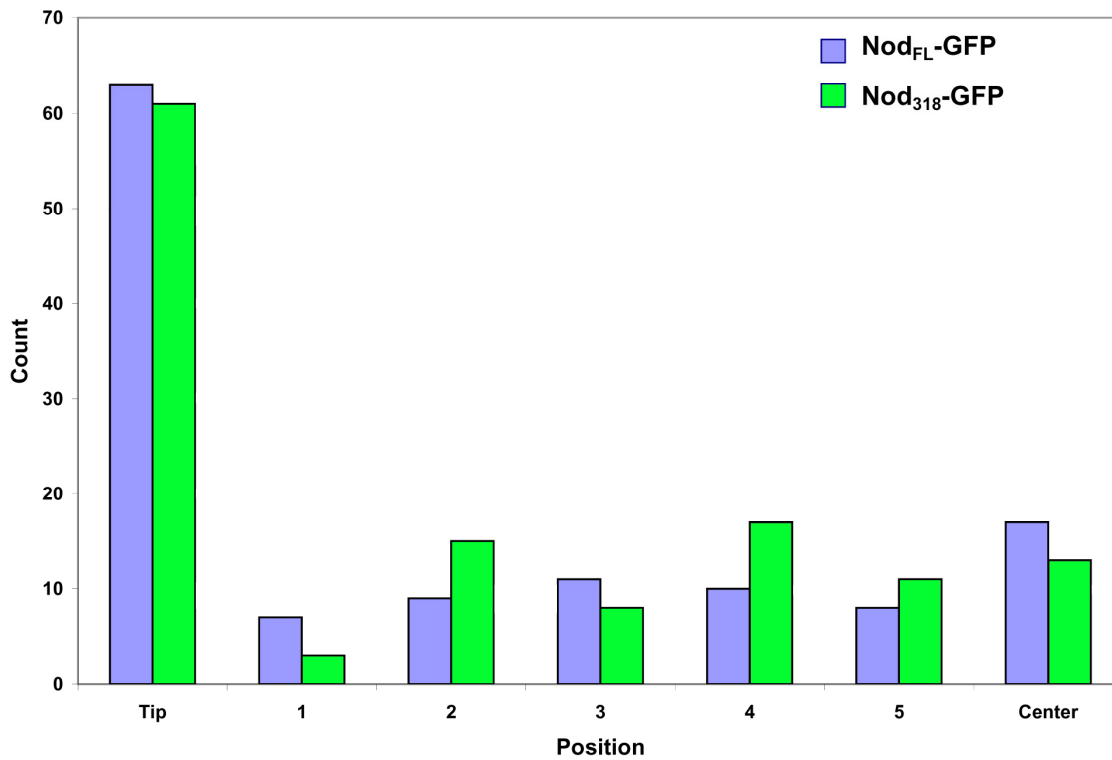
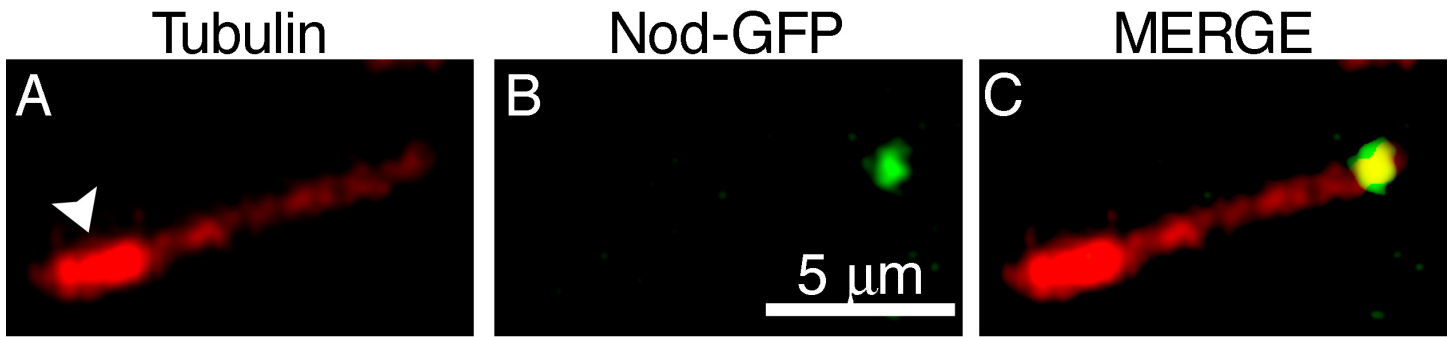


Figure 23. Distribution of Nod Binding Sites Along Microtubules

6.5.6 Figure 23 Legend

Distribution of Nod Binding Sites Along the Microtubule

The microtubule was divided into 7 segments from either end, such that 0 indicates both microtubule tips, and 50 the center of the microtubule. Thus the first 'bin' denotes those cases where the Nod focus fell at a point between 0 and 7% of the length of the microtubule, the second bin denotes those cases where the focus fell between 8 and 14% of the length of the microtubule, and so on. Because we are always measuring the distance from the GFP focus to the nearest tip of the microtubule the distance cannot exceed 50%. The bin size of seven reflects the fact that for those foci, which were close to, but not at, the tip, the minimum distance from focus to tip was 7% of the length. The frequency of Nod_{FL}-GFP and Nod₃₁₈-GFP localization to each segment is plotted. The microtubules scored for this localization are listed in Table 4. Each set of bars denotes the actual number of fluorescent foci found along the microtubule at the denoted segment.



Summary of Nod Binding Polarity Marked MTs

	Total MT	% MT Bound (#)	Lattice Binding (#)	Total End Binding (#)	Polarity Marked MTs % End Binding (#)	
					Plus End	Minus End
25 nM Nod₃₁₈-GFP	6934	4.1 (234)	28.2 (66)	71.8 (168)	31 (52)	1.8 (3)

Figure 24. Trapping of the Nod₃₁₈-GFP Collision Complex by Glutaraldehyde Fixation

6.5.7 Figure 24 Legend

Trapping of the Nod₃₁₈-GFP Collision Complex by Glutaraldehyde Fixation

Panels A-C show a polarity marked microtubule denoted by a bright seed at the minus end (arrowhead in A) bound at the dimmer plus-end by Nod₃₁₈-GFP. The average length of the microtubules counted was 4.63 ± 0.18 (SEM). The tubulin concentration was 0.5 μ M.

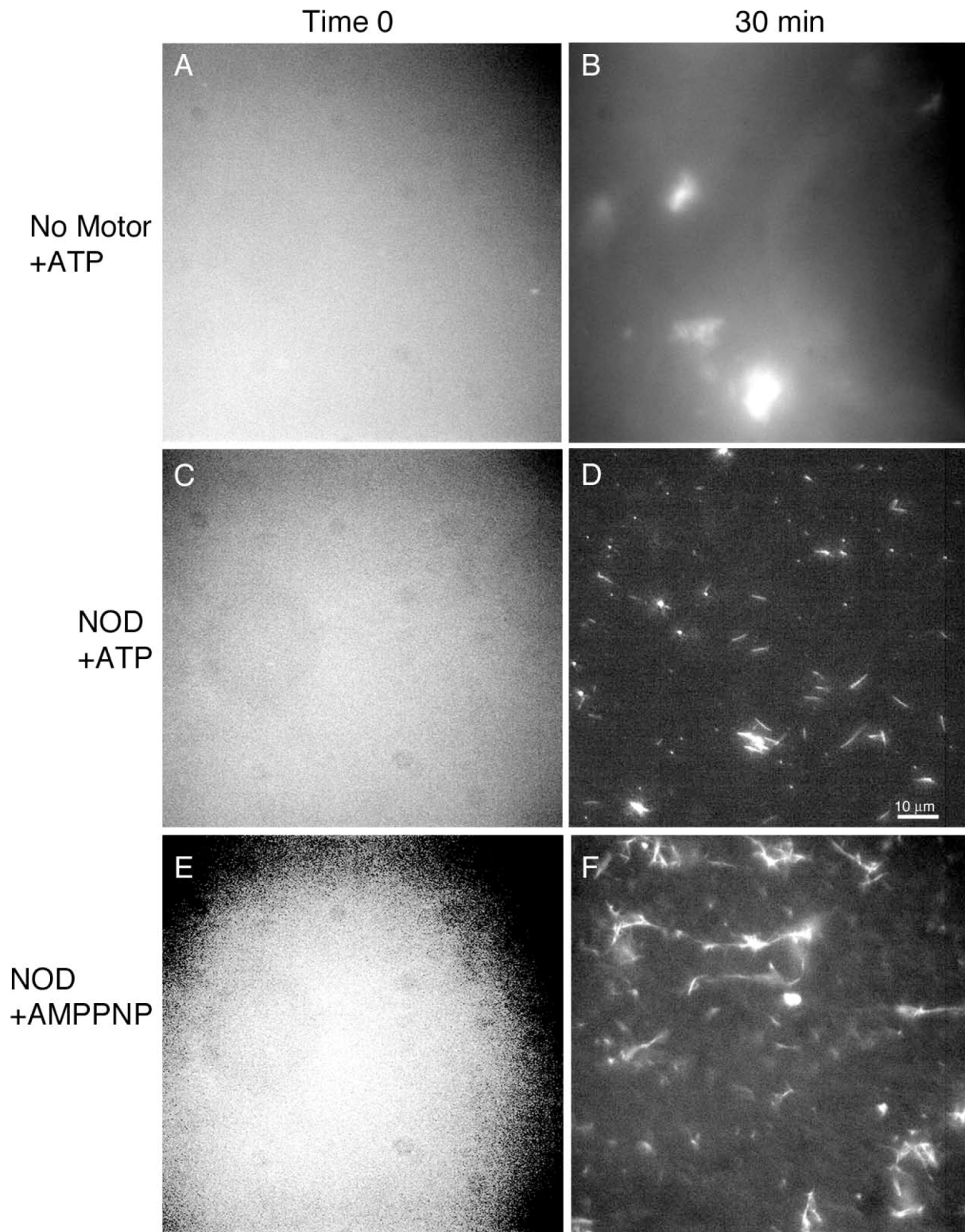


Figure 25. Nod Promotes Microtubule Polymerization *in vitro*

6.5.8 Figure 25 Legend

Nod Promotes Microtubule Polymerization *in vitro*

3 μ M soluble labeled tubulin was complexed with 50 nM Nod₃₁₈ in the presence of MgATP and the reaction was incubated for varying time points, at which time, 8 μ l was extracted and microtubule polymerization was visually assayed on a fluorescence microscope. Panels A, C, E show time 0. Panels B, D, F show 30 minutes. In panel B, little microtubule polymerization is observed in the absence of any motor. In panel D, in the presence of Nod₃₁₈ and MgATP, polymerization of individual microtubules can be observed. In panel F, in the presence of Nod₃₁₈ and MgAMPPNP, polymerization is also seen with bundling of the microtubules.

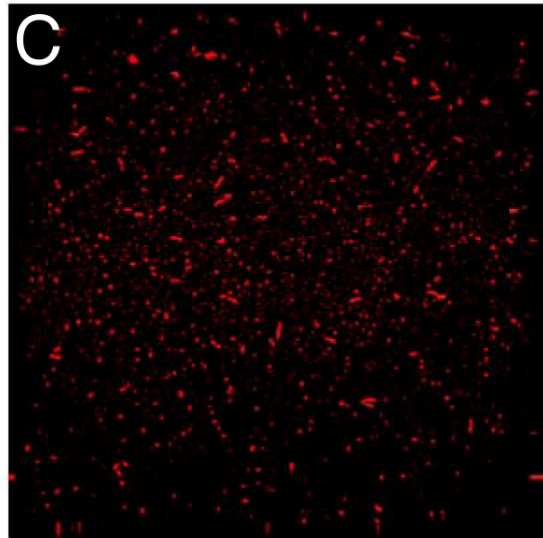
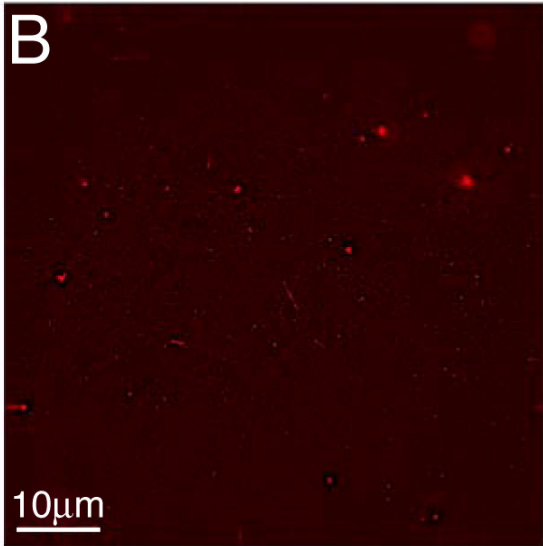
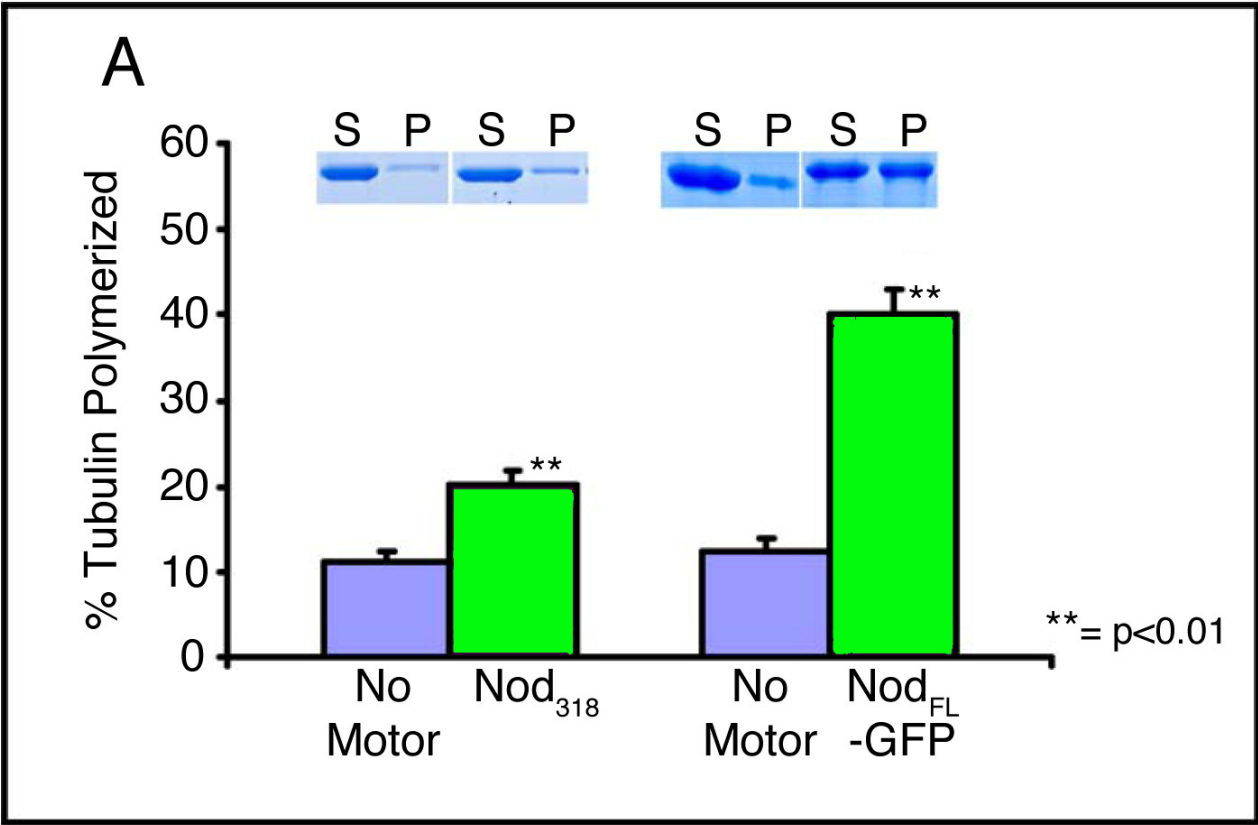


Figure 26. Sedimentation Analysis of the Effect of Nod on Microtubule Polymerization

6.5.9 Figure 26 Legend

Sedimentation Analysis of the Effect of Nod on Microtubule Polymerization

(A) Both Nod₃₁₈ (300 nM) and Nod_{FL} (150 nM) incubated with 3 μ M soluble tubulin promote microtubule polymerization over time in the presence of MgATP. The reactions were centrifuged, and the supernatant and pellet at equal volume for each reaction were analyzed by SDS-PAGE. The amount of tubulin that partitioned to the supernatant and to the pellet was quantified (see gel slices) (B and C). To ensure that the tubulin that partitioned to the pellet was polymerized tubulin (microtubules) and not aggregates of soluble tubulin, the experiment was repeated using rhodamine-tubulin, and the pellets were resuspended and examined using fluorescence microscopy. Each experiment was performed in duplicate on three separate occasions. The value presented in the histogram (A) is the average of those six repetitions. Error bars denote the standard error of the mean. Microsoft Excel Student T-test calculated the statistical differences between control samples and Nod treated samples.

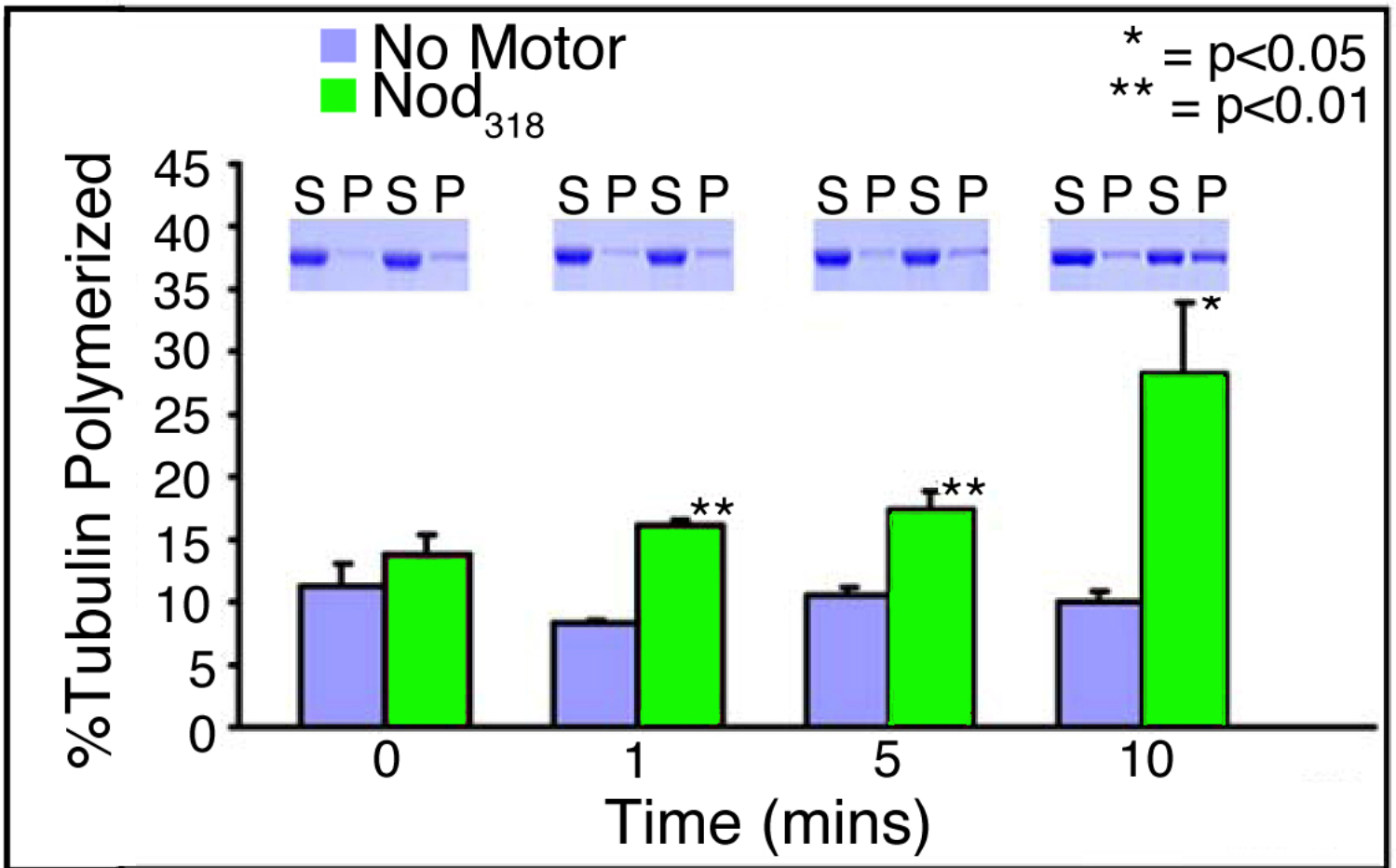


Figure 27. Nod Promotes Microtubule Polymerization in a Time-Dependent Manner

6.5.10 Figure 27 Legend

Nod Promotes Microtubule Polymerization in a Time-Dependent Manner

3 μ M soluble tubulin and 300 nM Nod₃₁₈ incubated with MgATP polymerizes tubulin as a function of time as indicated by the increase of tubulin partitioning to the pellet (see gel slices). Each experiment was performed in duplicate on three separate occasions. The value presented in the histogram is the average of those six repetitions. Error bars denote the standard error of the mean. Microsoft Excel Student T-test calculated the statistical differences between control samples and Nod treated samples.

MT Polymerization by *E.coli* Lysate

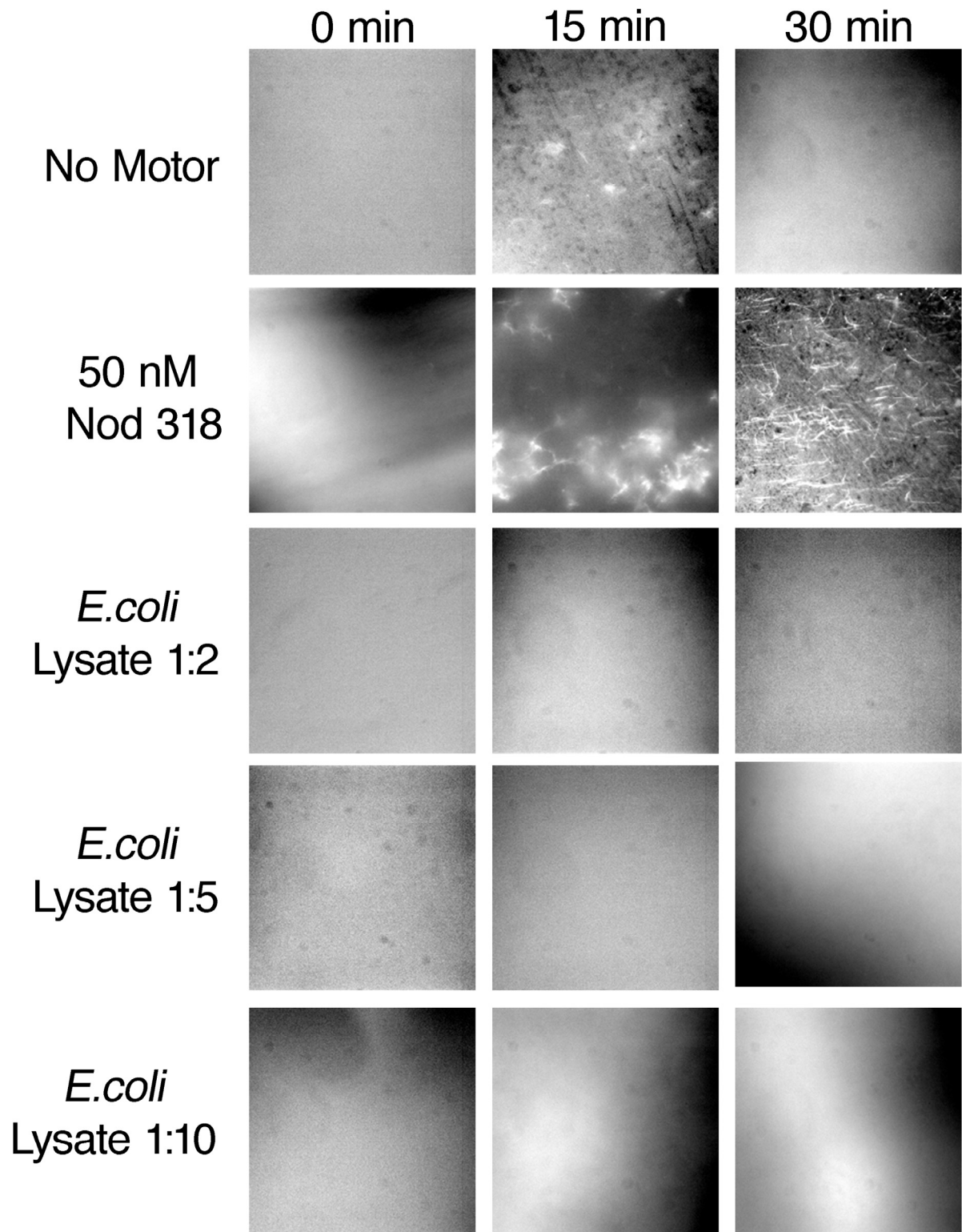


Figure 28. *E.coli* Lysate is Insufficient to Polymerize Microtubules

6.5.11 Figure 28 Legend

***E.coli* Lysate is Insufficient to Polymerize Microtubules**

Microtubule polymerization is visualized over time in the absence of motor (Row 1), in the presence of Nod₃₁₈-GFP purified from *E.coli* Lysate, (Row 2) or in the presence of diluted *E.coli* Lysate expressed without Nod (Rows 3-5). Note that the only individual microtubules polymerized are those polymerized in the presence of purified Nod.

7.0 DISCUSSION AND CONCLUSIONS

Over twenty years have passed since the discovery of Kinesin-1, a mighty motor that marched down microtubules of the axon hauling cargo [70]. In the intervening time, Kinesin-1, the founding member of the Kinesin superfamily has acquired more than 400 siblings that can be classified into 14 subgroups, while other kinesins evade classification and reside in the family as “orphans” (Figure 1). The subfamilies are classified based on their unique function, oligomeric state, location of the motor domain in the polypeptide chain, and conservation of subfamily-specific amino acid sequences within the motor domain. Kinesin-1s have two identical N-terminal catalytic domains that dimerize through C-terminal coiled-coil sequence. Kinesin-1 coordinates ATP hydrolysis to stepping hand-over-hand (asymmetrically) along the microtubule using their N-terminal catalytic “heads” (Figure 3). Most Kinesin-1s associate with cargo-specific light chains to form a heterotetramer. It is the C-terminus of the Kinesin-1 heterotetramer that forms the adaptor or cargo binding site. The high processivity of this molecular motor acts to pull the cargo toward the microtubule plus-ends for distances greater than 100 nm. (reviewed in [94]). However, Kinesin subfamilies 2-14 do not all mimic this role. Not surprisingly, the cell has not invested energy into 14 + copies of a protein for the same function. The sheer number of kinesin proteins suggests that they are specialized to function spatially and temporally. As the diversity of the Kinesin superfamily is probed, it becomes increasingly clear that a kinesin participates in nearly every cellular event.

My dissertation work has involved *in vitro* characterization of three unconventional kinesins, Kar3Cik1, Kar3Vik1, and Nod. The three kinesins differ from conventional kinesin, Kinesin-1 in that they do not walk along microtubules to transport vesicular cargo to the plus end. We find that Kar3Cik1 and Nod both function to

regulate microtubule dynamics. In contrast, Kar3Vik1 exhibits cooperative microtubule binding consistent with genetic phenotypes that allow us to propose that it may transport microtubules as cargo to the microtubule minus end. Our data and that of other labs, suggests that Kar3Vik1 acts to focus and maintain minus ends at the spindle pole body in yeast, similar to Ncd in *Drosophila* meiosis. The kinesins are similar in that they both play roles in regulating the dynamics of microtubules at the microtubule ends during specific times in the life cycles of the organisms in which they are found. My findings have provided further insight to the growing field of kinesin motor proteins that are found to target to a specific microtubule end *in vivo*, and at this site, utilize their intrinsic motor activity to act on the microtubule to ensure proper cellular functioning.

To address how different kinesins precisely interact with microtubules we used a combination of equilibrium binding techniques, microscopy, and steady state kinetics to characterize the kinesins Kar3Cik1, Kar3Vik1, and Nod. I defined the motors Kar3Cik1 and Kar3Vik1, as two distinct motors *in vitro*, and my results are supported by genetics and imaging of the two distinct motors *in vivo*. This work was the first to specifically define the interactions that Kar3Cik1 and Kar3Vik1, each have with single microtubules. My studies in collaboration with Drs. Wei Cui, and R. Scott Hawley with Nod identified a kinesin superfamily member with the responsibility of promoting microtubule polymerization. These results provide interesting clues to *in vivo* kinesin function and emphasize the diversity of the kinesin superfamily of motors.

7.1 KAR3, A GENETIC HISTORY

When I began my dissertation on Kar3, a rich genetic history existed for Kar3 and its heterodimeric partners Cik1 and Vik1. Genetic screens, deletions, and motor domain mutations showed that Kar3 was required during mating in yeast to act on the cytoplasmic microtubules in an ATP-dependent manner for the event of nuclear fusion [165, 169, 202]. The observation of longer microtubules in *kar3Δ* cells suggested that Kar3 acted to regulate microtubule dynamics [7, 8, 165, 169, 173, 174, 177, 178]. In addition, it was observed that *in vitro* Kar3 was able to destabilize microtubules from

both ends, with a preference for the minus end while motoring toward the microtubule minus end [192, 193]. This was the first report of a kinesin physically acting on the microtubule to regulate the microtubule length. Because karyogamy involves two nuclei moving in toward each other and then fusing, the model became: Kar3 motored to the minus ends in karyogamy while it cross-linked microtubules, and it then acted at the minus ends to shorten microtubules. Consistent with the *in vitro* report of Kar3 acting on both microtubule ends, *in vivo* localization data for Kar3 showed it to be at both the microtubule plus and minus ends [7, 8, 165, 169, 171, 173, 174, 177, 187-190, 193].

It was discovered that the Kar3 localization to cytoplasmic microtubules was dependent on a non-motor protein, Cik1 [187]. Kar3 and Cik1 deletions showed identical karyogamy phenotypes, and the two proteins co-immunoprecipitated. Further work predicted that the two formed a novel heterodimeric motor that looked like a dimeric kinesin, with two globular domains in close proximity. However unlike a heterodimeric kinesin, only one “head” would be catalytic [189]. Cik1, the “dead head”, would lie in close proximity to the catalytic head. When Kar3 bound the microtubule, Cik1 would then be close to the Kar3•microtubule interface. These data suggested that Cik1 likely regulated Kar3 and the Kar3 interaction with the microtubule. Distinct from karyogamy, Cik1 and Kar3 did not share identical mitotic phenotypes [188]. This observation suggested that during mitosis or vegetative growth Kar3 acted independently, or in partner with another protein.

A search of the yeast genome revealed an uncharacterized protein that was found to be of similar length with amino acid sequence identity and predicted structural similarity to Cik1 [188]. Genetics and *in vivo* localization showed that this protein, Vik1, was responsible for the localization of Kar3 to the spindle pole body in mitosis [188]. Prior to Vik1 discovery, it had been shown that during vegetative growth Kar3 plays an important role at the spindle pole body in balancing the forces between three different kinesins, Kip2, Cin8, and Kip1 to regulate microtubule dynamics [7, 8, 12, 173, 174, 177]. This was shown for both mitotic spindle and cytoplasmic microtubules. Again, it was thought that Kar3 acted to depolymerize microtubules at the minus ends to control proper length. The genetic phenotypes of *vik1*Δ are similar to those of *kar3*Δ, and not *cik1*Δ, suggesting that Vik1 and Cik1 are not redundant for function [188]. Absent from

this body of work on Kar3 were biochemical analyses of Kar3Cik1 and Kar3Vik1 as they interacted with the microtubule *in vitro* to delineate between the functions of the two. My dissertation research examined the specific Kar3Cik1- and Kar3Vik1-microtubule interactions *in vitro*.

7.2 CIK1 TARGETS THE MINUS END KINESIN DEPOLYMERASE KAR3 TO THE MICROTUBULE PLUS END

We purified the heterodimer Kar3Cik1 to determine its interactions with the microtubule to compare with the microtubule interactions of Kar3 motor domain, dimeric Ncd, a fellow Kinesin-14 family member, MCAK, a Kinesin-13 and robust microtubule depolymerase, and finally to a conventional Kinesin-1. Our results were novel and exciting in that they provided an explanation for the *in vivo* observations and localization data for Kar3 and Cik1. We defined a model for Kar3Cik1 function *in vivo*, and we characterized a novel kinesin depolymerase.

We showed using time-lapse fluorescence microscopy that Kar3Cik1 has the ability to slide and depolymerize microtubules (Figures 9D, 11, and Supplemental Movie 1). We found the depolymerization to be resistant to overly stable microtubules, consistent with the Kar3 localization to dynamic microtubules *in vivo* (Figure 10). The Kar3Cik1 depolymerization is plus-end targeted, meaning that Kar3Cik1 preferentially bound to and depolymerized microtubules from the plus end of the microtubule (Figures 11 & 12, Table 3). In addition, we found no evidence of Kar3Cik1 binding to soluble tubulin, or exhibiting an ATPase rate stimulated by soluble tubulin. These results suggest that Kar3Cik1 is unique as a depolymerase in that it does not release with the tubulin subunits being removed from the polymer, suggesting that it may remain tightly associated with the microtubule end, tracking with the depolymerizing microtubules. Support for this comes from solution assays of depolymerization where we observed the kinetics of depolymerization to fit a single exponential function, suggesting that one ATP turnover is coupled to one tubulin release event from the polymer (Figure 10). These

results contrast with those of the canonical Kinesin-13 depolymerases in which the kinetics are sigmoid.

Kinesin-13s do not appear to track with the shortening microtubule, as we propose for Kar3Cik1. Instead, it is known that Kinesin-13s, release with tubulin subunits and have an ATPase stimulated by soluble tubulin [14]. Kinesin-13s have sigmoid depolymerization kinetics in that several Kinesin-13s bind to the microtubule plus end, induce a conformational change in the lattice that triggers rapid microtubule catastrophe [156]. The Kinesin-13s couple ATP turnover to inducing conformational changes on the microtubule lattice, or cooperative end-binding, such that the microtubule ends curl, after which the microtubule undergoes catastrophe or rapid shortening [19, 20, 68, 83]. Our work highlights differences between the Kar3Cik1 depolymerase and the Kinesin-13s characterized to date.

Kar3Cik1 is unique as a Kinesin-14 in that unlike Kar3, Kar3Cik1 showed a preference for binding to the microtubule plus end (Tables 2 & 3). We propose that Kar3 is targeted to the microtubule plus end via interaction with Cik1. Ncd surprisingly showed an end binding preference as well, though Ncd targeted the lattice more frequently than Kar3Cik1 (Table 3). In addition, Ncd also showed microtubule destabilizing capabilities from both ends (Table 2). This work revealed that microtubule destabilization may be a property intrinsic to all Kinesin-14 family members, but one that is regulated or inhibited *in vivo*, as no published data exists for Ncd-promoted depolymerization *in vivo*.

Kar3Cik1 differs from conventional Kinesin-1 in that it has opposite microtubule gliding polarity, with a rate of gliding 30-fold slower than Kinesin-1 (Figure 9D & 14A). Kar3Cik1 has a different preferential microtubule-binding site: Kar3Cik1 targets the microtubule plus end and Kinesin-1 targets the microtubule lattice (Figure 12, Table 3). Kar3Cik1 has the ability to induce microtubule depolymerization, where at the same conditions Kinesin-1 only serves to stabilize or glide the microtubule (Figure 11, Table 2).

These results provide for the first time, a direct role for Kar3Cik1 in karyogamy, which we propose is Cik1 targeting Kar3 to microtubule plus ends. Kar3Cik1 then uses its motor activity to depolymerize microtubules from the plus to the minus end, to

facilitate nuclear fusion. A recent publication detailing Kar3 in karyogamy supports this hypothesis [168]. Our work has implications for the Kar3Cik1 role in mitosis where we propose that Kar3Cik1 may act on a subset of microtubule plus ends to depolymerize the microtubules to facilitate proper kinetochore attachment and chromosomal segregation.

7.3 VIK1 BINDS MICROTUBULES TO REGULATE KAR3 BINDING AND DEPOLYMERIZATION

We purified the Kar3Vik1 heterodimer to compare with the motor capabilities we determined for Kar3Cik1. Similar to Kar3Cik1 we find that Kar3Vik1 can glide microtubules and depolymerize them (Figure 14A & C). However, we find the depolymerization is significantly slower than that observed for Kar3Cik1, while the microtubule-sliding rate is the same (Figures 14C & A). Our results suggest that the microtubule interactions differ, and while depolymerization is intrinsic to Kar3, Vik1 may modulate Kar3 in such a way as to prevent microtubule depolymerization.

In comparison to Kar3Cik1, we find that Kar3Vik1 does not target to the microtubule plus end. Rather, Kar3Vik1 exhibits cooperative binding to the microtubule (Figure 16). This finding is in agreement with the *in vivo* localization data and genetics, which suggest that Kar3Vik1 concentrates at the microtubule spindle poles *in vivo* to organize and stabilize microtubule minus ends for proper mitotic and cytoplasmic microtubule organization [188]. The cooperative binding of Kar3Vik1 we observe *in vitro* stabilizes the microtubule against depolymerization (Figure 14D). We found that the cooperative binding may be facilitated in part by the Vik1 protein, which in the absence of Kar3 binds tightly to the microtubule (Figure 15). Accumulation of Kar3Vik1 at the microtubule minus ends at the spindle poles may provide the stabilizing force necessary to anchor and retain the microtubules at the spindle pole as the plus end directed BimC/Kinesin-5 motors Cin8 and Kip1 move toward the midline or cell periphery, crosslinking and pulling on the parallel and anti-parallel microtubules.

The genetic data in both *Saccharomyces cerevisiae* and *Schizosaccharomyces pombe* argue for Kar3Vik1 stabilizing microtubule minus ends. Both a *kar3* Δ and *vik1* Δ can suppress a collapsed spindle phenotype that is a result of a *cin8* Δ *kip1* Δ in *Saccharomyces cerevisiae* [188]. In *S. pombe*, overexpression of the Kar3Vik1 homologue, Pkl1, causes a splayed mitotic spindle with unfocused spindle pole microtubules [271]. Both phenotypes suggest that Kar3Vik1 acts at the spindle pole to counterbalance the forces applied to microtubules by plus end directed cross-linking kinesins, and to maintain minus end organization and anchoring. Our results provide a mechanism to explain the minus end Kar3Vik1 stabilization *in vivo*.

We propose that tight binding of Vik1 to the microtubule promotes Kar3 binding to the microtubule. Kar3 binding becomes tight in the presence of ATP, allows reorientation of the coiled-coil neck region toward the microtubule minus end which pulls the Vik1 subunit off the microtubule, similar to the power stroke observed for Ncd (Figure 17) [264]. This mechanism provides support for Kar3Vik1 translocation of microtubule cargoes toward the minus ends, as well as minus end directionality, both important for the Kar3Vik1 role at the spindle pole. Our model predicts that Kar3Vik1 is not processive, and following ATP hydrolysis dissociates from the microtubule in the Kar3Vik1•ADP bound solution state capable of rebinding and reiterating the cycle. However, Kar3Vik1 may be processive. If this is true, we suggest that Kar3Vik1 may be the perfect “inchworm model” kinesin candidate [269].

Despite the mechanism of arrival, we predict that once at the microtubule spindle pole, the tight binding of Vik1 and/or Kar3 may alter the conformation of the microtubule lattice such that multiple Kar3Vik1 motors can bind cooperatively, as we observed *in vitro*. The cooperative binding, and minus end directionality may serve to stabilize the minus ends at the pole by localizing many Kar3Vik1 motors at this site. Stabilizing the minus ends provides an opposing force to the plus end motors setting up the bipolar mitotic spindle. This stabilization may be similar to the role of Ncd. Both Kar3Vik1 and Ncd play important mitotic spindle pole roles. Further experiments must be performed on the single molecule and pre-steady state kinetic level to determine how the Kar3Vik1 two heads communicate and interact for function on the microtubule. It will be

interesting to look at the Kar3Vik1 nature of microtubule binding using cryoelectron microscopy compared to that of the Ncd motor.

7.4 CIK1 AND VIK1 CONFER DIFFERENT ROLES TO KINESIN KAR3

7.4.1 The Differences

The differences observed between Kar3Cik1 and Kar3Vik1 suggest that the heterodimeric pairings confer very different roles to the Kar3 motor protein. Cik1 serves to target Kar3 to the microtubule plus end and enhance the depolymerizing capabilities of Kar3 (Figures 11 & 12, Tables 2 & 3). In this manner, Cik1 may act like a plus-end microtubule binding protein. This role is consistent with the Kar3Cik1 proposed role *in vivo*. Molk *et al.* provide data that suggest that Bik1 may enhance or facilitate the Kar3Cik1 plus end tracking [168]. Single molecule work *in vitro* with Kar3Cik1 in the presence and absence of Bik1 will resolve these issues, and determine if Kar3Cik1 can intrinsically track with the microtubule as it shortens. We predict that tracking is important for the fidelity of nuclear fusion in karyogamy.

In contrast, Vik1 binds tightly to the microtubule and promotes Kar3Vik1 cooperative binding on the microtubule lattice. This cooperative binding serves to stabilize against the Kar3 depolymerizing activity. The binding properties we observe are consistent with the localization and microtubule-stabilizing role observed for Kar3 Vik1 *in vivo* at the spindle poles (Figures 14D & 16). Vik1, whose globular C-terminus looks like a kinesin motor domain (our unpublished results in collaboration with Drs. John Allingham and Ivan Rayment) may serve as a second motor, but as a 'dead head', important for Kar3 microtubule binding and gliding. Future studies with both heterodimers will further specify the individual interactions that Kar3Cik1 and Kar3Vik1 have with the microtubule.

7.4.2 The Unanswered Questions

For Kar3Cik1, the unknown question in karyogamy remains: What happens to the Kar3Cik1 N-terminus following cellular fusion? It is hypothesized that the N-terminus also bind microtubules [169, 187]. Alternatively, the N-terminus may interact with an unknown cortex binding protein (See Figure 29). We know Kar3Cik1 depolymerization is coordinated by Bik1 at the site of plus end interactions [168].

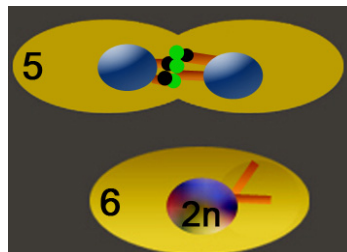


Figure 29. Kar3Cik1 (green) & Bik1 (black) at Depolymerizing Plus Ends Facilitate Nuclear Fusion.

Thus, one can imagine three possibilities for Kar3Cik1 N-terminal localization at the depolymerizing plus ends following cell fusion:

- 1) The N-termini of Kar3Cik1 bind adjacent microtubules, and as a result of the Cik1 targeting to the microtubule plus end, track with the depolymerizing microtubule. Bik1 acts to bridge the adjacent microtubules together, allowing Kar3Cik1 to track with the microtubules as they depolymerize.
- 2) Bik1 may physically interact with Kar3Cik1 at the N-terminus and promote the plus end tracking by providing the microtubule tether so that Kar3Cik1 can depolymerize from the plus to the minus ends.
- 3) Cortical scaffold proteins at this mid-zone may remain attached to the N-terminal region of Kar3Cik1 to facilitate microtubule depolymerization. Bik1 may mediate interactions between the plus-end of anti-parallel microtubules directly or indirectly through interaction with the Kar3Cik1 heterodimeric motor domain.

The improvement of cellular imaging and the continued discovery of microtubule regulating proteins suggest that this question will be answered. Examining Kar3Cik1

function at the nuclear fusion site will provide further insight to the Kar3Cik1 role in mitosis. No direct imaging of Cik1 has been performed in karyogamy or mitosis. All work has focused just on Kar3. Our work was pioneering in looking at the heterodimer interactions with the microtubule *in vitro*. *In vivo* imaging of the heterodimer would build on our work and provide further explanation for the mechanism of Kar3Cik1 action different from Kar3Vik1. In addition, work with the N-termini of both Kar3 and Cik1, the full-length proteins, and the Cik1 protein in the absence of Kar3 (like Vik1) will begin to provide more data for how the Kar3Cik1 ATPase mechanism is coordinated between the two domains for microtubule interaction. It may be that the same interactions Kar3Cik1 has with the microtubules in karyogamy apply in mitosis, however this question remains unanswered.

For Kar3Vik1, the question of how a catalytic head and a dead head coordinate to generate force for function *in vivo* must be solved. The unique similarity of the Vik1 protein fold to a kinesin provides some insight, but X-ray crystal structures of the Kar3Vik1 heterodimer will provide additional clues as well as cryo-electron microscopy of purified microtubule•Kar3Vik1 complexes. Cryoelectron tomography of yeast cells will provide additional insight into structural organization *in vivo*. To understand the mechanism of force generation, studies using transient state kinetic methodologies and single molecule mechanics will be required. These are experiments currently underway in our laboratory and with our collaborators. These experiments will also provide an understanding of the cooperative interactions between Kar3 with Cik1 and Vik1, as well as those interactions between the motors and the microtubule. The next years in the kinesin field promise to be exciting!

7.5 NOD, AN ORPHAN KINESIN THAT PROMOTES MICROTUBULE POLYMERIZATION

Our *in vitro* analysis of the *Drosophila melanogaster* orphan kinesin Nod revealed a kinesin able to promote polymerization of microtubules *in vitro* (Figures 25-27). In Nod mutants or null alleles, chromosomes “flew off” the metaphase plate and did not

undergo disjunction in female meiosis [208, 213, 298]. This suggested that forces were pulling the chromosomes off the metaphase plate. These pulling forces were hypothesized to be forces at the minus ends of the microtubules. The microtubule plus ends contact the chromosomes at the meiotic metaphase plate. It was proposed that Nod in some way provided a “polar ejection force” that served to eject the poles away from the chromosomal alignment at the metaphase plate. An attractive hypothesis for how Nod could accomplish this was to bind to both the chromosome and the microtubules. Structurally Nod would have to bind chromosomes through its C-terminus because it would bind microtubules using its N-terminal kinesin-like motor domain. It was shown that Nod could bind chromosomes, and all along the chromosomal arms [219, 220]. What was unknown was how it then promoted correct chromosomal alignment through interaction with the microtubule. My work in collaboration with Wei Cui probed this question using fluorescence microscopy to determine where Nod preferentially bound to microtubules. We found that Nod has a preference for binding to the microtubule plus end similar to Kar3Cik1, however Nod showed no ability to depolymerize the polymer (Figures 23 & 24, our unpublished results). Instead, Nod in the presence of soluble tubulin stimulated microtubule polymerization four-fold over soluble tubulin polymerization in the absence of Nod (Figure 26A & C). This exciting result led us to propose the model where Nod *in vivo* targets to the chromosome arms via elements found in the C-terminus. Our model predicts that the N-terminal Nod motor domain is exposed on the surface of the chromosomes. The surface of the chromosomes are constantly being probed by microtubule plus ends emanating from both spindle poles, which are organized and focused by the minus end directed kinesin Ncd. We propose that Nod binds to the microtubule plus end, for which it has a high affinity (Figures 23 and 24). We propose that Nod uses ATP turnover to release from the microtubule plus end and then rapidly rebind. Nod may physically add tubulin subunits onto the end of the growing microtubule, or Nod may serve to bind and stabilize the microtubule plus end promoting a GTP cap-like structure. Nod may release, allow tubulin subunits to add onto the polymerizing plus end, and rebind by stabilizing the microtubule plus end. Such a cycle promoted by Nod, would promote growth near the site of the chromosomes serving to push the microtubules and spindle

poles outward. This mechanism accounts for the proposed “polar ejection force” attributed earlier to Nod. How Nod promotes microtubule growth is unknown, but as imaging of single molecule interactions improves, this question will be one that can be answered.

7.6 CONCLUSIONS

My dissertation has centered on understanding and characterizing the mechanisms by which similar proteins interact with the same substrates to produce very different functions *in vivo*. My studies with Kar3Cik1 and Kar3Vik1 have shown that a single kinesin motor can act as two distinct motors by binding to one of two separate proteins that modulate the motor in very different ways. My collaborative work on the orphan kinesin Nod has shown that kinesin superfamily members can also regulate microtubule dynamics by inducing microtubule polymerization. This is novel and in contrast to the Kinesin-13s and our findings with Kar3Cik1 and Kar3Vik1. These studies are valuable in understanding how very different kinesin family members interact with the microtubule. Many diseases involve the microtubule cytoskeleton. To better understand and treat such diseases, a detailed understanding of the proteins that regulate the microtubule architecture is needed. Both Kar3 and Nod have human homologues, and the studies presented here may provide insight into functional roles that these homologs play in humans. As both Kar3 and Nod are involved and important for chromosomal segregation in their host organisms, determining their mechanism of action in this crucial event is beneficial to the scientific field at many levels. It is my hope that my contributions here will provide insight into kinesin motor function for human health, development, and treatment of disease associated with these proteins.

BIBLIOGRAPHY

1. Sweeney, H. L. & Holzbaur, E. L. (1996) Mutational analysis of motor proteins, *Annu Rev Physiol.* **58**, 751-92.
2. Titus, M. A. & Gilbert, S. P. (1999) The diversity of molecular motors: an overview, *Cell Mol Life Sci.* **56**, 181-3.
3. Vale, R. D. (2003) The molecular motor toolbox for intracellular transport, *Cell.* **112**, 467-80.
4. Gunawardena, S. & Goldstein, L. S. (2004) Cargo-carrying motor vehicles on the neuronal highway: transport pathways and neurodegenerative disease, *J Neurobiol.* **58**, 258-71.
5. Lakamper, S. & Meyhofer, E. (2006) Back on track - On the role of the microtubule for kinesin motility and cellular function, *J Muscle Res Cell Motil.* **27**, 161-71.
6. Wickstead, B. & Gull, K. (2006) A "holistic" kinesin phylogeny reveals new kinesin families and predicts protein functions, *Mol Biol Cell.* **17**, 1734-43.
7. Roof, D. M., Meluh, P. B. & Rose, M. D. (1992) Kinesin-related proteins required for assembly of the mitotic spindle, *J Cell Biol.* **118**, 95-108.
8. Saunders, W. S. & Hoyt, M. A. (1992) Kinesin-related proteins required for structural integrity of the mitotic spindle, *Cell.* **70**, 451-8.
9. Walczak, C. E., Mitchison, T. J. & Desai, A. (1996) XKCM1: a *Xenopus* kinesin-related protein that regulates microtubule dynamics during mitotic spindle assembly, *Cell.* **84**, 37-47.
10. Walczak, C. E. & Mitchison, T. J. (1996) Kinesin-related proteins at mitotic spindle poles: function and regulation, *Cell.* **85**, 943-6.

11. Gaglio, T., Saredi, A., Bingham, J. B., Hasbani, M. J., Gill, S. R., Schroer, T. A. & Compton, D. A. (1996) Opposing motor activities are required for the organization of the mammalian mitotic spindle pole, *J Cell Biol.* 135, 399-414.
12. Saunders, W., Lengyel, V. & Hoyt, M. A. (1997) Mitotic spindle function in *Saccharomyces cerevisiae* requires a balance between different types of kinesin-related motors, *Mol Biol Cell.* 8, 1025-33.
13. Walczak, C. E., Vernos, I., Mitchison, T. J., Karsenti, E. & Heald, R. (1998) A model for the proposed roles of different microtubule-based motor proteins in establishing spindle bipolarity, *Curr Biol.* 8, 903-13.
14. Desai, A., Verma, S., Mitchison, T. J. & Walczak, C. E. (1999) Kin I kinesins are microtubule-destabilizing enzymes, *Cell.* 96, 69-78.
15. Walczak, C. E. (2000) Microtubule dynamics and tubulin interacting proteins, *Curr Opin Cell Biol.* 12, 52-6.
16. Beach, D. L., Thibodeaux, J., Maddox, P., Yeh, E. & Bloom, K. (2000) The role of the proteins Kar9 and Myo2 in orienting the mitotic spindle of budding yeast, *Curr Biol.* 10, 1497-506.
17. Hunter, A. W. & Wordeman, L. (2000) How motor proteins influence microtubule polymerization dynamics, *J Cell Sci.* 113 Pt 24, 4379-89.
18. Kline-Smith, S. L. & Walczak, C. E. (2002) The microtubule-destabilizing kinesin XKCM1 regulates microtubule dynamic instability in cells, *Mol Biol Cell.* 13, 2718-31.
19. Hertzler, K. M., Ems-McClung, S. C. & Walczak, C. E. (2003) Kin I kinesins: insights into the mechanism of depolymerization, *Crit Rev Biochem Mol Biol.* 38, 453-69.
20. Moore, A. & Wordeman, L. (2004) The mechanism, function and regulation of depolymerizing kinesins during mitosis, *Trends Cell Biol.* 14, 537-46.
21. Goshima, G., Nedelec, F. & Vale, R. D. (2005) Mechanisms for focusing mitotic spindle poles by minus end-directed motor proteins, *J Cell Biol.* 171, 229-40.
22. Sousa, A. D., Berg, J. S., Robertson, B. W., Meeker, R. B. & Cheney, R. E. (2006) Myo10 in brain: developmental regulation, identification of a headless isoform and dynamics in neurons, *J Cell Sci.* 119, 184-94.
23. Hodge, T. & Cope, M. J. (2000) A myosin family tree, *J Cell Sci.* 113 Pt 19, 3353-4.

24. Dagenbach, E. M. & Endow, S. A. (2004) A new kinesin tree, *J Cell Sci.* 117, 3-7.
25. Asai, D. J. & Wilkes, D. E. (2004) The dynein heavy chain family, *J Eukaryot Microbiol.* 51, 23-9.
26. Hackney, D. D. (1996) The kinetic cycles of myosin, kinesin, and dynein, *Annu Rev Physiol.* 58, 731-50.
27. Schliwa, M. & Woehlke, G. (2003) Molecular motors, *Nature.* 422, 759-65.
28. Sablin, E. P. & Fletterick, R. J. (2004) Coordination between motor domains in processive kinesins, *J Biol Chem.* 279, 15707-10.
29. Mayer, T. U., Kapoor, T. M., Haggarty, S. J., King, R. W., Schreiber, S. L. & Mitchison, T. J. (1999) Small molecule inhibitor of mitotic spindle bipolarity identified in a phenotype-based screen, *Science.* 286, 971-4.
30. Straight, A. F., Cheung, A., Limouze, J., Chen, I., Westwood, N. J., Sellers, J. R. & Mitchison, T. J. (2003) Dissecting temporal and spatial control of cytokinesis with a myosin II Inhibitor, *Science.* 299, 1743-7.
31. Phelps, M. A., Foraker, A. B. & Swaan, P. W. (2003) Cytoskeletal motors and cargo in membrane trafficking: opportunities for high specificity in drug intervention, *Drug Discov Today.* 8, 494-502.
32. Downing, K. H. & Nogales, E. (1998) Tubulin structure: insights into microtubule properties and functions, *Curr Opin Struct Biol.* 8, 785-91.
33. Nogales, E., Whittaker, M., Milligan, R. A. & Downing, K. H. (1999) High-resolution model of the microtubule, *Cell.* 96, 79-88.
34. Greber, U. F. & Way, M. (2006) A superhighway to virus infection, *Cell.* 124, 741-54.
35. Schuyler, S. C. & Pellman, D. (2001) Search, capture and signal: games microtubules and centrosomes play, *J Cell Sci.* 114, 247-55.
36. Hyman, A. A. (1995) Microtubule dynamics. Kinetochores get a grip, *Curr Biol.* 5, 483-4.
37. Biggins, S. & Walczak, C. E. (2003) Captivating capture: how microtubules attach to kinetochores, *Curr Biol.* 13, R449-60.

38. Maiato, H., DeLuca, J., Salmon, E. D. & Earnshaw, W. C. (2004) The dynamic kinetochore-microtubule interface, *J Cell Sci.* 117, 5461-77.
39. DeLuca, J. G. & Salmon, E. D. (2004) Kinetochores: if you build it, they will come, *Curr Biol.* 14, R921-3.
40. Walczak, C. E. (2005) CLASP fluxes its mitotic muscles, *Nat Cell Biol.* 7, 5-7.
41. Cassimeris, L., Pryer, N. K. & Salmon, E. D. (1988) Real-time observations of microtubule dynamic instability in living cells, *J Cell Biol.* 107, 2223-31.
42. Mitchison, T. & Kirschner, M. (1984) Dynamic instability of microtubule growth, *Nature.* 312, 237-42.
43. Kristofferson, D., Mitchison, T. & Kirschner, M. (1986) Direct observation of steady-state microtubule dynamics, *J Cell Biol.* 102, 1007-19.
44. Walker, R. A., O'Brien, E. T., Pryer, N. K., Soboeiro, M. F., Voter, W. A., Erickson, H. P. & Salmon, E. D. (1988) Dynamic instability of individual microtubules analyzed by video light microscopy: rate constants and transition frequencies, *J Cell Biol.* 107, 1437-48.
45. Desai, A. & Mitchison, T. J. (1997) Microtubule polymerization dynamics, *Annu Rev Cell Dev Biol.* 13, 83-117.
46. Downing, K. H. & Nogales, E. (1998) New insights into microtubule structure and function from the atomic model of tubulin, *Eur Biophys J.* 27, 431-6.
47. Nogales, E. (1999) A structural view of microtubule dynamics, *Cell Mol Life Sci.* 56, 133-42.
48. Nogales, E. & Wang, H. W. (2006) Structural mechanisms underlying nucleotide-dependent self-assembly of tubulin and its relatives, *Curr Opin Struct Biol.* 16, 221-9.
49. Gelfand, V. I. (1991) Microtubule Dynamics: Mechanism Regulation and Function, *Annual Review of Cell Biology.* 7, 93-116.
50. Becker, B. E. & Cassimeris, L. (2005) Cytoskeleton: microtubules born on the run, *Curr Biol.* 15, R551-4.
51. Nogales, E., Wolf, S. G. & Downing, K. H. (1998) Structure of the alpha beta tubulin dimer by electron crystallography, *Nature.* 391, 199-203.

52. Heald, R. & Nogales, E. (2002) Microtubule dynamics, *J Cell Sci.* 115, 3-4.
53. Li, H., DeRosier, D. J., Nicholson, W. V., Nogales, E. & Downing, K. H. (2002) Microtubule structure at 8 Å resolution, *Structure.* 10, 1317-28.
54. Nogales, E. (2000) Structural insights into microtubule function, *Annu Rev Biochem.* 69, 277-302.
55. Vale, R. D., Coppin, C. M., Malik, F., Kull, F. J. & Milligan, R. A. (1994) Tubulin GTP hydrolysis influences the structure, mechanical properties, and kinesin-driven transport of microtubules, *J Biol Chem.* 269, 23769-75.
56. Drechsel, D. N. & Kirschner, M. W. (1994) The minimum GTP cap required to stabilize microtubules, *Curr Biol.* 4, 1053-61.
57. Tran, P. T., Walker, R. A. & Salmon, E. D. (1997) A metastable intermediate state of microtubule dynamic instability that differs significantly between plus and minus ends, *J Cell Biol.* 138, 105-17.
58. Mahadevan, L. a. M., T.J. (2005) Powerful Curves, *Nature.* 435, 895-896.
59. Niederstrasser, H., Salehi-Had, H., Gan, E. C., Walczak, C. & Nogales, E. (2002) XKCM1 acts on a single protofilament and requires the C terminus of tubulin, *J Mol Biol.* 316, 817-28.
60. Wang, H. a. N., E. (2005) The nucleotide-dependent bending flexibility of tubulin regulates microtubule assembly., *Nature.* 435, 911-915.
61. Tirnauer, J. S., Salmon, E. D. & Mitchison, T. J. (2004) Microtubule plus-end dynamics in *Xenopus* egg extract spindles, *Mol Biol Cell.* 15, 1776-84.
62. Maliga, Z. & Mitchison, T. J. (2006) Small-molecule and mutational analysis of allosteric Eg5 inhibition by monastrol, *BMC Chem Biol.* 6, 2.
63. von Massow, A., Mandelkow, E. M. & Mandelkow, E. (1989) Interaction between kinesin, microtubules, and microtubule-associated protein 2, *Cell Motil Cytoskeleton.* 14, 562-71.
64. Heins, S., Song, Y. H., Wille, H., Mandelkow, E. & Mandelkow, E. M. (1991) Effect of MAP2, MAP2c, and tau on kinesin-dependent microtubule motility, *J Cell Sci Suppl.* 14, 121-4.

65. Vasquez, R. J., Gard, D. L. & Cassimeris, L. (1999) Phosphorylation by CDK1 regulates XMAP215 function in vitro, *Cell Motil Cytoskeleton*. 43, 310-21.
66. Walczak, C. E. (2003) The Kin I kinesins are microtubule end-stimulated ATPases, *Mol Cell*. 11, 286-8.
67. McNally, F. (2003) Microtubule dynamics: new surprises from an old MAP, *Curr Biol*. 13, R597-9.
68. Wordeman, L. (2005) Microtubule-depolymerizing kinesins, *Curr Opin Cell Biol*. 17, 82-8.
69. Galjart, N. (2005) CLIPs and CLASPs and cellular dynamics, *Nat Rev Mol Cell Biol*. 6, 487-98.
70. Vale, R. D., Reese, T. S. & Sheetz, M. P. (1985) Identification of a novel force-generating protein, kinesin, involved in microtubule-based motility, *Cell*. 42, 39-50.
71. Vale, R. D., Schnapp, B. J., Mitchison, T., Steuer, E., Reese, T. S. & Sheetz, M. P. (1985) Different axoplasmic proteins generate movement in opposite directions along microtubules in vitro, *Cell*. 43, 623-32.
72. Scholey, J. M., Porter, M. E., Grissom, P. M. & McIntosh, J. R. (1985) Identification of kinesin in sea urchin eggs, and evidence for its localization in the mitotic spindle, *Nature*. 318, 483-6.
73. Gilbert, S. P. & Sloboda, R. D. (1986) Identification of a MAP 2-like ATP-binding protein associated with axoplasmic vesicles that translocate on isolated microtubules, *J Cell Biol*. 103, 947-56.
74. Hollenbeck, P. (1986) Organelle transport. Moving in different directions, *Nature*. 319, 724-5.
75. Kuznetsov, S. A. & Gelfand, V. I. (1986) Bovine brain kinesin is a microtubule-activated ATPase, *Proc Natl Acad Sci U S A*. 83, 8530-4.
76. Cohn, S. (1987) Microtubule activation of kinesin ATPase activity, *Nature*. 326, 16-7.
77. Saxton, W. M., Porter, M. E., Cohn, S. A., Scholey, J. M., Raff, E. C. & McIntosh, J. R. (1988) Drosophila kinesin: characterization of microtubule motility and ATPase, *Proc Natl Acad Sci U S A*. 85, 1109-13.

78. Kull, F. J., Sablin, E. P., Lau, R., Fletterick, R. J. & Vale, R. D. (1996) Crystal structure of the kinesin motor domain reveals a structural similarity to myosin, *Nature*. 380, 550-5.
79. Yang, J. T., Laymon, R. A. & Goldstein, L. S. (1989) A three-domain structure of kinesin heavy chain revealed by DNA sequence and microtubule binding analyses, *Cell*. 56, 879-89.
80. Weiss, A., Schiaffino, S. & Leinwand, L. A. (1999) Comparative sequence analysis of the complete human sarcomeric myosin heavy chain family: implications for functional diversity, *J Mol Biol*. 290, 61-75.
81. Menetrey, J., Bahloul, A., Wells, A. L., Yengo, C. M., Morris, C. A., Sweeney, H. L. & Houdusse, A. (2005) The structure of the myosin VI motor reveals the mechanism of directionality reversal, *Nature*. 435, 779-85.
82. Malik, F. & Vale, R. (1990) Cell biology. A new direction for kinesin, *Nature*. 347, 713-4.
83. Helenius, J., Brouhard, G., Kalaidzidis, Y., Diez, S. & Howard, J. (2006) The depolymerizing kinesin MCAK uses lattice diffusion to rapidly target microtubule ends, *Nature*. 441, 115-9.
84. Bloom, G. S., Wagner, M. C., Pfister, K. K. & Brady, S. T. (1988) Native structure and physical properties of bovine brain kinesin and identification of the ATP-binding subunit polypeptide, *Biochemistry*. 27, 3409-16.
85. Yang, J. T., Saxton, W. M. & Goldstein, L. S. (1988) Isolation and characterization of the gene encoding the heavy chain of *Drosophila* kinesin, *Proc Natl Acad Sci U S A*. 85, 1864-8.
86. Kuznetsov, S. A., Vaisberg, E. A., Shanina, N. A., Magretova, N. N., Chernyak, V. Y. & Gelfand, V. I. (1988) The quaternary structure of bovine brain kinesin, *Embo J*. 7, 353-6.
87. Sellers, J. R. (1996) Kinesin and NCD, two structural cousins of myosin, *J Muscle Res Cell Motil*. 17, 173-5.
88. Amos, L. A. & Cross, R. A. (1997) Structure and dynamics of molecular motors, *Curr Opin Struct Biol*. 7, 239-46.
89. Kozielski, F., Sack, S., Marx, A., Thormahlen, M., Schonbrunn, E., Biou, V., Thompson, A., Mandelkow, E. M. & Mandelkow, E. (1997) The crystal structure

- of dimeric kinesin and implications for microtubule-dependent motility, *Cell*. 91, 985-94.
90. Vale, R. D. & Fletterick, R. J. (1997) The design plan of kinesin motors, *Annu Rev Cell Dev Biol*. 13, 745-77.
 91. Asbury, C. L., Fehr, A. N. & Block, S. M. (2003) Kinesin moves by an asymmetric hand-over-hand mechanism, *Science*. 302, 2130-4.
 92. Kaseda, K., Higuchi, H. & Hirose, K. (2003) Alternate fast and slow stepping of a heterodimeric kinesin molecule, *Nat Cell Biol*. 5, 1079-82.
 93. Yildiz, A., Tomishige, M., Vale, R. D. & Selvin, P. R. (2004) Kinesin walks hand-over-hand, *Science*. 303, 676-8.
 94. Asbury, C. L. (2005) Kinesin: world's tiniest biped, *Curr Opin Cell Biol*. 17, 89-97.
 95. Sablin, E. P., Kull, F. J., Cooke, R., Vale, R. D. & Fletterick, R. J. (1996) Crystal structure of the motor domain of the kinesin-related motor ncd, *Nature*. 380, 555-9.
 96. Gulick, A. M., Song, H., Endow, S. A. & Rayment, I. (1998) X-ray crystal structure of the yeast Kar3 motor domain complexed with Mg.ADP to 2.3 Å resolution, *Biochemistry*. 37, 1769-76.
 97. Kozielski, F., De Bonis, S., Burmeister, W. P., Cohen-Addad, C. & Wade, R. H. (1999) The crystal structure of the minus-end-directed microtubule motor protein ncd reveals variable dimer conformations, *Structure*. 7, 1407-16.
 98. Shipley, K., Hekmat-Nejad, M., Turner, J., Moores, C., Anderson, R., Milligan, R., Sakowicz, R. & Fletterick, R. (2004) Structure of a kinesin microtubule depolymerization machine, *Embo J*. 23, 1422-32.
 99. Ogawa, T., Nitta, R., Okada, Y. & Hirokawa, N. (2004) A common mechanism for microtubule destabilizers-M type kinesins stabilize curling of the protofilament using the class-specific neck and loops, *Cell*. 116, 591-602.
 100. Hackney, D. D. (1988) Kinesin ATPase: rate-limiting ADP release, *Proc Natl Acad Sci U S A*. 85, 6314-8.
 101. Hackney, D. D., Malik, A. S. & Wright, K. W. (1989) Nucleotide-free kinesin hydrolyzes ATP with burst kinetics, *J Biol Chem*. 264, 15943-8.

102. Howard, J. (1993) Kinesin ATPase, *Nature*. 364, 396.
103. Hackney, D. D. (1994) The rate-limiting step in microtubule-stimulated ATP hydrolysis by dimeric kinesin head domains occurs while bound to the microtubule, *J Biol Chem*. 269, 16508-11.
104. Gilbert, S. P. & Johnson, K. A. (1994) Pre-steady-state kinetics of the microtubule-kinesin ATPase, *Biochemistry*. 33, 1951-60.
105. Ma, Y. Z. & Taylor, E. W. (1995) Kinetic mechanism of kinesin motor domain, *Biochemistry*. 34, 13233-41.
106. Ma, Y. Z. & Taylor, E. W. (1997) Interacting head mechanism of microtubule-kinesin ATPase, *J Biol Chem*. 272, 724-30.
107. Gilbert, S. P., Moyer, M. L. & Johnson, K. A. (1998) Alternating site mechanism of the kinesin ATPase, *Biochemistry*. 37, 792-9.
108. Schnitzer, M. J., Visscher, K. & Block, S. M. (2000) Force production by single kinesin motors, *Nat Cell Biol*. 2, 718-23.
109. Xing, J., Wriggers, W., Jefferson, G. M., Stein, R., Cheung, H. C. & Rosenfeld, S. S. (2000) Kinesin has three nucleotide-dependent conformations. Implications for strain-dependent release, *J Biol Chem*. 275, 35413-23.
110. Rosenfeld, S. S., Jefferson, G. M. & King, P. H. (2001) ATP reorients the neck linker of kinesin in two sequential steps, *J Biol Chem*. 276, 40167-74.
111. Rosenfeld, S. S., Xing, J., Jefferson, G. M., Cheung, H. C. & King, P. H. (2002) Measuring kinesin's first step, *J Biol Chem*. 277, 36731-9.
112. Sindelar, C. V., Budny, M. J., Rice, S., Naber, N., Fletterick, R. & Cooke, R. (2002) Two conformations in the human kinesin power stroke defined by X-ray crystallography and EPR spectroscopy, *Nat Struct Biol*. 9, 844-8.
113. Rice, S., Cui, Y., Sindelar, C., Naber, N., Matuska, M., Vale, R. & Cooke, R. (2003) Thermodynamic properties of the kinesin neck-region docking to the catalytic core, *Biophys J*. 84, 1844-54.
114. Gilbert, S. P., Webb, M. R., Brune, M. & Johnson, K. A. (1995) Pathway of processive ATP hydrolysis by kinesin, *Nature*. 373, 671-6.

115. Hackney, D. D. (1995) Highly processive microtubule-stimulated ATP hydrolysis by dimeric kinesin head domains, *Nature*. 377, 448-50.
116. Ma, Y. Z. & Taylor, E. W. (1995) Mechanism of microtubule kinesin ATPase, *Biochemistry*. 34, 13242-51.
117. Farrell, C. M., Mackey, A. T., Klumpp, L. M. & Gilbert, S. P. (2002) The role of ATP hydrolysis for kinesin processivity, *J Biol Chem*. 277, 17079-87.
118. Rosenfeld, S. S., Fordyce, P. M., Jefferson, G. M., King, P. H. & Block, S. M. (2003) Stepping and stretching. How kinesin uses internal strain to walk processively, *J Biol Chem*. 278, 18550-6.
119. Klumpp, L. M., Mackey, A. T., Farrell, C. M., Rosenberg, J. M. & Gilbert, S. P. (2003) A kinesin switch I arginine to lysine mutation rescues microtubule function, *J Biol Chem*. 278, 39059-67.
120. Klumpp, L. M., Hoenger, A. & Gilbert, S. P. (2004) Kinesin's second step, *Proc Natl Acad Sci U S A*. 101, 3444-9.
121. Sablin, E. P. & Fletterick, R. J. (1995) Crystallization and preliminary structural studies of the ncd motor domain, *Proteins*. 21, 68-9.
122. Endow, S. A. & Waligora, K. W. (1998) Determinants of kinesin motor polarity, *Science*. 281, 1200-2.
123. Sablin, E. P., Case, R. B., Dai, S. C., Hart, C. L., Ruby, A., Vale, R. D. & Fletterick, R. J. (1998) Direction determination in the minus-end-directed kinesin motor ncd, *Nature*. 395, 813-6.
124. Endow, S. A. (1999) Determinants of molecular motor directionality, *Nat Cell Biol*. 1, E163-7.
125. Hirose, K., Lockhart, A., Cross, R. A. & Amos, L. A. (1995) Nucleotide-dependent angular change in kinesin motor domain bound to tubulin, *Nature*. 376, 277-9.
126. Hoenger, A., Sablin, E. P., Vale, R. D., Fletterick, R. J. & Milligan, R. A. (1995) Three-dimensional structure of a tubulin-motor-protein complex, *Nature*. 376, 271-4.
127. Hirose, K., Fan, J. & Amos, L. A. (1995) Re-examination of the polarity of microtubules and sheets decorated with kinesin motor domain, *J Mol Biol*. 251, 329-33.

128. Hirose, K., Lockhart, A., Cross, R. A. & Amos, L. A. (1996) Three-dimensional cryoelectron microscopy of dimeric kinesin and ncd motor domains on microtubules, *Proc Natl Acad Sci U S A.* **93**, 9539-44.
129. Hoenger, A. & Milligan, R. A. (1997) Motor domains of kinesin and ncd interact with microtubule protofilaments with the same binding geometry, *J Mol Biol.* **265**, 553-64.
130. Woehlke, G., Ruby, A. K., Hart, C. L., Ly, B., Hom-Booher, N. & Vale, R. D. (1997) Microtubule interaction site of the kinesin motor, *Cell.* **90**, 207-16.
131. Hoenger, A., Sack, S., Thormahlen, M., Marx, A., Muller, J., Gross, H. & Mandelkow, E. (1998) Image reconstructions of microtubules decorated with monomeric and dimeric kinesins: comparison with x-ray structure and implications for motility, *J Cell Biol.* **141**, 419-30.
132. Mandelkow, E. & Hoenger, A. (1999) Structures of kinesin and kinesin-microtubule interactions, *Curr Opin Cell Biol.* **11**, 34-44.
133. Hirose, K., Lowe, J., Alonso, M., Cross, R. A. & Amos, L. A. (1999) Congruent docking of dimeric kinesin and ncd into three-dimensional electron cryomicroscopy maps of microtubule-motor ADP complexes, *Mol Biol Cell.* **10**, 2063-74.
134. Hirose, K., Lowe, J., Alonso, M., Cross, R. A. & Amos, L. A. (1999) 3D electron microscopy of the interaction of kinesin with tubulin, *Cell Struct Funct.* **24**, 277-84.
135. Kikkawa, M., Okada, Y. & Hirokawa, N. (2000) 15 Å resolution model of the monomeric kinesin motor, KIF1A, *Cell.* **100**, 241-52.
136. Hoenger, A., Thormahlen, M., Diaz-Avalos, R., Doerhoefer, M., Goldie, K. N., Muller, J. & Mandelkow, E. (2000) A new look at the microtubule binding patterns of dimeric kinesins, *J Mol Biol.* **297**, 1087-103.
137. Hoenger, A., Doerhoefer, M., Woehlke, G., Tittmann, P., Gross, H., Song, Y. H. & Mandelkow, E. (2000) Surface topography of microtubule walls decorated with monomeric and dimeric kinesin constructs, *Biol Chem.* **381**, 1001-11.
138. Krebs, A., Goldie, K. N. & Hoenger, A. (2004) Complex formation with kinesin motor domains affects the structure of microtubules, *J Mol Biol.* **335**, 139-53.

139. Klumpp, L. M., Brendza, K. M., Gatial, J. E., 3rd, Hoenger, A., Saxton, W. M. & Gilbert, S. P. (2004) Microtubule-kinesin interface mutants reveal a site critical for communication, *Biochemistry*. 43, 2792-803.
140. Marx, A., Muller, J., Mandelkow, E. M., Hoenger, A. & Mandelkow, E. (2006) Interaction of kinesin motors, microtubules, and MAPs, *J Muscle Res Cell Motil*. 27, 125-37.
141. Sack, S., Kull, F. J. & Mandelkow, E. (1999) Motor proteins of the kinesin family. Structures, variations, and nucleotide binding sites, *Eur J Biochem*. 262, 1-11.
142. Kull, F. J. & Endow, S. A. (2002) Kinesin: switch I & II and the motor mechanism, *J Cell Sci*. 115, 15-23.
143. Yun, M., Zhang, X., Park, C. G., Park, H. W. & Endow, S. A. (2001) A structural pathway for activation of the kinesin motor ATPase, *Embo J*. 20, 2611-8.
144. Kikkawa, M., Sablin, E. P., Okada, Y., Yajima, H., Fletterick, R. J. & Hirokawa, N. (2001) Switch-based mechanism of kinesin motors, *Nature*. 411, 439-45.
145. Sablin, E. P. & Fletterick, R. J. (2001) Nucleotide switches in molecular motors: structural analysis of kinesins and myosins, *Curr Opin Struct Biol*. 11, 716-24.
146. Nitta, R., Kikkawa, M., Okada, Y. & Hirokawa, N. (2004) KIF1A alternately uses two loops to bind microtubules, *Science*. 305, 678-83.
147. Sosa, H., Dias, D. P., Hoenger, A., Whittaker, M., Wilson-Kubalek, E., Sablin, E., Fletterick, R. J., Vale, R. D. & Milligan, R. A. (1997) A model for the microtubule-Ncd motor protein complex obtained by cryo-electron microscopy and image analysis, *Cell*. 90, 217-24.
148. Ovechkina, Y. & Wordeman, L. (2003) Unconventional motoring: an overview of the Kin C and Kin I kinesins, *Traffic*. 4, 367-75.
149. Duhl, D. M. & Renhowe, P. A. (2005) Inhibitors of kinesin motor proteins--research and clinical progress, *Curr Opin Drug Discov Devel*. 8, 431-6.
150. Nagle, A., Hur, W. & Gray, N. S. (2006) Antimitotic agents of natural origin, *Curr Drug Targets*. 7, 305-26.
151. Wordeman, L. & Mitchison, T. J. (1995) Identification and partial characterization of mitotic centromere-associated kinesin, a kinesin-related protein that associates with centromeres during mitosis, *J Cell Biol*. 128, 95-104.

152. Ems-McClung, S. C. & Walczak, C. E. (2004) Catastrophic kinesins: piecing together their mechanism by 3D reconstruction, *Cell*. 116, 485-6.
153. Kinoshita, K., Noetzel, T. L., Arnal, I., Drechsel, D. N. & Hyman, A. A. (2006) Global and local control of microtubule destabilization promoted by a catastrophe kinesin MCAK/XKCM1, *J Muscle Res Cell Motil*. 27, 107-14.
154. Moores, C. A., Yu, M., Guo, J., Beraud, C., Sakowicz, R. & Milligan, R. A. (2002) A mechanism for microtubule depolymerization by KinI kinesins, *Mol Cell*. 9, 903-9.
155. Moores, C. A., Hekmat-Nejad, M., Sakowicz, R. & Milligan, R. A. (2003) Regulation of KinI kinesin ATPase activity by binding to the microtubule lattice, *J Cell Biol*. 163, 963-71.
156. Hunter, A. W., Caplow, M., Coy, D. L., Hancock, W. O., Diez, S., Wordeman, L. & Howard, J. (2003) The kinesin-related protein MCAK is a microtubule depolymerase that forms an ATP-hydrolyzing complex at microtubule ends, *Mol Cell*. 11, 445-57.
157. Moore, A. T., Rankin, K. E., von Dassow, G., Peris, L., Wagenbach, M., Ovechkina, Y., Andrieux, A., Job, D. & Wordeman, L. (2005) MCAK associates with the tips of polymerizing microtubules, *J Cell Biol*. 169, 391-7.
158. Walker, R. A., Inoue, S. & Salmon, E. D. (1989) Asymmetric behavior of severed microtubule ends after ultraviolet-microbeam irradiation of individual microtubules in vitro, *J Cell Biol*. 108, 931-7.
159. Walker, R. A., Pryer, N. K. & Salmon, E. D. (1991) Dilution of individual microtubules observed in real time in vitro: evidence that cap size is small and independent of elongation rate, *J Cell Biol*. 114, 73-81.
160. Moore, A. & Wordeman, L. (2004) C-terminus of mitotic centromere-associated kinesin (MCAK) inhibits its lattice-stimulated ATPase activity, *Biochem J*. 383, 227-35.
161. Hertzler, K. M., Ems-McClung, S. C., Kline-Smith, S. L., Lipkin, T. G., Gilbert, S. P. & Walczak, C. E. (2006) Full-length dimeric MCAK is a more efficient microtubule depolymerase than minimal domain monomeric MCAK, *Mol Biol Cell*. 17, 700-10.
162. Maney, T., Wagenbach, M. & Wordeman, L. (2001) Molecular dissection of the microtubule depolymerizing activity of mitotic centromere-associated kinesin, *J Biol Chem*. 276, 34753-8.

163. Ovechkina, Y., Wagenbach, M. & Wordeman, L. (2002) K-loop insertion restores microtubule depolymerizing activity of a "neckless" MCAK mutant, *J Cell Biol.* 159, 557-62.
164. Tytell, J. D. & Sorger, P. K. (2006) Analysis of kinesin motor function at budding yeast kinetochores, *J Cell Biol.* 172, 861-74.
165. Maddox, P. S., Stemple, J. K., Satterwhite, L., Salmon, E. D. & Bloom, K. (2003) The minus end-directed motor Kar3 is required for coupling dynamic microtubule plus ends to the cortical shmoo tip in budding yeast, *Curr Biol.* 13, 1423-8.
166. Maddox, P. S. (2005) Microtubules: Kar3 eats up the track, *Curr Biol.* 15, R622-4.
167. Sproul, L. R., Anderson, D. J., Mackey, A. T., Saunders, W. S. & Gilbert, S. P. (2005) Cik1 targets the minus-end kinesin depolymerase kar3 to microtubule plus ends, *Curr Biol.* 15, 1420-7.
168. Molk, J. N., Salmon, E. D. & Bloom, K. (2006) Nuclear congression is driven by cytoplasmic microtubule plus end interactions in *S. cerevisiae*, *J Cell Biol.* 172, 27-39.
169. Meluh, P. B. & Rose, M. D. (1990) KAR3, a kinesin-related gene required for yeast nuclear fusion, *Cell.* 60, 1029-41.
170. Bascom-Slack, C. A. & Dawson, D. S. (1997) The yeast motor protein, Kar3p, is essential for meiosis I, *J Cell Biol.* 139, 459-67.
171. Trelles-Sticken, E., Loidl, J. & Scherthan, H. (2003) Increased ploidy and KAR3 and SIR3 disruption alter the dynamics of meiotic chromosomes and telomeres, *J Cell Sci.* 116, 2431-42.
172. Shanks, R. M., Bascom-Slack, C. & Dawson, D. S. (2004) Analysis of the kar3 meiotic arrest in *Saccharomyces cerevisiae*, *Cell Cycle.* 3, 363-71.
173. Hoyt, M. A., He, L., Totis, L. & Saunders, W. S. (1993) Loss of function of *Saccharomyces cerevisiae* kinesin-related CIN8 and KIP1 is suppressed by KAR3 motor domain mutations, *Genetics.* 135, 35-44.
174. Saunders, W., Hornack, D., Lengyel, V. & Deng, C. (1997) The *Saccharomyces cerevisiae* kinesin-related motor Kar3p acts at preanaphase spindle poles to limit the number and length of cytoplasmic microtubules, *J Cell Biol.* 137, 417-31.

175. Cottingham, F. R. & Hoyt, M. A. (1997) Mitotic spindle positioning in *Saccharomyces cerevisiae* is accomplished by antagonistically acting microtubule motor proteins, *J Cell Biol.* **138**, 1041-53.
176. Schoch, C. L., Br-uning, A. R., Entian, K. D., Pretorius, G. H. & Prior, B. A. (1997) A *Saccharomyces cerevisiae* mutant defective in the kinesin-like protein Kar3 is sensitive to NaCl-stress, *Curr Genet.* **32**, 315-22.
177. Huyett, A., Kahana, J., Silver, P., Zeng, X. & Saunders, W. S. (1998) The Kar3p and Kip2p motors function antagonistically at the spindle poles to influence cytoplasmic microtubule numbers, *J Cell Sci.* **111** (Pt 3), 295-301.
178. Straight, A. F., Sedat, J. W. & Murray, A. W. (1998) Time-lapse microscopy reveals unique roles for kinesins during anaphase in budding yeast, *J Cell Biol.* **143**, 687-94.
179. Cottingham, F. R., Gheber, L., Miller, D. L. & Hoyt, M. A. (1999) Novel roles for *saccharomyces cerevisiae* mitotic spindle motors, *J Cell Biol.* **147**, 335-50.
180. Zeng, X., Kahana, J. A., Silver, P. A., Morphew, M. K., McIntosh, J. R., Fitch, I. T., Carbon, J. & Saunders, W. S. (1999) Slk19p is a centromere protein that functions to stabilize mitotic spindles, *J Cell Biol.* **146**, 415-25.
181. Hildebrandt, E. R. & Hoyt, M. A. (2000) Mitotic motors in *Saccharomyces cerevisiae*, *Biochim Biophys Acta.* **1496**, 99-116.
182. Gardner, R. D., Poddar, A., Yellman, C., Tavormina, P. A., Monteagudo, M. C. & Burke, D. J. (2001) The spindle checkpoint of the yeast *Saccharomyces cerevisiae* requires kinetochore function and maps to the CBF3 domain, *Genetics.* **157**, 1493-502.
183. Hoepfner, D., Schaerer, F., Brachat, A., Wach, A. & Philippsen, P. (2002) Reorientation of mispositioned spindles in short astral microtubule mutant *spc72Delta* is dependent on spindle pole body outer plaque and Kar3 motor protein, *Mol Biol Cell.* **13**, 1366-80.
184. Mayer, M. L., Pot, I., Chang, M., Xu, H., Aneliunas, V., Kwok, T., Newitt, R., Aebersold, R., Boone, C., Brown, G. W. & Hieter, P. (2004) Identification of protein complexes required for efficient sister chromatid cohesion, *Mol Biol Cell.* **15**, 1736-45.

185. Tanaka, K., Mukae, N., Dewar, H., van Breugel, M., James, E. K., Prescott, A. R., Antony, C. & Tanaka, T. U. (2005) Molecular mechanisms of kinetochore capture by spindle microtubules, *Nature*. 434, 987-94.
186. Page, B. D. & Snyder, M. (1992) CIK1: a developmentally regulated spindle pole body-associated protein important for microtubule functions in *Saccharomyces cerevisiae*, *Genes Dev.* 6, 1414-29.
187. Page, B. D., Satterwhite, L. L., Rose, M. D. & Snyder, M. (1994) Localization of the Kar3 kinesin heavy chain-related protein requires the Cik1 interacting protein, *J Cell Biol.* 124, 507-19.
188. Manning, B. D., Barrett, J. G., Wallace, J. A., Granok, H. & Snyder, M. (1999) Differential regulation of the Kar3p kinesin-related protein by two associated proteins, Cik1p and Vik1p, *J Cell Biol.* 144, 1219-33.
189. Barrett, J. G., Manning, B. D. & Snyder, M. (2000) The Kar3p kinesin-related protein forms a novel heterodimeric structure with its associated protein Cik1p, *Mol Biol Cell.* 11, 2373-85.
190. Shanks, R. M., Kamieniecki, R. J. & Dawson, D. S. (2001) The Kar3-interacting protein Cik1p plays a critical role in passage through meiosis I in *Saccharomyces cerevisiae*, *Genetics.* 159, 939-51.
191. Manning, B. D., Padmanabha, R. & Snyder, M. (1997) The Rho-GEF Rom2p localizes to sites of polarized cell growth and participates in cytoskeletal functions in *Saccharomyces cerevisiae*, *Mol Biol Cell.* 8, 1829-44.
192. Endow, S. A., Kang, S. J., Satterwhite, L. L., Rose, M. D., Skeen, V. P. & Salmon, E. D. (1994) Yeast Kar3 is a minus-end microtubule motor protein that destabilizes microtubules preferentially at the minus ends, *Embo J.* 13, 2708-13.
193. Middleton, K. & Carbon, J. (1994) KAR3-encoded kinesin is a minus-end-directed motor that functions with centromere binding proteins (CBF3) on an in vitro yeast kinetochore, *Proc Natl Acad Sci U S A.* 91, 7212-6.
194. Hoepfner, D., Brachat, A. & Philippsen, P. (2000) Time-lapse video microscopy analysis reveals astral microtubule detachment in the yeast spindle pole mutant *cnm67*, *Mol Biol Cell.* 11, 1197-211.
195. Giepmans, B. N., Adams, S. R., Ellisman, M. H. & Tsien, R. Y. (2006) The fluorescent toolbox for assessing protein location and function, *Science.* 312, 217-24.

196. Maddox, P., Chin, E., Mallavarapu, A., Yeh, E., Salmon, E. D. & Bloom, K. (1999) Microtubule dynamics from mating through the first zygotic division in the budding yeast *Saccharomyces cerevisiae*, *J Cell Biol.* 144, 977-87.
197. McDonald, H. B., Stewart, R. J. & Goldstein, L. S. (1990) The kinesin-like *ncd* protein of *Drosophila* is a minus end-directed microtubule motor, *Cell.* 63, 1159-65.
198. McDonald, H. B. & Goldstein, L. S. (1990) Identification and characterization of a gene encoding a kinesin-like protein in *Drosophila*, *Cell.* 61, 991-1000.
199. Walker, R. A. (1995) *ncd* and kinesin motor domains interact with both alpha- and beta-tubulin, *Proc Natl Acad Sci U S A.* 92, 5960-4.
200. Foster, K. A., Correia, J. J. & Gilbert, S. P. (1998) Equilibrium binding studies of non-claret disjunctional protein (*Ncd*) reveal cooperative interactions between the motor domains, *J Biol Chem.* 273, 35307-18.
201. Foster, K. A., Mackey, A. T. & Gilbert, S. P. (2001) A mechanistic model for *Ncd* directionality, *J Biol Chem.* 276, 19259-66.
202. Mackey, A. T., Ph.D. (2002) *Comparative Analysis of the Kinesin, Ncd, and Kar3 Molecular Motors*, University of Pittsburgh, Pittsburgh, Pennsylvania.
203. Carpenter, A. T. (1973) A meiotic mutant defective in distributive disjunction in *Drosophila melanogaster*, *Genetics.* 73, 393-428.
204. Grell, R. F. (1962) A new model for secondary nondisjunction: the role of distributive pairing, *Genetics.* 47, 1737-54.
205. Grell, R. F. (1976) *Distributive Pairing*, Academic Press, New York.
206. Hawley, R. S. (1988) *Exchange and chromosome segregation in eucaryotes.*, American Society for Microbiology, Washington, D.C.
207. Hawley, R. S. (1989) Genetic and molecular analysis of a simple disjunctional system in *Drosophila melanogaster*, *Prog Clin Biol Res.* 311, 277-302.
208. Zhang, P., Knowles, B. A., Goldstein, L. S. & Hawley, R. S. (1990) A kinesin-like protein required for distributive chromosome segregation in *Drosophila*, *Cell.* 62, 1053-62.

209. Endow, S. A., Henikoff, S. & Soler-Niedziela, L. (1990) Mediation of meiotic and early mitotic chromosome segregation in *Drosophila* by a protein related to kinesin, *Nature*. 345, 81-3.
210. Zhang, P. & Hawley, R. S. (1990) The genetic analysis of distributive segregation in *Drosophila melanogaster*. II. Further genetic analysis of the nod locus, *Genetics*. 125, 115-27.
211. Knowles, B. A. & Hawley, R. S. (1991) Genetic analysis of microtubule motor proteins in *Drosophila*: a mutation at the nod locus is a dominant enhancer of nod, *Proc Natl Acad Sci U S A*. 88, 7165-9.
212. Endow, S. A. (1992) Meiotic chromosome distribution in *Drosophila* oocytes: roles of two kinesin-related proteins, *Chromosoma*. 102, 1-8.
213. Theurkauf, W. E. & Hawley, R. S. (1992) Meiotic spindle assembly in *Drosophila* females: behavior of nonexchange chromosomes and the effects of mutations in the nod kinesin-like protein, *J Cell Biol*. 116, 1167-80.
214. Orr-Weaver, T. L. (1995) Meiosis in *Drosophila*: seeing is believing, *Proc Natl Acad Sci U S A*. 92, 10443-9.
215. Karpen, G. H., Le, M. H. & Le, H. (1996) Centric heterochromatin and the efficiency of achiasmate disjunction in *Drosophila* female meiosis, *Science*. 273, 118-22.
216. Rieder, C. L., Davison, E. A., Jensen, L. C., Cassimeris, L. & Salmon, E. D. (1986) Oscillatory movements of monooriented chromosomes and their position relative to the spindle pole result from the ejection properties of the aster and half-spindle, *J Cell Biol*. 103, 581-91.
217. Rasooly, R. S., New, C. M., Zhang, P., Hawley, R. S. & Baker, B. S. (1991) The lethal(1)TW-6cs mutation of *Drosophila melanogaster* is a dominant antimorphic allele of nod and is associated with a single base change in the putative ATP-binding domain, *Genetics*. 129, 409-22.
218. Rasooly, R. S., Zhang, P., Tibolla, A. K. & Hawley, R. S. (1994) A structure-function analysis of NOD, a kinesin-like protein from *Drosophila melanogaster*, *Mol Gen Genet*. 242, 145-51.
219. Afshar, K., Scholey, J. & Hawley, R. S. (1995) Identification of the chromosome localization domain of the *Drosophila* nod kinesin-like protein, *J Cell Biol*. 131, 833-43.

220. Afshar, K., Barton, N. R., Hawley, R. S. & Goldstein, L. S. (1995) DNA binding and meiotic chromosomal localization of the *Drosophila* nod kinesin-like protein, *Cell*. **81**, 129-38.
221. Matthies, H. J., Baskin, R. J. & Hawley, R. S. (2001) Orphan kinesin NOD lacks motile properties but does possess a microtubule-stimulated ATPase activity, *Mol Biol Cell*. **12**, 4000-12.
222. Clark, I. E., Jan, L. Y. & Jan, Y. N. (1997) Reciprocal localization of Nod and kinesin fusion proteins indicates microtubule polarity in the *Drosophila* oocyte, epithelium, neuron and muscle, *Development*. **124**, 461-70.
223. Matthies, H. J., Messina, L. G., Namba, R., Greer, K. J., Walker, M. Y. & Hawley, R. S. (1999) Mutations in the alpha-tubulin 67C gene specifically impair achiasmate segregation in *Drosophila melanogaster*, *J Cell Biol*. **147**, 1137-44.
224. Cui, W., Sproul, L. R., Gustafson, S. M., Matthies, H. J., Gilbert, S. P. & Hawley, R. S. (2005) *Drosophila* Nod protein binds preferentially to the plus ends of microtubules and promotes microtubule polymerization in vitro, *Mol Biol Cell*. **16**, 5400-9.
225. Hackney, D. D. (1994) Evidence for alternating head catalysis by kinesin during microtubule-stimulated ATP hydrolysis, *Proc Natl Acad Sci U S A*. **91**, 6865-9.
226. Moyer, M. L., Gilbert, S. P. & Johnson, K. A. (1998) Pathway of ATP hydrolysis by monomeric and dimeric kinesin, *Biochemistry*. **37**, 800-13.
227. Alonso, M. C., van Damme, J., Vandekerckhove, J. & Cross, R. A. (1998) Proteolytic mapping of kinesin/ncd-microtubule interface: nucleotide-dependent conformational changes in the loops L8 and L12, *Embo J*. **17**, 945-51.
228. Amos, L. A. (2000) Focusing-in on microtubules, *Curr Opin Struct Biol*. **10**, 236-41.
229. Manning, B. D. & Snyder, M. (2000) Drivers and passengers wanted! the role of kinesin-associated proteins, *Trends Cell Biol*. **10**, 281-9.
230. Gilbert, S. P. & Johnson, K. A. (1993) Expression, purification, and characterization of the *Drosophila* kinesin motor domain produced in *Escherichia coli*, *Biochemistry*. **32**, 4677-84.
231. Borisy, G. G., Olmsted, J. B., Marcum, J. M. & Allen, C. (1974) Microtubule assembly in vitro, *Fed Proc*. **33**, 167-74.

232. Campbell, D. H., Luescher, E. & Lerman, L. S. (1951) Immunologic Adsorbents: I. Isolation of Antibody by Means of a Cellulose-Protein Antigen, *Proc Natl Acad Sci U S A.* 37, 575-8.
233. Cochran, J. C., Sontag, C. A., Maliga, Z., Kapoor, T. M., Correia, J. J. & Gilbert, S. P. (2004) Mechanistic analysis of the mitotic kinesin Eg5, *J Biol Chem.* 279, 38861-70.
234. Gilbert, S. P. & Mackey, A. T. (2000) Kinetics: a tool to study molecular motors, *Methods.* 22, 337-54.
235. Ems-McClung, S. C., Zheng, Y. & Walczak, C. E. (2004) Importin alpha/beta and Ran-GTP regulate XCTK2 microtubule binding through a bipartite nuclear localization signal, *Mol Biol Cell.* 15, 46-57.
236. Maddox, P. S., Bloom, K. S. & Salmon, E. D. (2000) The polarity and dynamics of microtubule assembly in the budding yeast *Saccharomyces cerevisiae*, *Nat Cell Biol.* 2, 36-41.
237. Miller, R. K., Heller, K. K., Frisen, L., Wallack, D. L., Loayza, D., Gammie, A. E. & Rose, M. D. (1998) The kinesin-related proteins, Kip2p and Kip3p, function differently in nuclear migration in yeast, *Mol Biol Cell.* 9, 2051-68.
238. Hwang, E., Kusch, J., Barral, Y. & Huffaker, T. C. (2003) Spindle orientation in *Saccharomyces cerevisiae* depends on the transport of microtubule ends along polarized actin cables, *J Cell Biol.* 161, 483-8.
239. Correia, J. J., Gilbert, S. P., Moyer, M. L. & Johnson, K. A. (1995) Sedimentation studies on the kinesin motor domain constructs K401, K366, and K341, *Biochemistry.* 34, 4898-907.
240. Mackey, A. T. & Gilbert, S. P. (2003) The ATPase cross-bridge cycle of the Kar3 motor domain. Implications for single head motility, *J Biol Chem.* 278, 3527-35.
241. Maney, T., Hunter, A. W., Wagenbach, M. & Wordeman, L. (1998) Mitotic centromere-associated kinesin is important for anaphase chromosome segregation, *J Cell Biol.* 142, 787-801.
242. Rose, M. D. (1996) Nuclear fusion in the yeast *Saccharomyces cerevisiae*, *Annu Rev Cell Dev Biol.* 12, 663-95.
243. Rickard, J. E. & Kreis, T. E. (1996) CLIPs for organelle-microtubule interactions, *Trends Cell Biol.* 6, 178-83.

244. Ligon, L. A., Shelly, S. S., Tokito, M. & Holzbaur, E. L. (2003) The microtubule plus-end proteins EB1 and dynactin have differential effects on microtubule polymerization, *Mol Biol Cell*. 14, 1405-17.
245. Maekawa, H. & Schiebel, E. (2004) CLIP-170 family members: a motor-driven ride to microtubule plus ends, *Dev Cell*. 6, 746-8.
246. Ligon, L. A., Shelly, S. S., Tokito, M. K. & Holzbaur, E. L. (2006) Microtubule binding proteins CLIP-170, EB1, and p150Glued form distinct plus-end complexes, *FEBS Lett*. 580, 1327-32.
247. Tirnauer, J. S., O'Toole, E., Berrueta, L., Bierer, B. E. & Pellman, D. (1999) Yeast Bim1p promotes the G1-specific dynamics of microtubules, *J Cell Biol*. 145, 993-1007.
248. Carvalho, P., Gupta, M. L., Jr., Hoyt, M. A. & Pellman, D. (2004) Cell cycle control of kinesin-mediated transport of Bik1 (CLIP-170) regulates microtubule stability and dynein activation, *Dev Cell*. 6, 815-29.
249. Schwartz, K., Richards, K. & Botstein, D. (1997) BIM1 encodes a microtubule-binding protein in yeast, *Mol Biol Cell*. 8, 2677-91.
250. Trueheart, J., Boeke, J. D. & Fink, G. R. (1987) Two genes required for cell fusion during yeast conjugation: evidence for a pheromone-induced surface protein, *Mol Cell Biol*. 7, 2316-28.
251. Berlin, V., Styles, C. A. & Fink, G. R. (1990) BIK1, a protein required for microtubule function during mating and mitosis in *Saccharomyces cerevisiae*, colocalizes with tubulin, *J Cell Biol*. 111, 2573-86.
252. Pierre, P., Scheel, J., Rickard, J. E. & Kreis, T. E. (1992) CLIP-170 links endocytic vesicles to microtubules, *Cell*. 70, 887-900.
253. Wolyniak, M. J., Blake-Hodek, K., Kosco, K., Hwang, E., You, L. & Huffaker, T. C. (2006) The regulation of microtubule dynamics in *Saccharomyces cerevisiae* by three interacting plus-end tracking proteins, *Mol Biol Cell*. 17, 2789-98.
254. van Breugel, M., Drechsel, D. & Hyman, A. (2003) Stu2p, the budding yeast member of the conserved Dis1/XMAP215 family of microtubule-associated proteins is a plus end-binding microtubule destabilizer, *J Cell Biol*. 161, 359-69.

255. Asbury, C. L., Gestaut, D. R., Powers, A. F., Franck, A. D. & Davis, T. N. (2006) The Dam1 kinetochore complex harnesses microtubule dynamics to produce force and movement, *Proc Natl Acad Sci U S A.* 103, 9873-8.
256. Gupta, M. L., Jr. (2006) Plus end-specific depolymerase activity of Kip3, a kinesin-8 protein, explains its role in positioning the yeast mitotic spindle, *Nat Cell Biol.* epub ahead of print: 13 August 2006; DOI:10.1038/ncb1457
257. Pellman, D., Bagget, M., Tu, Y. H., Fink, G. R. & Tu, H. (1995) Two microtubule-associated proteins required for anaphase spindle movement in *Saccharomyces cerevisiae*, *J Cell Biol.* 130, 1373-85.
258. Lin, H., de Carvalho, P., Kho, D., Tai, C. Y., Pierre, P., Fink, G. R. & Pellman, D. (2001) Polyploids require Bik1 for kinetochore-microtubule attachment, *J Cell Biol.* 155, 1173-84.
259. Hirokawa, N. & Takemura, R. (2004) Kinesin superfamily proteins and their various functions and dynamics, *Exp Cell Res.* 301, 50-9.
260. Mazumdar, M. & Misteli, T. (2005) Chromokinesins: multitalented players in mitosis, *Trends Cell Biol.* 15, 349-55.
261. Miki, H., Okada, Y. & Hirokawa, N. (2005) Analysis of the kinesin superfamily: insights into structure and function, *Trends Cell Biol.* 15, 467-76.
262. Chu, H. M., Yun, M., Anderson, D. E., Sage, H., Park, H. W. & Endow, S. A. (2005) Kar3 interaction with Cik1 alters motor structure and function, *Embo J.* 24, 3214-23.
263. Krzysiak, T. C., Wendt, T., Sproul, L. R., Tittmann, P., Gross, H., Gilbert, S. P. & Hoenger, A. (2006) A structural model for monastrol inhibition of dimeric kinesin Eg5, *Embo J.* 25, 2263-73.
264. Wendt, T. G., Volkmann, N., Skiniotis, G., Goldie, K. N., Muller, J., Mandelkow, E. & Hoenger, A. (2002) Microscopic evidence for a minus-end-directed power stroke in the kinesin motor ncd, *Embo J.* 21, 5969-78.
265. deCastro, M. J., Ho, C. H. & Stewart, R. J. (1999) Motility of dimeric ncd on a metal-chelating surfactant: evidence that ncd is not processive, *Biochemistry.* 38, 5076-81.

266. Pechatnikova, E. & Taylor, E. W. (1999) Kinetics processivity and the direction of motion of Ncd, *Biophys J.* 77, 1003-16.
267. Karabay, A. & Walker, R. A. (2003) Identification of Ncd tail domain-binding sites on the tubulin dimer, *Biochem Biophys Res Commun.* 305, 523-8.
268. Wendt, T., Karabay, A., Krebs, A., Gross, H., Walker, R. & Hoenger, A. (2003) A structural analysis of the interaction between ncd tail and tubulin protofilaments, *J Mol Biol.* 333, 541-52.
269. Hua, W., Chung, J. & Gelles, J. (2002) Distinguishing inchworm and hand-over-hand processive kinesin movement by neck rotation measurements, *Science.* 295, 844-8.
270. Troxell, C. L., Sweezy, M. A., West, R. R., Reed, K. D., Carson, B. D., Pidoux, A. L., Cande, W. Z. & McIntosh, J. R. (2001) pkl1(+) and klp2(+): Two kinesins of the Kar3 subfamily in fission yeast perform different functions in both mitosis and meiosis, *Mol Biol Cell.* 12, 3476-88.
271. Pidoux, A. L., LeDizet, M. & Cande, W. Z. (1996) Fission yeast pkl1 is a kinesin-related protein involved in mitotic spindle function, *Mol Biol Cell.* 7, 1639-55.
272. Hatsumi, M. & Endow, S. A. (1992) Mutants of the microtubule motor protein, nonclaret disjunctional, affect spindle structure and chromosome movement in meiosis and mitosis, *J Cell Sci.* 101 (Pt 3), 547-59.
273. Hagan, I. & Yanagida, M. (1992) Kinesin-related cut7 protein associates with mitotic and meiotic spindles in fission yeast, *Nature.* 356, 74-6.
274. Hoyt, M. A., He, L., Loo, K. K. & Saunders, W. S. (1992) Two *Saccharomyces cerevisiae* kinesin-related gene products required for mitotic spindle assembly, *J Cell Biol.* 118, 109-20.
275. Heck, M. M., Pereira, A., Pesavento, P., Yannoni, Y., Spradling, A. C. & Goldstein, L. S. (1993) The kinesin-like protein KLP61F is essential for mitosis in *Drosophila*, *J Cell Biol.* 123, 665-79.
276. Sawin, K. E. & Mitchison, T. J. (1995) Mutations in the kinesin-like protein Eg5 disrupting localization to the mitotic spindle, *Proc Natl Acad Sci U S A.* 92, 4289-93.

277. Kashina, A. S., Rogers, G. C. & Scholey, J. M. (1997) The bimC family of kinesins: essential bipolar mitotic motors driving centrosome separation, *Biochim Biophys Acta*. 1357, 257-71.
278. Endow, S. A. (1993) Chromosome distribution, molecular motors and the claret protein, *Trends Genet.* 9, 52-5.
279. Endow, S. A., Chandra, R., Komma, D. J., Yamamoto, A. H. & Salmon, E. D. (1994) Mutants of the *Drosophila* ncd microtubule motor protein cause centrosomal and spindle pole defects in mitosis, *J Cell Sci.* 107 (Pt 4), 859-67.
280. Wilson, P. G., Simmons, R. & Saighal, S. (2004) Novel nuclear defects in KLP61F-deficient mutants in *Drosophila* are partially suppressed by loss of Ncd function, *J Cell Sci.* 117, 4921-33.
281. Endres, N. F., Yoshioka, C., Milligan, R. A. & Vale, R. D. (2006) A lever-arm rotation drives motility of the minus-end-directed kinesin Ncd, *Nature.* 439, 875-8.
282. Ito, M., Morii, H., Shimizu, T. & Tanokura, M. (2006) Coiled coil in the stalk region of ncd motor protein is nonlocally sustained, *Biochemistry.* 45, 3315-24.
283. Mackey, A. T., Sproul, L. R., Sontag, C. A., Satterwhite, L. L., Correia, J. J. & Gilbert, S. P. (2004) Mechanistic analysis of the *Saccharomyces cerevisiae* kinesin Kar3, *J Biol Chem.* 279, 51354-61.
284. Riparbelli, M. G. & Callaini, G. (2005) The meiotic spindle of the *Drosophila* oocyte: the role of centrosomin and the central aster, *J Cell Sci.* 118, 2827-36.
285. Goshima, G. & Vale, R. D. (2003) The roles of microtubule-based motor proteins in mitosis: comprehensive RNAi analysis in the *Drosophila* S2 cell line, *J Cell Biol.* 162, 1003-16.
286. Rice, S., Lin, A. W., Safer, D., Hart, C. L., Naber, N., Carragher, B. O., Cain, S. M., Pechatnikova, E., Wilson-Kubalek, E. M., Whittaker, M., Pate, E., Cooke, R., Taylor, E. W., Milligan, R. A. & Vale, R. D. (1999) A structural change in the kinesin motor protein that drives motility, *Nature.* 402, 778-84.
287. Case, R. B., Rice, S., Hart, C. L., Ly, B. & Vale, R. D. (2000) Role of the kinesin neck linker and catalytic core in microtubule-based motility, *Curr Biol.* 10, 157-60.
288. Cui, W. & Hawley, R. S. (2005) The HhH2/NDD domain of the *Drosophila* Nod chromokinesin-like protein is required for binding to chromosomes in the oocyte nucleus, *Genetics.* 171, 1823-35.

289. Brendza, R. P., Serbus, L. R., Duffy, J. B. & Saxton, W. M. (2000) A function for kinesin I in the posterior transport of oskar mRNA and Stauf protein, *Science*. 289, 2120-2.
290. Dickinson, R. B. & Purich, D. L. (2002) Clamped-filament elongation model for actin-based motors, *Biophys J*. 82, 605-17.
291. Januschke, J., Gervais, L., Dass, S., Kaltschmidt, J. A., Lopez-Schier, H., St Johnston, D., Brand, A. H., Roth, S. & Guichet, A. (2002) Polar transport in the Drosophila oocyte requires Dynein and Kinesin I cooperation, *Curr Biol*. 12, 1971-81.
292. Li, M., McGrail, M., Serr, M. & Hays, T. S. (1994) Drosophila cytoplasmic dynein, a microtubule motor that is asymmetrically localized in the oocyte, *J Cell Biol*. 126, 1475-94.
293. Brendza, R. P., Serbus, L. R., Saxton, W. M. & Duffy, J. B. (2002) Posterior localization of dynein and dorsal-ventral axis formation depend on kinesin in Drosophila oocytes, *Curr Biol*. 12, 1541-5.
294. Cha, B. J., Serbus, L. R., Koppetsch, B. S. & Theurkauf, W. E. (2002) Kinesin I-dependent cortical exclusion restricts pole plasm to the oocyte posterior, *Nat Cell Biol*. 4, 592-8.
295. Serbus, L. R., Cha, B. J., Theurkauf, W. E. & Saxton, W. M. (2005) Dynein and the actin cytoskeleton control kinesin-driven cytoplasmic streaming in Drosophila oocytes, *Development*. 132, 3743-52.
296. Shiroguchi, K., Ohsugi, M., Edamatsu, M., Yamamoto, T. & Toyoshima, Y. Y. (2003) The second microtubule-binding site of monomeric kid enhances the microtubule affinity, *J Biol Chem*. 278, 22460-5.
297. Howard, J. & Hyman, A. A. (2003) Dynamics and mechanics of the microtubule plus end, *Nature*. 422, 753-8.
298. Hawley, R. S. & Theurkauf, W. E. (1993) Requiem for distributive segregation: achiasmate segregation in Drosophila females, *Trends Genet*. 9, 310-7.